Centre for Ore Deposit and Exploration Studies

FAULTING AND MINERALISATION OF WESTERN TASMANIA

AMIRA/ARC Project P.291A

Report No.1
May 1994

UNIVERSITY OF TASMANIA

Contents

Summary

Project P291 on faulting and mineralisation in Western Tasmania applied the regional structure of the Dundas Trough to improve ore deposit and exploration models in the area. Two aspects arising out this project required further study. A major aim of P291A is to use structure, geochemistry and sedimentology to test the model for Cambrian extensional faulting proposed in P291. A secondary aim was to tackle inconsistencies in the Devonian structure remaining from previous studies, and to further test the regional sections with gravity and magnetics.

AMIRA project P291A started with a meeting on 18 October 1993. Commonwealth ARC funding for the cooperative research grant began on 1 January 1994. The agreed program for 1994 included four items from the planned list of nine.

2. Examine the structural and stratigraphic evidence for the Cambrian extensional faults along the western boundary of the Dundas Group from Zeehan to Que River.

The initial work on the Stitt Quartzite supported previous interpretation of a turbidite origin but suggested these lithologies formed above storm wave base. No evidence of a close western source was found on this limb of the syncline. Access difficulties have slowed the progress in studies closer to the basin bounding fault. Field work will continue into the next field season.

6. Investigate lithostratigraphic correlations within the Dundas Group and between the Dundas and Central Volcanic Complex.

The Mount Read Volcanics have been subdivided into three depositional cycles, based on a literature review, each with a distinct basin geometry and history. Samples of sandstones have been collected from each of these cycles. Detailed petrography on these rocks has been started with a view to finding distinguishing characteristics for each cycle and variations in provenance within the belt.

8. The spatial and temporal relationship between cleavage formation, folding and faulting along the Rosebery Fault from Rosebery Lodes to the Pieman River.

There is a close spatial relationship between the Rosebery Fault and a late N-striking cleavage (S_2). This cleavage occurs in the hanging wall at Rosebery but in the footwall in the Pieman River. The style of the cleavage reflects the thermal conditions during Devonian granitoid emplacement. An earlier cleavage was recognised at all localities. This cleavage was not visible in the most intense zones of S_2 cleavage development but overprinting was found on the edge of the zone of S_2 development. The earlier cleavage has a composite origin including both a NNW-striking Devonian cleavage and a N-striking cleavage of Devonian or Cambrian age.

9. The isotopic signature of veins related to discrete structural events in a transect from the Pieman River to the Murchison Dam.

A preliminary study of both quartz and carbonate has been undertaken. The Devonian quartz bearing veins have oxygen isotopic values related to their distance from the granite. Cambrian and Devonian hydrothermal carbonates have distinctly different carbon and oxygen isotope values. Devonian veins in faults show inherited Cambrian isotopic values where there is no granite contribution.

Sampling has been carried out for an initial study on the application of laser ablation sulfur isotope methods to the detection/characterisation of Cambrian structures. Evidence from seafloor and ancient settings indicates that areas of shallow seawater convection are likely to be the isotopically detectable.

All the proposed sections have been started but only the cleavage study along the Rosebery Fault has reached an advanced stage. The results of further work on item 2 have pointed out future difficulties in accessing well exposed rocks. The isotopic work has supported the need to use an approach based on a range of techniques.

Preliminary Report: Sedimentology of the Dundas Group with reference to a possible syn-depositional growth fault west of Rosebery

Stuart W. Bull
CODES Key Centre

INTRODUCTION

Regional structural studies have led to the proposal that a N–S trending structure west of the Rosebery Fault in the Rosebery region was a growth fault, with an associated WNW–ESE trending transfer, which was active in the Cambrian (Berry and Keele 1993; Fig.1). The aim of this study is to test this model by examining the sediments of the Dundas Group in the Rosebery area for evidence of structural control on Cambrian sedimentation. Such evidence could include facies and/or provenance patterns, ideally in conjunction with palaeocurrent indicators.

STRATIGRAPHY

The Dundas Group in the Rosebery area can be considered in terms of four stratigraphic subdivisions. The stratigraphic names used here are after Green (1983), however, the status of these names is apparently informal.

The basal unit of the Dundas Group in the Rosebery area, the White Spur Formation, consists of lithicwacke, siltstone, mudstone and quartz-feldspar-phyric tuff (Corbett & McNeill 1986). Where observed by the author outcrop of the White Spur Formation consists of massive altered volcaniclastics and black slate (Chamberlain shale). Although the volcaniclastics clearly have implications for provenance, no palaeocurrent indicators would be expected in these deposits. The middle unit of the Dundas Group in the Rosebery area, the Stitt Quartzite, consists of quartzwacke interbedded with black phyllitic mudstone, grey siltstone and minor conglomerate (Corbett & McNeill 1986). This unit is considered to have the best potential to record the sedimentological features required by this study. The upper unit of the Dundas Group in the Rosebery area, the Westcott argillite, consists of dolomitic siltstone and sandstone (Corbett & McNeill 1986), with intercalated conglomerate deposits (?Salisbury conglomerate equivalents) interpreted as debris flows (Green 1983). The conglomerate deposits could prove useful provenance indicators, however, they are massive and structureless where they have currently been observed by the author. This is consistent with the debris flow interpretation and no palaeocurrent indicators would be expected.

Stitt quartzite

Exposures of the Stitt Quartzite have been examined at six localities in the Rosebery area (Fig. 1) and sedimentological sections have been measured from four of these localities. Sections Stitt quartzite 1 (Fig. 2) and Stitt quartzite 2 (Fig. 3) were measured on the Flume Road at Rosebery Mine. They are generalised facies logs which represent the overall nature of the Stitt quartzite from its base (Stitt quartzite 1) up through the middle level of the unit (Stitt quartzite 2). Sections Stitt quartzite 4 (Fig. 4) and Stitt quartzite 6 (Fig. 5) are detailed bed for bed logs which document the internal detail of the facies defined in the Stitt quartzite.

Four facies have been defined from the measured sedimentary sections through the Stitt quartzite. These are the *mudstone facies*, the *thin-bedded sandstone/siltstone/mudstone facies*, the *medium/thin-bedded sandstone facies* and the *thick-bedded sandstone facies*. All facies are present in the generalised facies logs Stitt quartzite 1 and Stitt quartzite 2 (Figs 2 and 3) and more internal detail can be seen in the detailed

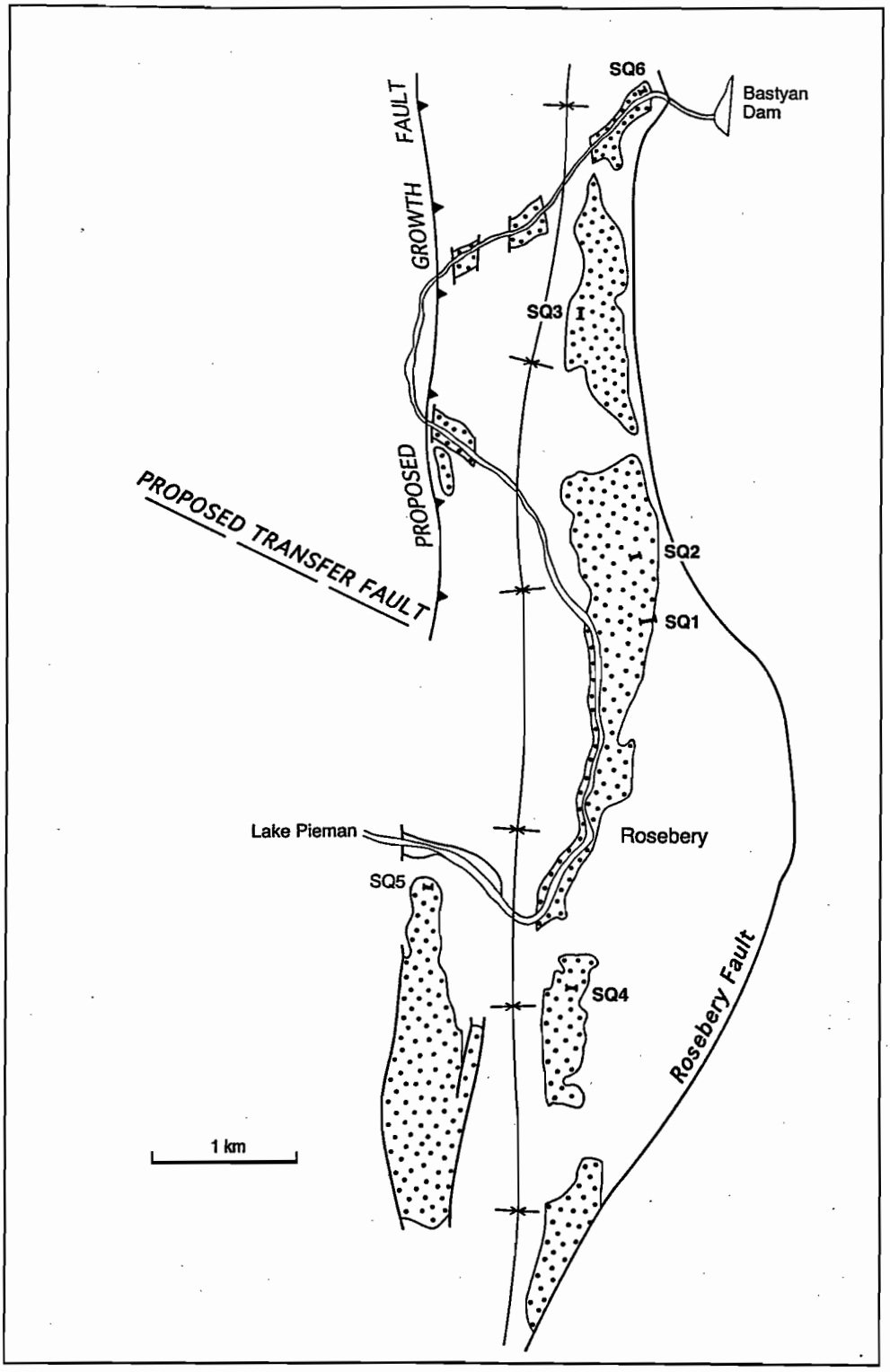

FIG. 1 — Extent of the Stitt quartzite in the Rosebery area (after Corbett and McNeill 1986) showing the section localities for this study.

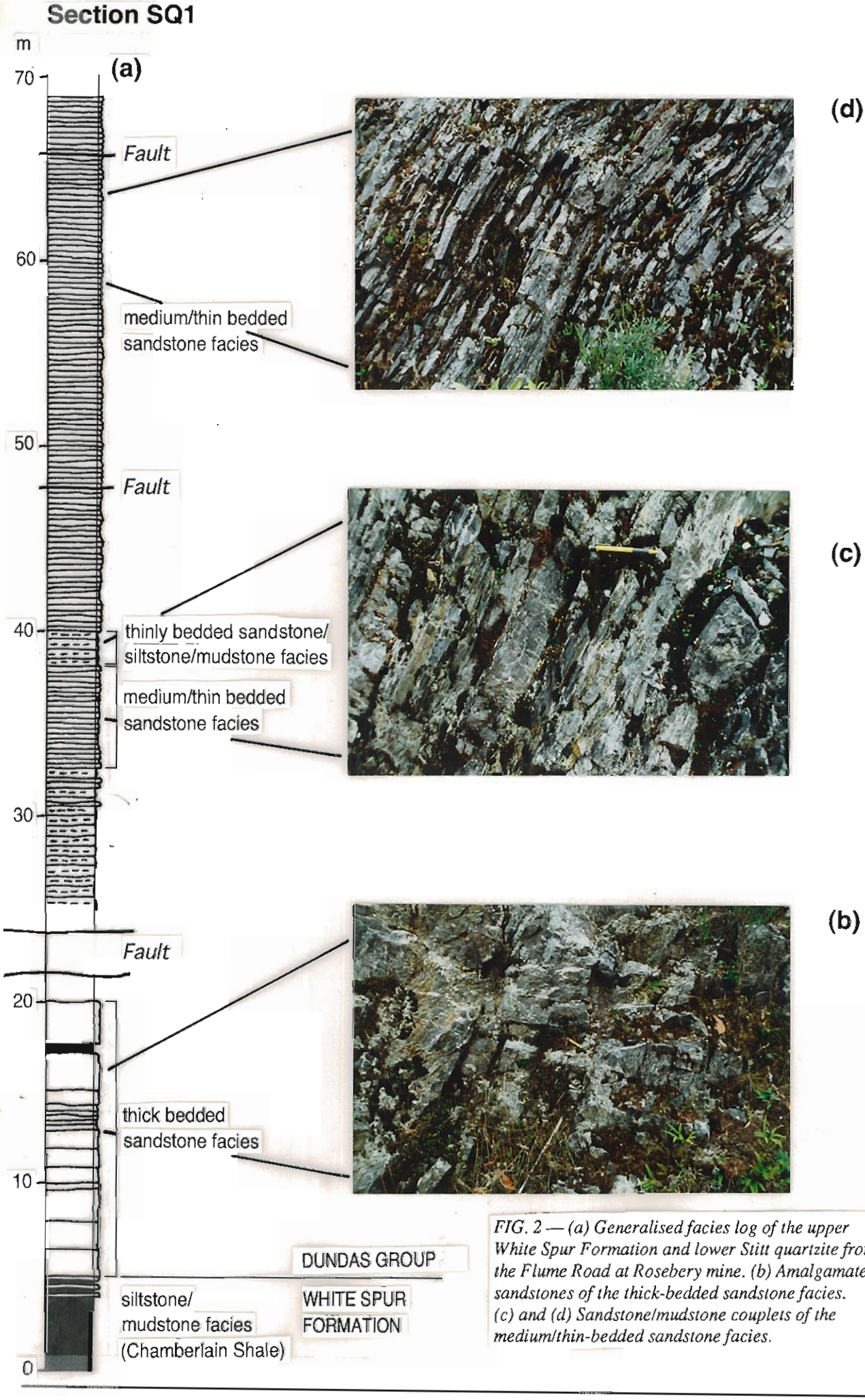

FIG. 2 — (a) Generalised facies log of the upper White Spur Formation and lower Stitt quartzite from the Flume Road at Rosebery mine. (b) Amalgamated sandstones of the thick-bedded sandstone facies. (c) and (d) Sandstone/mudstone couplets of the medium/thin-bedded sandstone facies.

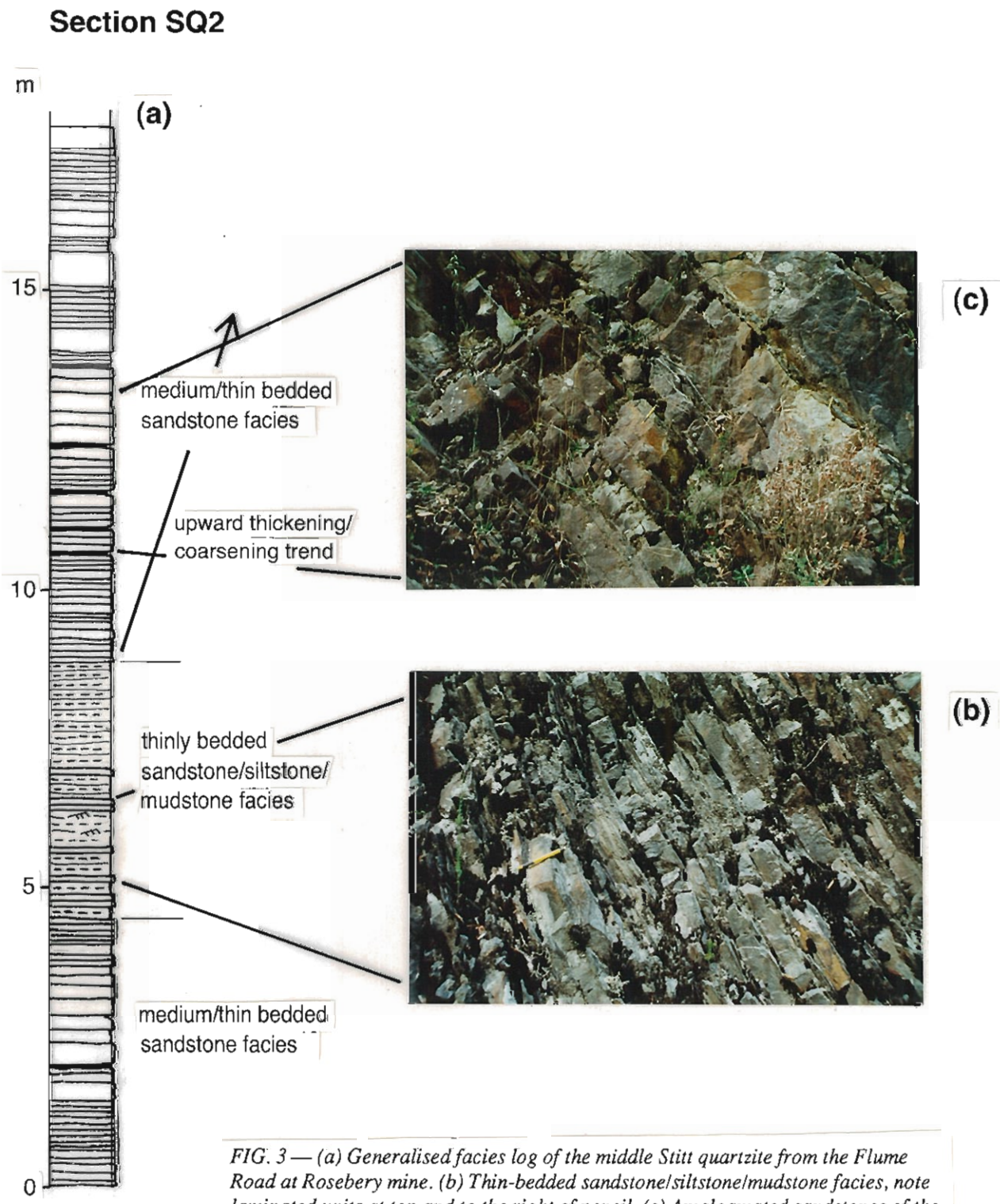

FIG. 3 — (a) Generalised facies log of the middle Stitt quartzite from the Flume Road at Rosebery mine. (b) Thin-bedded sandstone/siltstone/mudstone facies, note laminated units at top and to the right of pencil. (c) Amalgamated sandstones of the medium/thin-bedded sandstone facies.

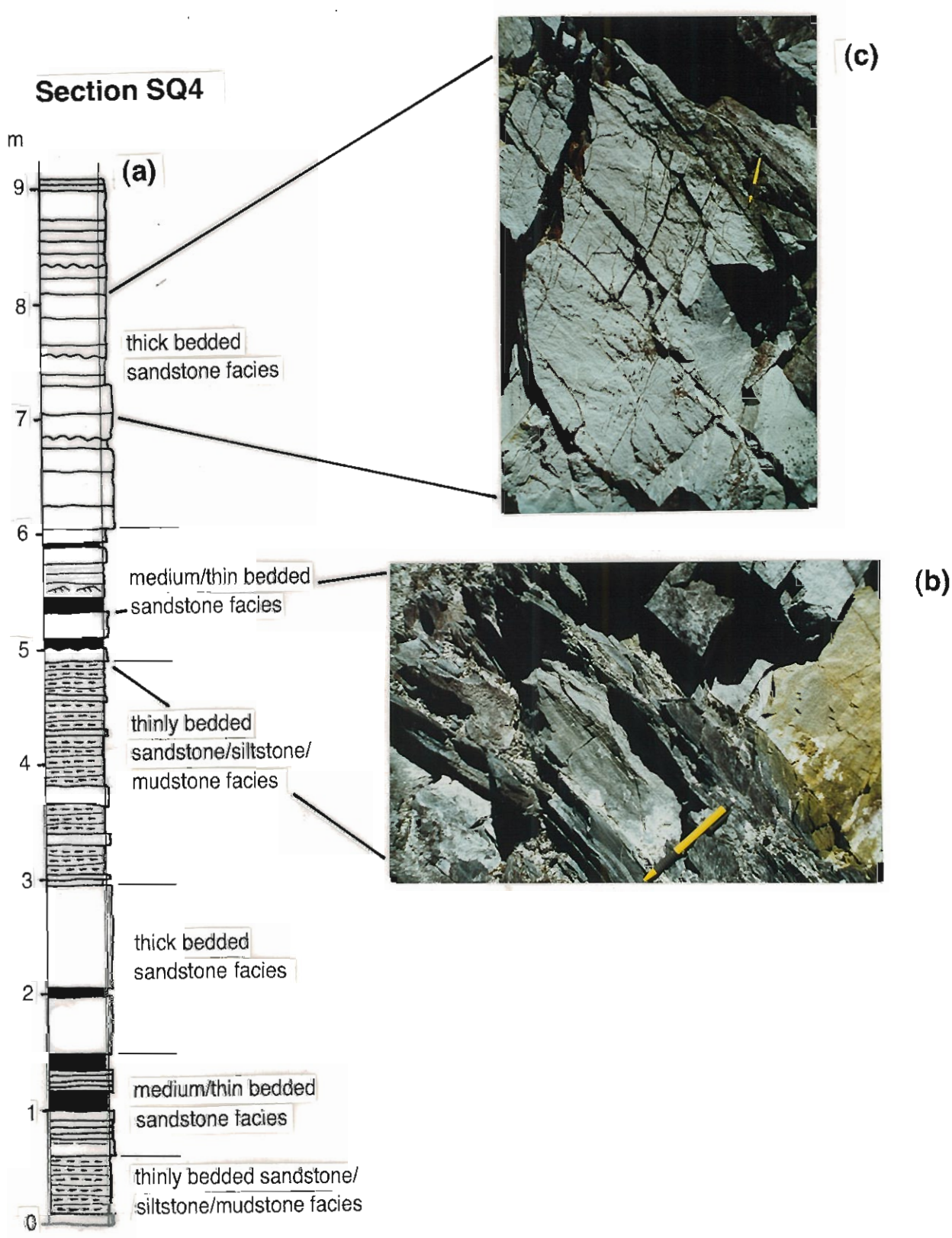

FIG. 4 — (a) Detailed bed-for-bed log of the Stitt quartzite in a quarry exposure 1.5 km SW of Rosebery. (b) Sandstone beds separated by mudstone intervals in the medium/thin-bedded sandstone facies. (c) Amalgamated sandstone beds of the thick-bedded sandstone facies. Note ripple pavement on second bed top to the left of pencil.

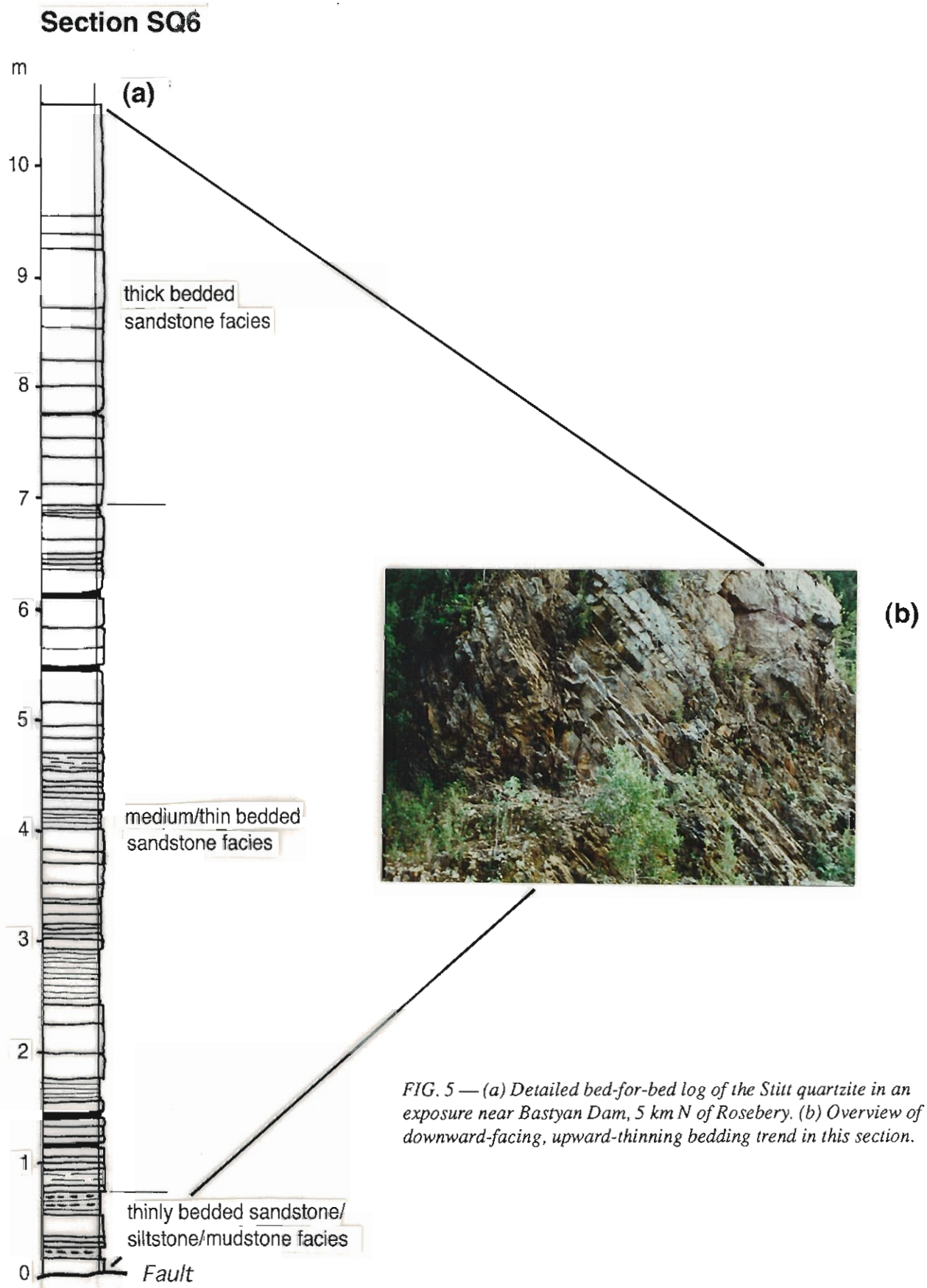

FIG. 5 — (a) Detailed bed-for-bed log of the Stitt quartzite in an exposure near Bastyan Dam, 5 km N of Rosebery. (b) Overview of downward-facing, upward-thinning bedding trend in this section.

bed for bed sections Stitt quartzite 4 and Stitt quartzite 6 (Figs 4 and 5).

The *mudstone facies* proper is only sparsely represented in the Stitt quartzite, and is best developed in the underlying Chamberlain shale which is the uppermost unit of the White Spur Formation (see the base of section Stitt quartzite 1; Fig. 2). It consists of massive black mudstone (now slate) with varying proportions of intercalated pale grey siltstone to fine-grained sandstone. Where present, the siltstone/sandstone occurs as 1 to 3 cm thick beds which have sharp bases, graded tops and are clearly turbiditic in character.

The *thin-bedded sandstone/siltstone/mudstone facies* also contains a significant proportion of mudstone (up to 50%), but in this case it is always intercalated with thinly bedded (i.e. < 10 cm) fine-grained sandstone and siltstone (Fig. 3b). Some of these deposits have the sharp bases and graded tops indicative of turbiditic emplacement, however, in many cases the sandstone and siltstone occurs in diffusely bounded intervals which are internally dominated by planar laminations and ripples. Most of the palaeocurrent indicators present in the Stitt quartzite are ripples in this facies.

The *medium/thin-bedded sandstone facies* is dominated by fine-grained sandstone beds which range in thickness from 4 to 20 cm. Individual beds are clearly turbiditic in character, and they may be amalgamated (e.g. Fig. 3c) or separated by lesser thicknesses of siltstone/mudstone (e.g. Fig. 2c and d; Fig. 4b). Overall siltstone and mudstone comprises < 30% of this facies.

The *thick-bedded sandstone facies* is similar to the *medium/thin-bedded sandstone facies* except that the beds are thicker (i.e. up to 2 m) and they are almost always amalgamated (e.g. Fig. 4c). As a result siltstone/mudstone comprises < 5% of this facies. An additional feature unique to this facies is the occasional presence of symmetrical ripples on the upper surface of some beds (e.g. Fig. 4c below and to left of pen).

Taken overall, bedded, turbiditic sandstone-dominated facies comprise at least 70% of each section in the Stitt quartzite. This may be partly an outcrop bias due to the fact that the sandstone dominated packages are relatively resistant and form the best exposures. However, a reconnaissance traverse of the Flume Road at Rosebery Mine which exposes much of the Stitt quartzite stratigraphy confirms its sandstone-dominated character. The main form of sedimentation active during the accumulation of the Stitt quartzite was, therefore, via sandy turbidity currents.

Turbidite accumulations are generally considered in terms of the submarine fan depositional model (e.g. Shanmugam and Moiola 1985; Fig. 6). In this model turbidity currents are delivered to the margin of a developing fan via channels and deposit their load in lobes at channel mouths. In general, in ancient successions, channels are recognised as upward thinning/fining sequences and lobes as upward thickening/coarsening sequences (Fig. 6). Examples of upward thinning and upward thickening bedding sequences in the Stitt quartzite have been reported by Green (1983), and others have been documented in this study (e.g. a 5 m thick crudely upward thickening/coarsening sequence is present in section Stitt quartzite 2 from 9 m to around 14 m [Fig. 3] and section Stitt quartzite 6, which is downward facing, consists entirely of a 10 m thick upward thinning/fining sequence [Fig. 5]). The presence of these bed thickness trends indicates that the turbidite deposits of the Stitt quartzite could have accumulated in some form of fan system.

Although in general terms a turbidite fan model appears to apply to the Stitt quartzite, caution needs to be used when applying submarine fan models to ancient successions. This is because fan models are generally based on examples which occur at present day continental margins. In such systems turbidity currents are delivered across the continental shelf via drowned river systems and the fan develops in very deep water in the continental slope/base of slope area. However, turbidity currents can occur in any significant water body which has a marginal sediment supply (e.g. on continental shelves and in marginal and intra-continental rift basins). Turbidite fans will accumulate in these settings as long as sediment is supplied via a point source, and the fans will be preserved as long as a relatively quiet (ie. sub wave-base) environment exists such that the deposits are protected from post-depositional reworking.

It is unclear to the author whether a continental margin setting is an appropriate model for the Cambrian of western Tasmania, however, several factors suggest that the Stitt quartzite does not represent deposition at great water depths. In a "classic" submarine fan model sedimentation occurs in very deep water beyond the range of wave-generated effects and other current activity. In consequence, ambient background deposition between the geologically instantaneous turbidity current events consists entirely of hemi-pelagic mudstone accumulation. Although mudstone is present throughout the Stitt quartzite there is less than would be expected in this model. In many places ambient depositional conditions between turbidite events are represented by the *thin-bedded sandstone/siltstone/mudstone facies*. Although this facies contains significant mudstone, it is characterised by the presence of planar laminated

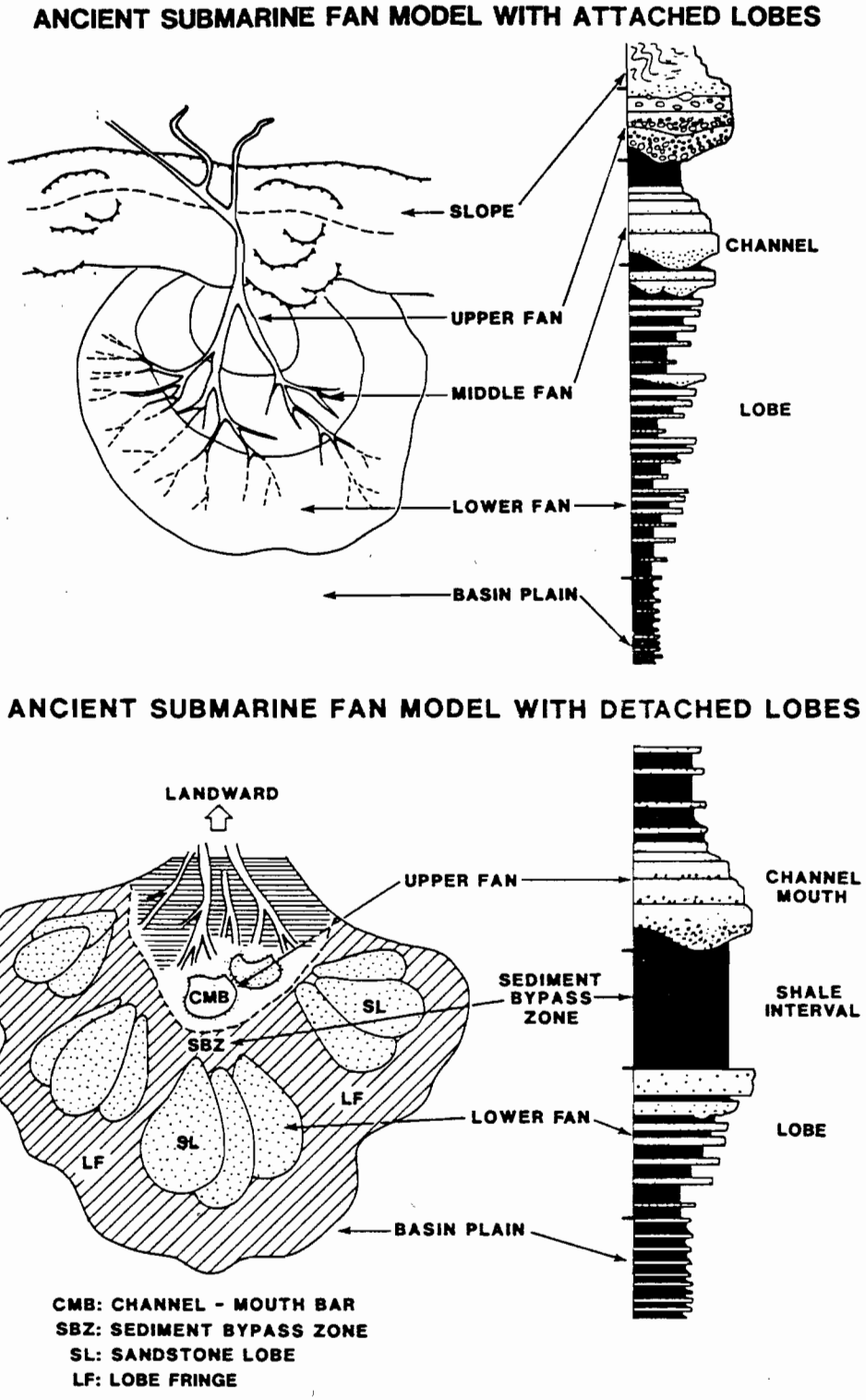

FIG. 6 — Top: Ancient submarine fan model with attached lobes; vertical progradational sequence showing thinning-upward channel and thickening-upward lobe cycles. Bottom: Ancient submarine fan model with detached lobes (after Shanmugan and Miola 1985).

and ripple siltstone (Fig. 3b). This indicates that between turbidite events the sediment surface was subjected to significant reworking by bottom currents (? tidal or longshore currents). In addition, the symmetrical ripples which occur on the upper surfaces of sandstone beds (Fig. 4c) at two localities suggest occasional wave-generated reworking. The overall impression is that the Stitt quartzite accumulated in quiet conditions, but the sediment surface was subjected to occasional reworking by relatively low energy currents. The most likely depositional setting is considered to be just below wave base. The depth of wave base for a particular water body depends on its geometry, but a reasonable range would be < 50 m to several hundred metres.

DISCUSSION

It is proposed that the Stitt quartzite represents a turbidite fan system which accumulated in a largely sub-wave base environment. With respect to what effects an active N–S trending growth fault to the west would have had on this system, two main possibilities are envisaged. Firstly, the fault could be expected to manifest itself as a N–S trending scarp with the downthrown hanging wall block to the east. If this scarp had sufficient relief, the situation could have existed where the eastern downthrown hanging wall block hosted sub-wave base sedimentation, while the western footwall block remained in relatively energetic shallow water or subaerial conditions. This type of system should manifest itself in the rock record as an erosional disconformity in older hanging wall rocks to the west, which acted as a source for eastward-directed coarse-grained clastic sediment. If the water depth was sufficient that the both footwall and hanging wall blocks occurred in a relatively quiet subaqueous environment then the effects of a scarp would be more subtle. It is possible, however, that the resultant N–S trending, eastward inclined slope would lead to an elongate zone of slumping and soft-sediment deformation. In either case, if a N–S trending active growth fault was present to the west of the Stitt quartzite system, the expected palaeocurrent pattern in the turbidite deposits should indicate a western source.

None of the effects expected if an active N–S trending growth fault was present to the west of Rosebery area during the deposition of the Stitt quartzite have been documented in this study. No material coarser than medium-grained sandstone was observed in the Stitt quartzite, although minor conglomerate deposits have been reported (Corbett and McNeill 1986), none have been described from the Rosebery area. This would seem to indicate that if the growth fault existed, then there was no steep fault scarp and/or the western footwall block was not uplifted into shallow or emergent environment. No particular zone of slumping or soft-sediment deformation has been defined either, although this part of the study has been hampered by the lack of exposure of those deposits which would have been closest to the fault, those of the western limb of the syncline within which the Stitt quartzite is exposed (Fig. 1).

The biggest problem encountered in testing the growth fault model in this study was, however, the lack of the critical palaeocurrent data from the right facies. Almost all of the palaeoflow indicators come from the *thin-bedded sandstone/siltstone/mudstone facies*. As outlined above, these deposits are interpreted to represent reworking of the sediment surface in between turbidity current events. The palaeoflow indicators present will, therefore, record the directions of the reworking currents. These could easily be longshore directed and need in no way reflect the direction of primary sediment supply via turbidity currents. In fact the palaeocurrent measurements (Fig. 7) give no clear pattern. The apparent W–SE trend is thought to be a sample bias arising from the fact that most of the measured sections are normal to steeply dipping N-S striking bedding. Given that most of the palaeoflow indicators are small ripples, it is much easier to recognise palaeoflow indicators which are either downdip (i.e. E to W) or updip (i.e. W to E) in the upward facing beds on the eastern limb of the syncline which comprise the bulk of the sections. Many more ripple pavements were present in the *thin-bedded sandstone/siltstone/mudstone facies* from which no palaeoflow direction could be recorded, and these could easily have been N to S or S to N palaeoflow indicators. The overall picture that emerges during times of reworking is of a slightly agitated environment with

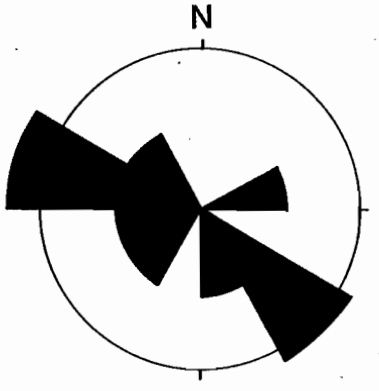

FIG. 7 — Palaeocurrent data from the Stitt quartzite (number of readings = 14).

no strong superimposed palaeoflow direction.

The type of palaeoflow indicators needed to properly test the active growth fault model are ripples from within the sandstone turbidite beds themselves (i.e. C-division cross-lamination; Bouma 1962). These proved to be very rare in the Stitt quartzite sections, so no evidence as to the direction of the source for the turbidity currents was recorded. In fact this absence of C-division cross-lamination and the associated B-division planar lamination from the Stitt quartzite turbidites is consistent with the sub-wave base depositional model proposed. This is because turbidity currents need to be fully turbulent and expanded (i.e. to have travelled a significant distance) to allow the particles enough freedom to produce laminated deposits. The sub-wave base model proposed is likely to be relatively proximal to source and, as such, poorly expanded, massive turbiditic sandstones would be expected.

Looking at the whole Dundas Group in the Rosebery area, mudstone/siltstone appears to represent ambient depositional conditions from at least the upper White Spur Formation (i.e. Chamberlain shale) through the Stitt quartzite to the Westcott argillite (where the fine-grained sediment becomes dolomitic; Corbett and McNeill 1986). This overall sequence can be interpreted in two ways. The system could be interpreted as a stable, relatively deep, quiet depositional environment with no syn-depositional faulting. Alternatively, if the sub-wave base depositional model proposed here for the 350 m thick Stitt quartzite is correct, it could be argued that relatively continuous tectonic subsidence on active growth faults would have been required to maintain the sub-wave base conditions throughout the deposition of this unit. In the Dundas Group sequence observed so far, the lithology which appears most likely to represent erosion of a fault scarp is the conglomerate intercalated with the dolomitic siltstones of the Westcott argillite (?Salisbury conglomerate and equivalents). Although they appear to be massive debris flow deposits and are, therefore, unlikely to yield palaeocurrent indicators, these deposits have distinctive clast types such as fuchsite and tholeiite lithologies and length slow spherulitic chert (Green 1983). They may, therefore, be suitable for a provenance study.

CONCLUSIONS

1. The Stitt quartzite is essentially a succession of fine-grained turbiditic sandstones.

2. These turbidites accumulated in some form of fan system just below wave base. In periods between turbidity current events the sediment surface was subjected to minor reworking via wave-generated and other current activity.

3. The Stitt quartzite records no evidence of a proximal growth fault to the west which had a scarp of sufficient relief such that the western hanging wall block was subjected to erosion in a shallow or subaerial environment. However, the critical palaeocurrent evidence of the direction of the turbidite source is lacking, and a growth fault scarp could have been present if it occurred entirely within the relatively quiet host depositional environment.

4. In the whole Dundas Group observed so far, the facies most likely to represent erosion of a fault scarp is considered to be the conglomeratic deposits intercalated with the Westcott argillite.

FUTURE WORK

1. To examine sections of the Stitt quartzite on the western limb of the syncline in Lake Pieman to look for evidence of slumping or soft-sediment deformation.

2. In order to confirm the sedimentological interpretation of the Stitt quartzite it would be useful to examine the unit in drill core.

3. To evaluate the potential of the conglomerate units within the Westcott argillite as provenance indicators by field work and drill core analysis.

REFERENCES

Berry, R. F. and Keele, R. A. 1993. Cambrian structure in western Tasmania. *In* Structure and mineralization of western Tasmania, AMIRA Project P.291 Final Report: 55-68.

Bouma, A. H. 1962. *SEDIMENTOLOGY OF SOME FLYSCH DEPOSITS.* Amsterdam: Elsevier: 168pp.

Corbett, K. D. and McNeill, A. W. 1986. Geological Survey of Tasmania-Department of Mines Hobart, Mt Read Volcanics Project, Map 2. Geology of Rosebery-Mt Block area.

Green, G. R. 1983. The geological setting and formation of the Rosebery volcanic-hosted massive sulphide orebody, Tasmania. Unpubl. PhD thesis, Geology Department, University of Tasmania.

Shanmugam, G. and Moiola, R. J. 1985. Submarine fan models: Problems and solutions. *In* Bouma, A. H., Normark, W. R. and Barnes, N. E. (eds): *Submarine fans and related turbidite systems.* Springer-Verlag New York: 29-34.

Isotope study: Preliminary Investigations

Paul A. Kitto
CODES Key Centre

ABSTRACT

A preliminary isotope study of both quartz and carbonate veins from the Pieman River and the Mackintosh Dam was undertaken to establish whether the isotopic signatures can characterise fault histories. These histories are a test of the tectonic model proposed for western Tasmania in the AMIRA project P291.

Oxygen isotope values in association with fluid inclusions studies have successfully characterised the Devonian quartz bearing veins. This information, in association with detailed gravity interpretations of the underlying Devonian granite ridge, can predict the position of district scale Sn–Cu–Pb–Zn telescoped metal zonation patterns. Fluid inclusion studies should assist in characterising the remaining quartz populations.

Cambrian and Devonian hydrothermal carbonates have distinctly different carbon and oxygen isotope values which can be used in conjunction with fluid inclusion investigations to establish the types of fluid responsible for carbonate mineralisation. Isotopic analysis of carbonate minerals within faults can therefore establish whether Cambrian or Devonian hydrothermal fluids were responsible for carbonate deposition, and in conjunction with kinematic indicators predict the fault history.

The isotopic results thus far provide a framework for future investigations. Fluid inclusion studies will complement any isotopic investigations. Access to gravity interpretations of the morphology of the Devonian granites that underlay the area of study would assist oxygen isotope interpretations of quartz. Possible new areas of research may include C/O isotope studies of the host rocks to vein carbonates. This could allow fluid/rock calculations and fluid circulation models to be considered. Strontium and carbon isotope studies of hydrothermal carbonates may also assist the evaluation of the proposed tectonic models for western Tasmania.

INTRODUCTION

Classification of deformation structures into either Cambrian or Devonian structures using isotopic signatures should provide a substantial test of the proposed tectonic model for Western Tasmania. Ore deposit research has shown that Cambrian ore fluids are substantially different to Devonian ore fluids and therefore isotopic and chemical signatures of vein material within variously mineralised faults should record the structural history of these faults. This project aims to look initially at faults in a transect from the Pieman River to the Murchison Dam (Fig. 1) because according to the initial study, AMIRA project P291, the faults in this transect include those which were:

(i) active in the Cambrian,
(ii) Cambrian faults reactivated in the Devonian, and
(iii) Devonian faults with no apparent Cambrian movement.

This investigation aims to test the structural history of these faults using the isotopic and chemical signatures of the veins associated with faulting. The isotopic section of the project will provide additional criteria for the interpretation of the structural controls on VHMS mineralisation and thus aid future exploration within the Mount Read Volcanic belt to find new world-class Pb–Zn–Cu–Au deposits. Devonian isotopic investigations are significant also for determination of the structural controls on tin and possibly gold mineralisation. The isotopic signature of

Devonian regional faults provide a basis for the recognition of halos above granite related mineralisation, such as the major Renison deposit and will provide essential criteria to differentiate Cambrian structures from Devonian structures.

The Devonian data collected and referred to in this report has been funded by an ARC large grant to R. Large, D. Cooke & P. Kitto.

BACKGROUND INFORMATION

The formation of brittle tensional fractures is typically associated with overpressured volatile-rich aqueous magmatic fluids that exceed both the minimum compressive stress and the tensile strength of the surrounding country rocks (Burnham 1979, Allman-Ward et al. 1982, Plimer 1987). Mineral deposition results from venting of the magmatic fluid from the lithostatic igneous source regime into the overlying hydrostatic environment where the magmatic fluids may cool, undergo phase separation and/or interact with wall rocks and/or fluids of meteoric, connate, seawater or metamorphic origin (Henley & McNabb 1978, Heinrich et al. 1989, Heinrich 1990). The resulting structurally hosted mineral assemblage will have its own unique set of characteristic such as structural deformations, mineralogy, geochemistry, fluid inclusions and isotopic signature which can be used in conjunction with other fault populations to characterise, on a deposit scale or regional scale, individual faults and their subsequent tectonic histories.

Oxygen isotope geochemistry, in association with other investigative techniques (such as, C, S, D/H, Rb/Sr and Pb isotopes, fluid inclusions and mineragraphy) is an excellent tool for investigating fault controlled hydrothermal ore deposits. Oxygen isotope data can give valuable information on the temperature of mineral deposition, source(s) of hydrothermal fluids and the extent of water–rock interaction (e.g. Taylor 1967, 1974, 1979). In particular, oxygen isotopes have been used successfully to investigate the origin and evolution of fluids in a variety of settings such as volcanic-hosted massive sulphide deposits (e.g. Green 1983, Munha et al. 1986), tungsten and lead–zinc skarns (e.g. Bowman et al. 1985, Shimazaki & Kusakabe 1990), mesothermal Ag–Pb–Zn districts (Lynch et al. 1990) and modern geothermal systems (e.g. Truesdell 1984).

Carbon isotopes have not been used as extensively in ore deposit research as the other stable isotopes (H, O, and S) because the carbon-bearing minerals usually post data the main stages of mineralisation (Kerrich 1987). Nevertheless, investigation of C isotopic composition of carbon bearing species in ore deposits and geothermal systems may provide valuable hydrologic and geochemical information.

Oxygen and carbon isotopes from carbonate minerals could prove most helpful in the interpretation of fault histories in western Tasmania, as carbonate mineralogies have been associated extensively with both Cambrian and Devonian mineralisation. Hydrothermal carbonates from both mineralising events have distinctly different isotopic signatures and could be employed in differentiating Cambrian and Devonian structures as well as unravelling complex fault histories due to reactivation. If this succeeds an attempt will be made to interpret the data in terms of fluid circulation models for both Cambrian VHMS style alteration and Devonian granite related mineralisation. The isotopic signature of regional scale structures has the potential to produce a model for crustal scale fluid flow in both Cambrian and Devonian events. This type of modelling has been tried with some success in the Canadian Cordillera (e.g. Nesbitt et al. 1986, Kyser et al. 1986, Kerrich 1977, 1987, Kerrich et al. 1984).

RESEARCH INVESTIVATION

This report presents the preliminary findings of a stable isotopes investigation into fault histories and mineralisation of Cambrian and Devonian faults in western Tasmania. The report has been divided into two sections that deal with specific types of stable isotope work undertaken and places these findings into context with previous investigations from western Tasmania.

Part 1 deals with oxygen isotope investigations of quartz mineralisation in faults in western Tasmania and presents a summary of the research findings thus far and recommendations for future research.

Part 2 discusses carbon and oxygen isotope investigations of fault hosted carbonate mineralisation in western Tasmania and presents a summary of the research findings thus far and recommendations for future research.

This investigation aimed to test the structural history of a number of faults from the Pieman River to the Murchison Dam (Figs 1, 2 and 3) to differentiate those faults which had been active during the Cambrian from those which were reactivated in the Devonian, together with Devonian faults with no Cambrian movement. The structural history of these faults was to be tested using both isotopic and chemical signatures of the veins associated with faulting. This approach to testing the tectonic models proposed in the initial study, AMIRA project P291, was based on the knowledge that Cambrian ore

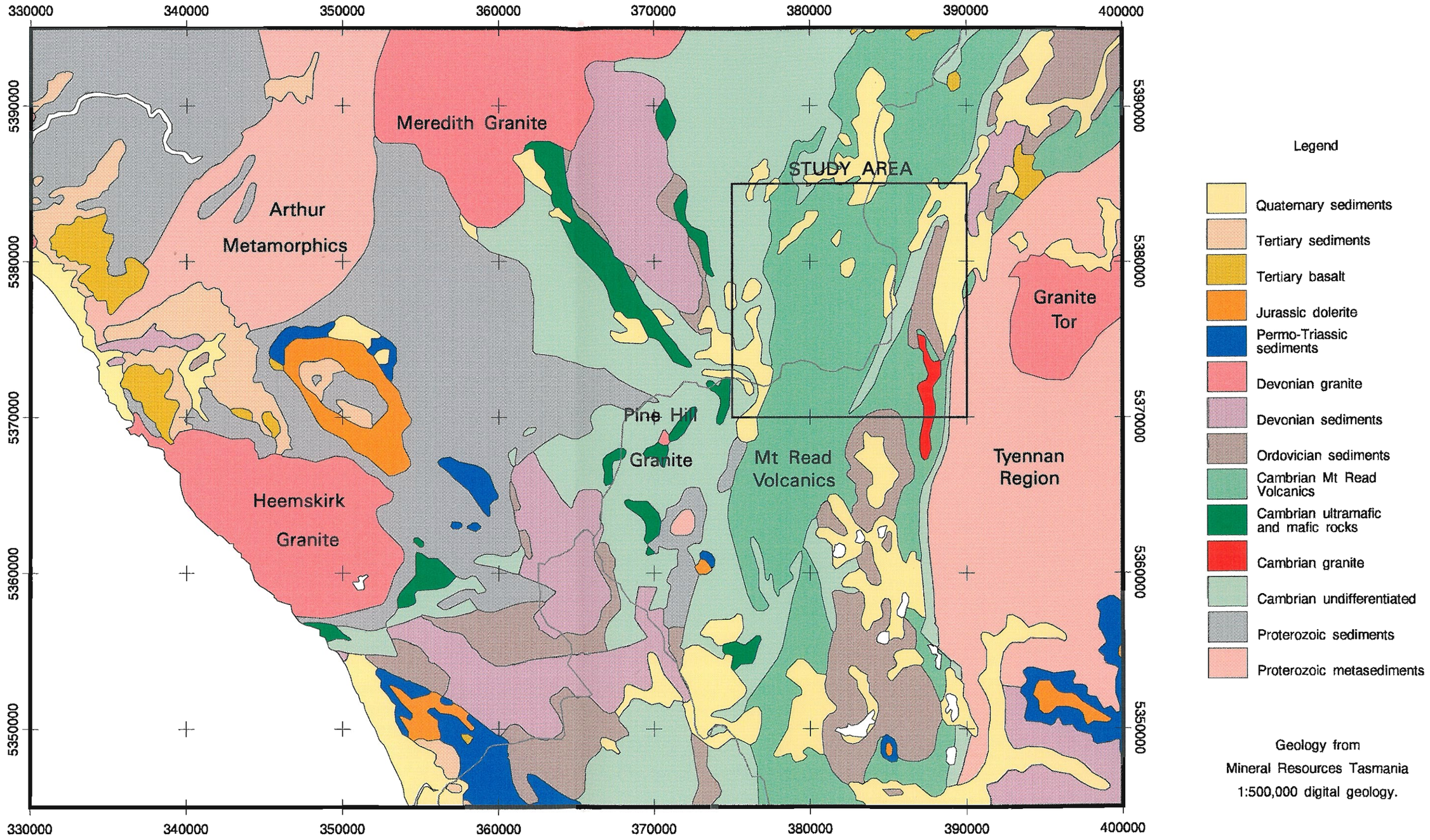

Geology from
Mineral Resources Tasmania
1:500,000 digital geology.

Scale: 1:250,000

0 5 10 15 20 25

km

Grid: Australian Map Grid, Zone 55.

WESTERN TASMANIA
GEOLOGY

Figure 1

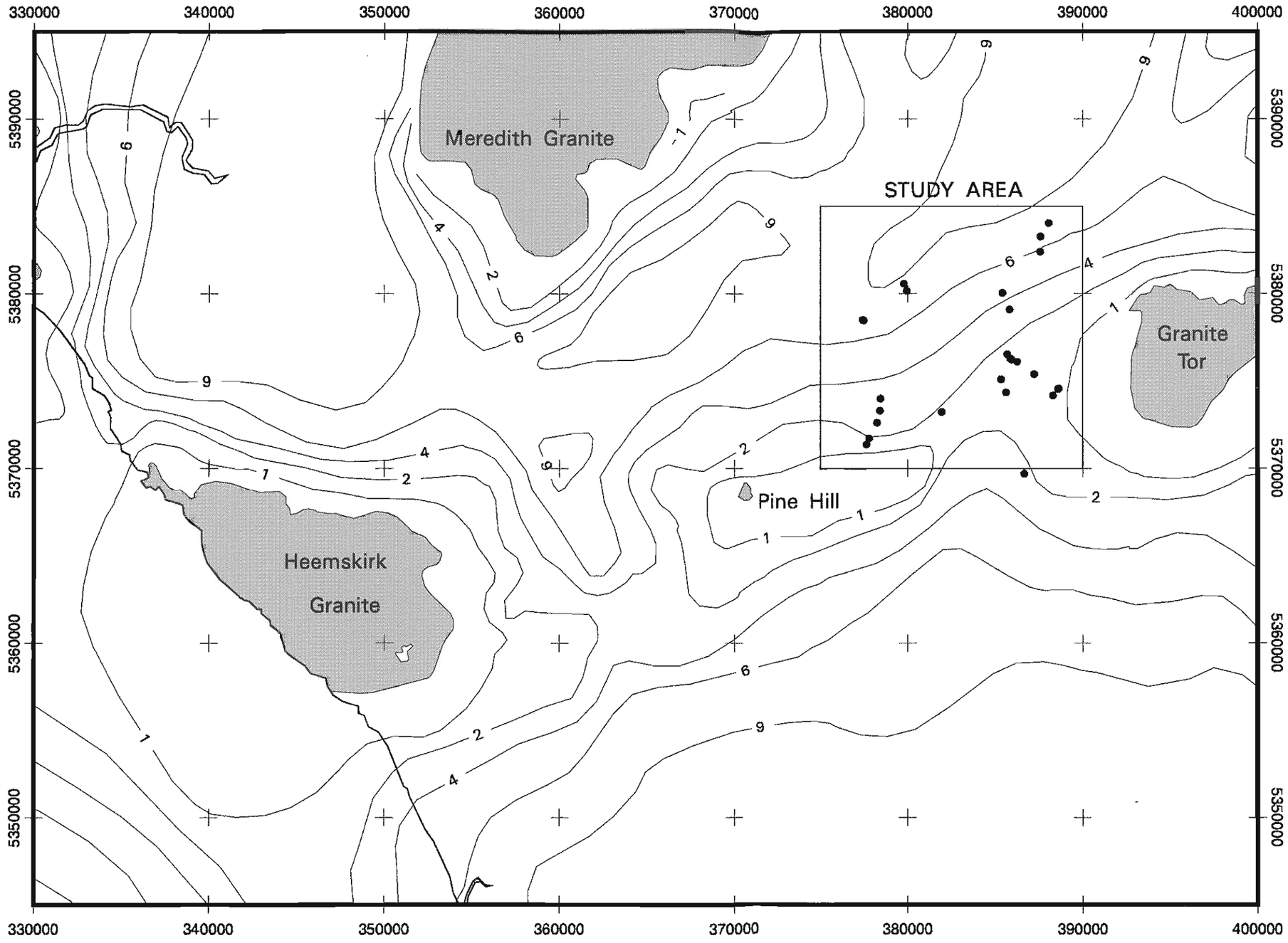

• Sample Locations

Granite contours interpreted from gravity data.
From Leaman and Richardson, 1989.
Depth contours in km.

Scale: 1:250,000

0 5 10 15 20 25

km

Grid: Australian Map Grid, Zone 55.

WESTERN TASMANIA CONTOURS OF DEPTH TO DEVONIAN GRANITE

Figure 2

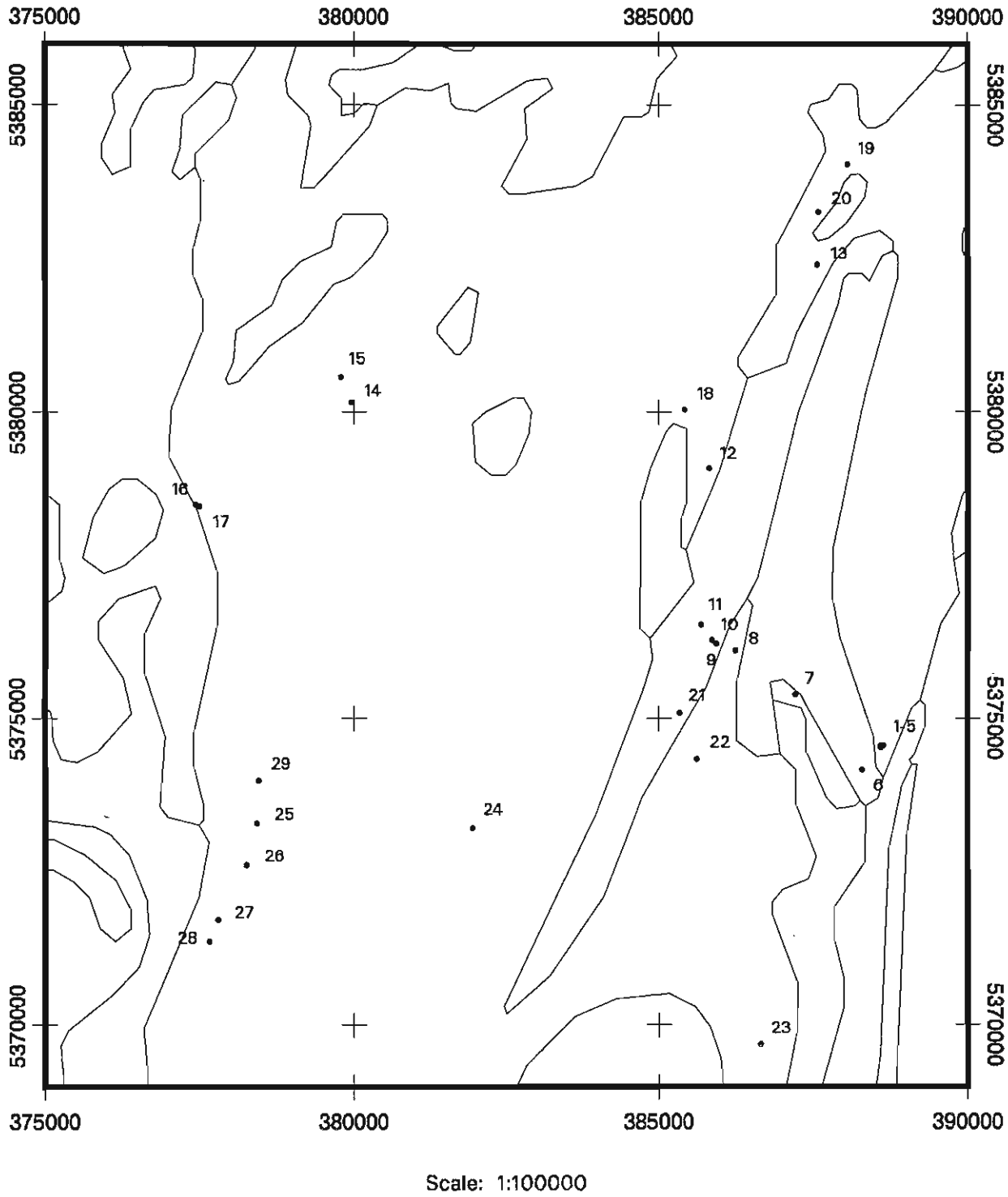

FIG. 3 — Sample location points from the study area. See Appendix 1 for detailed description of samples, isotopic analyses and exact co-ordinates.

fluids have different carbon and oxygen isotope signatures compared to Devonian ore fluids. The rationale, therefore, implies that fluids of different compositions were circulating through the major fault structures during the different phases of deformation and minerals precipitated by these circulating fluids should have characteristic geochemical and isotopic signatures. An assumption was made that minimal seawater circulation took place during the Devonian Tabberabberan uplifting event but significant seawater circulation occurred during Cambrian times, even distal to mineralisation.

PART 1

OXYGEN ISOTOPES IN QUARTZ FROM FAULT STRUCTURES

INTRODUCTION

The premise to undertaking an oxygen isotope investigation into variability in $\delta^{18}O_{qz}$ values arose from preliminary investigations at the Renison Tin Mine that indicate a fault controlled magmatic fluid, associated spatially and temporally with the Devonian Pine Hill Granite, was responsible for the zoned Renison–Dundas mineral field (Kitto 1993). The $\delta^{18}O_{qtz}$ values illustrate systematic zonal changes sympathetic with the observed metal zonations. These conclusions were based on geophysical, mineralogical and isotopic evidence.

As $\delta^{18}O_{qz}$ values from fault structures within the designated field area could assist in the recognition of the histories of the various fault generations and reactivations. Samples were analysed at the University of Tasmania by Gerrit Kuipers, using standard BrF_5 conversion techniques, after Clayton & Mayeda (1962). The reproducibility of the oxygen isotope analyses was within ±0.2‰ for the analysed samples.

Faults, Fluids and Mineralisation

The genesis of many zoned ore districts is thought to be intimately associated with mesothermal granitic intrusions. Ascending hydrothermal fluids are believed to evolve via changes in temperature, pressure and chemistry both temporally and spatially during fluid migration along fissures. This can result in the deposition of different suites of minerals in nested, concentric zones at increasing distances from a granitic source. The causes of regional metal zonation are still being debated however, as the complexities inherent in such hydrothermal systems are numerous and poorly understood (e.g. Kutina 1963, Pouba & Stemprok 1970, Ruxton & Plummer 1984, Gilbert & Park 1986). Highly fractionated, volatile-rich, magmatic intrusions have been proposed as the source of both ore-forming fluids and ore metals (Burnham 1967, Whitney 1975, Taylor et al. 1984, Pollard & Taylor 1986). Such bodies also provide the heat required to circulate externally-derived hydrothermal ore fluids (Burnham 1979, Lehmann 1990). Base metal zonation could result, therefore, from a systematic change in the physico-chemical conditions affecting a single ore fluid as it migrates from its granitic source. Alternatively, it could result from the mixing of magmatic fluids and hydrothermal solutions of different origins, e.g. meteoric, metamorphic, seawater or connate waters (Kelly & Tuneaure 1970, Kelly & Rye 1979, Patterson et al. 1981, Jackson et al. 1982, Sun and Eadington 1987, Lehmann & Mahawat 1989). Ore deposition and zonation may also be influenced by fluid–rock interactions between the magmatic-hydrothermal fluids and the country rocks (Heinrich & Eadington 1986).

$\delta^{18}O_{qz}$ at Renison

Renison is the world's largest operating underground tin mine and as such has provided a unique opportunity to study a large, accessible, and economic paleo-hydrothermal system.

Structural investigations have shown that the forceful emplacement of a volatile-rich Devonian granitic magma modified the regional stress field around Renison and structurally prepared the overlying sediments, via extensive normal faulting. The first, second and third order fault structures were the focus for metal-rich hydrothermal brines which reacted with the late Precambrian to early Cambrian dolomite horizons and resulted in significant carbonate replacement (tin-rich) ore bodies.

A number of traditional investigative techniques (i.e. petrology, mineralogy, fluid inclusions, stable and radiogenic isotopes) were integrated to better evaluate the genesis of the cassiterite–sulphide mineralisation at Renison. In particular, oxygen isotope and fluid inclusion studies have demonstrated that the main stage ore fluids interacted only minimally with the host sediments on ascent, before the hydrothermal fluids reacted with the host dolomite horizons and produced stratabound sulphide mineralisation. Oxygen isotope signatures for quartz from the main stage mineralisation (quartz–arsenopyrite–pyrrhotite–cassiterite) on the

Federal–Bassett Fault show a systematic increase from +11.2‰ to 17.1‰ within the fault structure and clearly illustrate the focussed nature of the ore fluids; the hydrothermal palaeoflow directions; the sites of economic Sn mineralisation; and a correlation between $\delta^{18}O_{qtz}$ quartz values and telescoped mineral zonation as the mineralised fluids cooled outward along fault structures distal to the underlying granite intrusion (Kitto 1993).

$\delta^{18}O_{qz}$ in Renison–Dundas District

Based on the success of the $\delta^{18}O_{qtz}$ investigation at Renison a preliminary analysis of samples from the Renison–Dundas mineral district was undertaken to assess the usefulness of $\delta^{18}O_{qtz}$ values for evaluating mechanisms of ore deposition and metal zonation (W–Sn–Cu–Au–Pb–Ag–Zn) on a district scale.

Before presenting the results of this investigation it would be prudent to discuss granite related styles of mineralisation associated with the Heemskirk–Pine Hill–Granite Tor region.

Granite Related Mineralisation In Western Tasmania

The intimate association between Devonian granites and tin mineralisation in Tasmania, and in particular western Tasmania, has long been recognised (Twelvetrees 1900, 1906, Waller 1902, Loftus Hills 1921, Reid 1925). Two northeast trending corridors of tin mineralisation, with Ag–Pb–Zn haloes, occur in western Tasmania (Fig. 4). These trends, interpreted from residual gravity surveys (Leaman et al. 1980), occur along the northern and southern margins of a large "batholith" of Devonian granite (Fig. 4; inset). The operating Renison mine, and the former tin mines of Razorback, and Grand Prize together with a tin prospect at Queen Hill and St Dizier, occur along the southern margin. A number of tin and tourmaline-bearing deposits, as well as Ag–Pb–Zn vein deposits at Zeehan, Dundas and Mount Farrell, occur within a zone outlined by the northeast trending granite ridge (Figs 2, 5). A number of these deposits are closely associated with major faults (e.g. Henty Fault and Rosebery Fault) and suggest the direct involvement of the granite ridge in the formation of and/or mobilisation of mineralisation along Cambrian and/or Devonian fault structures (Taheri & Green 1990, Khin Zaw 1991).

Zeehan Mineral Field

In the zoned Zeehan mineral field, east of the Heemskirk granite (Fig. 4), most Ag–Pb–Zn veins are genetically associated with, and centred on the Queen Hill–Severn massive sulphide–cassiterite deposit above an apophysis in the Heemskirk Granite (Lutley 1975, Solomon 1981, Collins & Williams 1986, Collins *et al.* 1989, Leaman & Richardson 1989, Solomon & Groves 1994). The highest silver:lead ratios all occur within 2km of this focus (Solomon 1981, Collins & Williams 1986, Green 1990). The steeply dipping ore shoots trend between NNW and NNE and are hosted by veins that intersect Proterozoic to Early Devonian sediments. The west to east zoning of the pyritic to sideritic ores, thought to be related to the thermal environment established by the Heemskirk Granite (Both & Williams 1968, Both et al. 1969, Stanton 1972) are now considered to result from increased f_{CO2} in the ore fluids around Queen Hill, due to dissolution of carbonates or mixing of hydrothermal magmatic ore fluids with CO_2-rich ground waters (Solomon 1981, Collins & Williams 1986, Solomon & Groves 1994).

Farrell Mineral Field

In the Farrell mineral field, west of Granite Tor (Fig. 4), a number of small vein style Ag–Pb–Zn orebodies occur with a NNE trend, along a 14 km strike length of the Cambrian Farrell Slates, as two distinct fracture zones associated with the Henty Fault (Brooks 1962 Rivers 1975, Pŏlya et al. 1986). Mineralisation associated with emplacement of the Devonian Granite Tor intrusion consists of an inner zone of pyrite–arsenopyrite–pyrrhotite–cassiterite–quartz and an outer argentiferous galena and sphalerite zone with minor pyrite ± chalcopyrite ± arsenopyrite ± jamesonite and tetrahedrite in a quartz and siderite gangue (Polya et al. 1986, Collins et al. 1989). Taheri & Green (1990) reported that the highest temperature minerals (Sn zone) occurred directly above the Granite Tor ridge 1km from its buried surface and that the Ag–Pb–Zn dominated mineralisation was located at least 3 km away from the granite–sediment interface.

A Cambrian volcanogenic origin has been suggested for the Farrell Lodes (Solomon 1981, Polya et al 1986) but lead isotope compositions (Gulson & Porritt 1987) and zinc/lead ratios (Large & Huston 1986) discount this possibility and confirm a Devonian age for mineralisation.

The Lakeside and Sterling Valley tin prospects in the Farrell Field, described by Taheri and Green (1990), have an unusual gold–tin mineral association. This contrasts with the majority of Sn and Ag–Pb–Zn rich deposits in the Dundas Trough, which are typically gold-poor. The gold-tin association is thought to be related to Devonian vein deposits hosted by, or in rocks overlying the Mount Read Volcanics (Fig. 4) and where the underlying granite ridge is intersected by major faults, such as the Rosebery and Henty faults (Taheri & Green 1990, Herman, pers. comm. 1993).

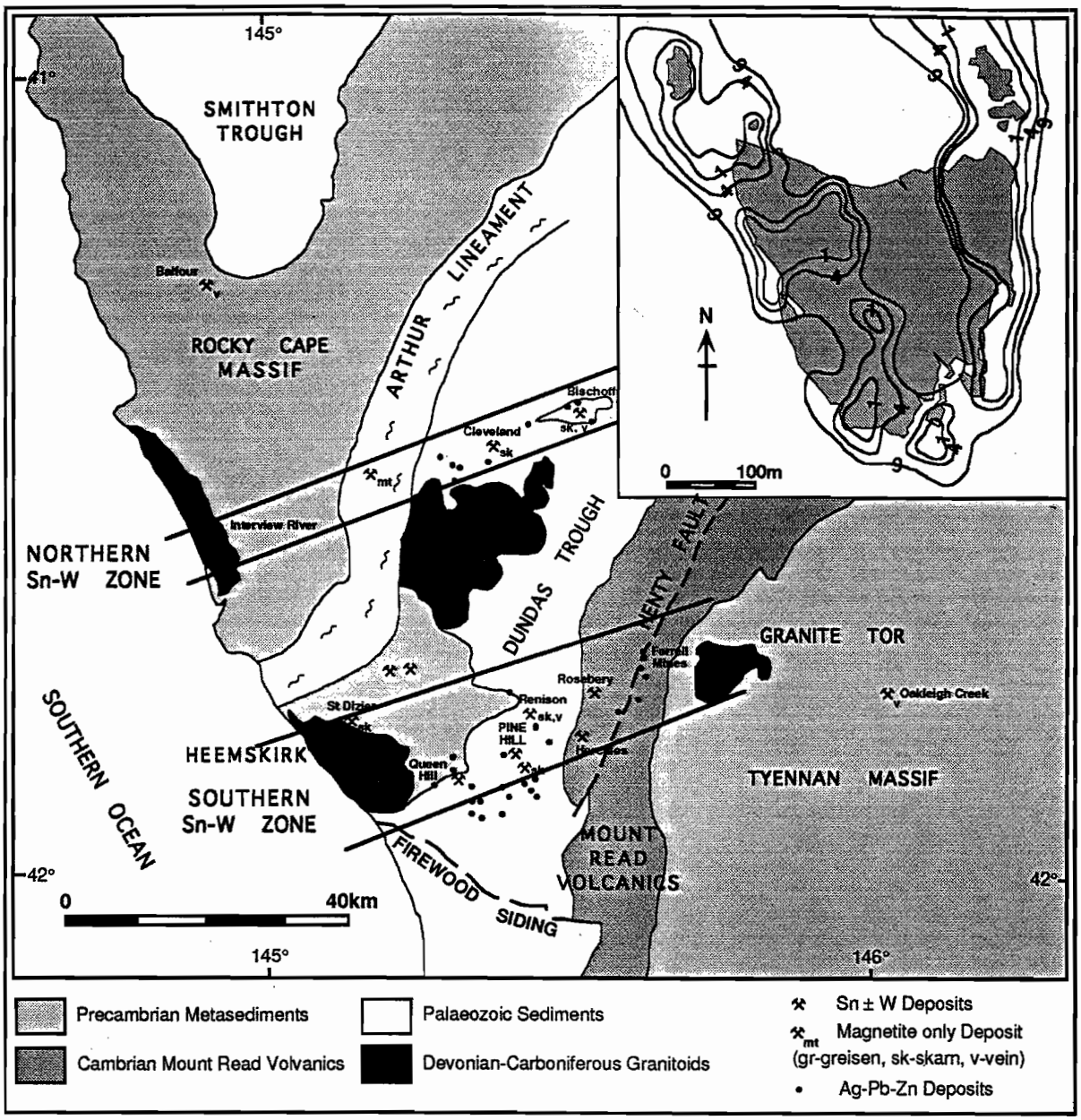

FIG. 4 — Western Tasmania and the position of the 'Devonian Batholith" together with the NNE trending zones of mineralisation.

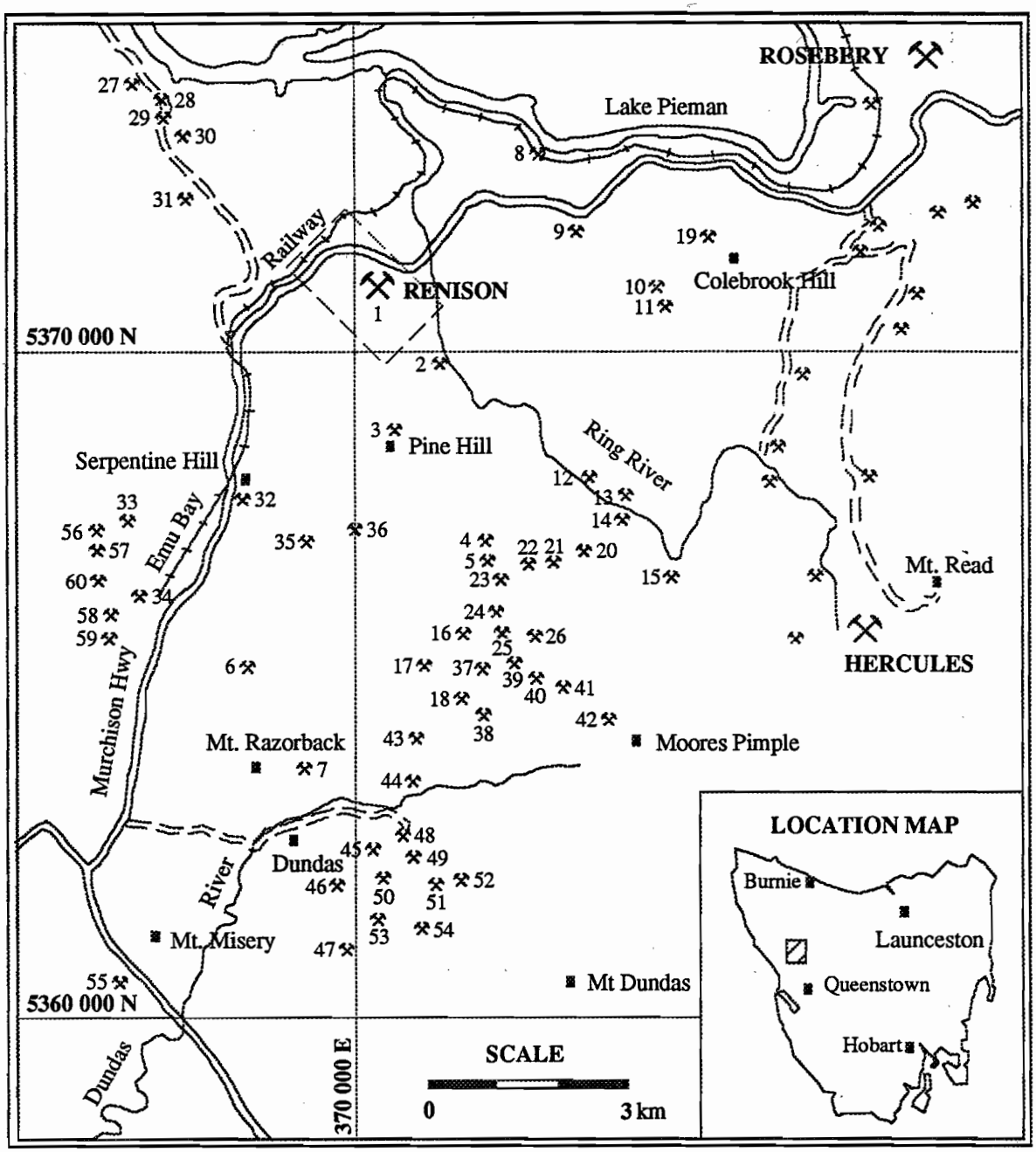

FIG. 5 — Location map of the mines and prospects in the Renison–Dundas mineral field. See Table 1 & 2 for details of the mineralogy and structural controls to ore deposition.

A hypothetical model to explain the gold–tin association might invoke deeply circulating, fault controlled, Devonian granite related hydrothermal fluids remobilising gold from the Mount Read Volcanic succession and depositing it together with the more typical Devonian vein styles of mineralisation.

Renison–Dundas District

Mineralisation in the Renison–Dundas district (Fig. 5) has a well defined zonal distribution. Previous investigators have noted the existence of a weak metal zonation with a central tin zone surrounded by a discontinuous zone of minor copper–silver and lead–zinc deposits, but details of the exact nature of this mineral field have not been forth coming (Blissett 1962, Groves 1968, Patterson 1979, Herman & White 1989). Kitto (1993b, 1994) was the first to recognise and discuss the intimate association between metal zonation and the shape of the Pine Hill Granite intrusion.

The Renison–Dundas mineral field covers an area of approximately 200 km^2, and occurs south of Lake Pieman to a line east of the Murchison Highway from Misery Hill to Mt Dundas, and includes the abandoned mining townships of Renison Bell and Dundas (Fig. 5). The Pine Hill Granite outcrops in the central-northern region of this mineral field. Mining operations have occurred discontinuously since the discovery of the field in the late 1880s and early 1890s. The largest period of mining activity occurred prior to World War I when the Dundas township was one of the largest in Tasmania. Since that time sporadic mining operations have occurred but the Renison Tin Mine is the only fully operational mine in the district today. A number of small-scale operations still extract secondary minerals such as crocoite ($PbCrO_4$) and cerussite ($PbCO_3$) for sale to gem collectors (e.g. Adelaide Mine, Red Lead Mine). Specimen quality, purple bladed axinite is also collected from an opencut at Colebrook Hill.

Mineralogical and structural details on each of the sixty identified mines and prospects located in the Renison–Dundas district have been summarised in Tables 1 and 2. Much of the information tabulated has been obtained from past geological records (e.g. Montgomery 1986, Twelvetrees 1900 & 1906, Waller 1902, Reid 1925, Elliston 1950, Blissett 1962, Forsythe 1969, Herman & White 1989) and from visits to the majority of these mines and prospects. A number of generalisations can been made regarding mineralisation in the Renison–Dundas district.

Structural Controls on Mineralisation

All of the deposits in the district are associated with or occur as fracture filled fissure veins or as mineralised breccia zones. Two major structural trends hosting mineralisation are immediately obvious from Table 1. These structural trends consist of sets of major NW- and NNE-trending faults that act as hosts to mineralisation (Reid 1925, Blissett 1962). These fault sets are interpreted as extensional conjugate faults that developed above the flattened roof zone of the Pine Hill Granite batholith during emplacement of that body. Structural contours for the granite–sediment contact in the area highlights the flat topped nature of the batholith and the distribution of ore deposits along the margins of the granite.

The NW-trending set of faults are the preferential sites for mineralisation. They are normal to the minimum compressive stress (S_3) during granite emplacement and were dilated by the high fluid pressures associated with mineralisation.

Major mineralised faults observed at the South Comet Mine (No. 54, Fig. 5, Tables 1, 2) and at the Curtin Davis Mines (Nos 21–26, Fig. 5, Tables 1, 2) have kinematic indicators which suggests that initial dip-slip movement was followed by dextral reactivation. This scenario is similar to Renison where initial dip slip movement associated with granite emplacement is overprinted by a dextral reactivation of the Federal–Bassett Fault as the granite related stress field decayed and the regional Devonian Tabberabberan stress field began to dominate. At Renison this strike slip reactivation produced a dilational jog in the Federal–Bassett Fault which contains the major Federal orebody. The orientation of S_3 in the Renison–Dundas mineral field, associated with dilation of the northwest trending faults is consistent with the conclusions drawn from the Renison deposit. District scale mineralisation occurred under similar conditions to those recorded at Renison and is associated with the emplacement of the Pine Hill Granite.

Mineralised veins occurs in brittle shear zones, and in the case of the Curtin Davis deposits along bedding-controlled dilation zones in the hinges and limbs of tightly folded sediments. Vein textures and kinematic indicators, similar to Renison, indicate that mineralisation and deformation which caused the vein-hosted shear zones, developed synchronously at low mean stress due to high fluid pressures.

The large majority of vein deposits in the district contain steeply plunging ore shoots located at the intersection of two sub parallel fault planes (e.g. South Comet Mine, Bartlett 1993). Because of the undulating nature of the fault surfaces the steeply plunging ore shoots pinch and swell, are discontinuous along strike and do not extend more than a few hundred metres down dip. This style of deposit has made mining on a large scale difficult. Most veins are too small to be economic.

Table 1 — Prospects and mines from the Renison–Dundas mineral field and a list of their styles of mineralisation together with their structural trends. Filled circles, crosses and open circles represent major, intermediate and minor commodities at each prospect.

No.	DEPOSIT NAME	1	2	3	4	5	6	7	8	Sn	W	As	Cu	Sb	Bi	Pb	Zn	Ag	Au	Ni	TREND
	Sn DEPOSITS																				
1	Renison District		X		X				X	•	o	X	X		o	o	o	o		o	NW
2	Karlson Riley			X	X					•		X	o						o		NW
3	Penzance	X			X					•	X	X									NW
4	Fraser				X					X		•	•	o	X	o	o	X	o		NNW/NNE
5	Greens		X	X	X				X	•	X	X	X	X		X	X	o	o		NW/NNE
6	Grand Prize			X	X					•		X	o								NNW
7	Razorback		X	X	X					•		o				o	o			o	NNW
8	Exe River				X					•		X	X								NNW
9	X Proprietary				X				X	•	o	X	X								NNW
10	Olympic				X					•		X									NNW
11	Athena				X					•		X									NW
	Cu DEPOSITS																				
12	Bonnie Dundee				X				X	o		X	•	•				•			NNE/NNW
13	Fahl				X		X	X	X			X	•	X	X	X		•	o		NNW
14	Rich P. A.				X			X	X			X	•	X	X			•			NNW
15	Svengali							X					•	X		o		•			NW
16	Hecla							X	X	o	o	X	X	•	•	X	X	•			NNE
17	Great Northern Creek					X		X	X	o	o	X	X	•		•	X	•			NNW
18	Ramdale						X						X	X		•	X	•			NNE
19	Colebrook Hill		X							o		o	•	o		o	o				N-S
20	Blocks 291						X	X	X			X	•	X	X	•	X	•	o		NW
21	Curtain Davis							X	X	o		X	•	X	X	•	o	•	o		NNW
22	Curtain Davis Extended							X					X	o	X	•	X	•			NNW
23	Crown Curtain Davis								X			X	X	•	X	o		•	o		NNE
24	S. W. Curtain Davis							X	X			X	•	•	X			•			NNE/NNW
25	South Curtain Davis							X	X	o		X	•	•	X	•	X	•			NNW
26	No.1 Curtain Davis						X	X	X	o		X	•	•	X	X	X	•	o		NNW
	Pb-Zn DEPOSITS																				
27	Success Extended							X				o	o			•	o	•			NW
28	Bon Accord							X								•		•			NW
29	Owen Meridith							X								•		•			NW
30	Success							X								•		•			NW
31	Poseiden							X					X			•		•			NNW
32	Argent Tunnel					X										•		•			E
33	Lead Blocks							X								•	X	•			NNW
34	McKinnie							X								•		•			N
35	Melba					X								X		•	X	•			NW
36	Kapi			X												•	X	•		o	NNW
37	Evendon					X		X		o		X	o		o	•	X	•			NNW
38	Carbine					X		X					X	X		•	X	•			NNW
39	Curtain Davis Consol					X			X	X		X	o	X	o	•	X	•	o		NNW
40	Scout Hut (Higgins)				X				X			o	X	o		•	X	•			NNE
41	Wallace				X		X		X	X		X	X	•		•	X	•	o		NNW
42	Moores Pimple			X				X					o			•	X	•			NNW
43	Unnamed Prospect							X								•	X	•			NNW
44	North Comet				X																NNW
45	West Comet							X								•	X	•			NNE
46	Adelaide			X				X						X		•	X	•			NNW
47	Red Lead			X				X						X		•	X	•			NNW
48	Comet			X				X				o	o	o		•	X	•			NW
49	Maestries			X				X				o	o	o		•	X	•			NNW
50	Platt			X										o		•	X	•	o		NW
51	Banner Cross							X						X		•	X	•			NNW
52	Ainslie					X		X						o		•	X	•			NW
53	Kominski					X		X				o		o		•	X	•			NW
54	South Comet							X					o	o		•	•	•			NNW
55	Mt. Misery		X						X				o			•	X	•			NE
	Cu-Ni DEPOSITS																				
56	Genets			X									•							•	N
57	North Cuni			X									•							•	N
58	Vaudeau			X									•							•	N
59	Nickel Reward			X									•							•	N
60	South Cuni			X									•							•	N
		GREISEN	CARBONATE REPLACEMENT	ALTERED ULTRAMAFICS	QZ VEINS - asp, py, po etc.	QZ STRINGERS - py, gn, sph etc.	MASSIVE/VEIN - jamesonite	MASSIVE/VEIN - siderite	WALLROCK BRECCIA - asp ± py												

Table 2 — Prospects and mines from the Renison–Dundas mineral field and a list of their mineralogies.

No.	DEPOSIT NAME	1	2	3	4	5	6	7	8	9	10	11	12	13	14	15	16	17	18	19	20	21	22	23	24	25	26	27	28	29
	Sn DEPOSITS																													
1	Renison District	•	•	•	•	•	•	•				•	•	•	•			•	•											
2	Karlson Riley		•	•	•	•		•																						
3	Penzance	•	•	•	•	•	•	•																						
4	Fraser	•	•	•	•	•		•				•		•				•												
5	Greens		•	•	•	•						•			•			•	•											
6	Grand Prize		•	•	•	•		•											•											
7	Razorback		•	•	•	•		•											•											
8	Exe River	•	•	•	•	•		•				•																		
9	X Proprietary	•	•	•	•	•	•	•																						
10	Olympic		•	•	•	•		•																						
11	Athena		•	•	•	•		•																						
	Cu DEPOSITS																													
12	Bonnie Dundee		•	•	•				•			•				•													
13	Fahl		•	•	•			•	•		•	•			•		•													
14	Rich P. A.		•	•				•	•		•	•																		
15	Svengali		•		•				•			•			•		•													
16	Hecla		•	•	•			•	•			•		•	•		•	•		•										
17	Great Northern Creek		•		•			•	•		•	•		•	•		•			•										
18	Ramdale				•				•		•	•		•	•															
19	Colebrook Hill		•	•	•			•	•			•		•	•		•	•										•	•	
20	Blocks 291		•		•				•		•	•			•		•													
21	Curtain Davis		•	•	•			•	•		•	•		•	•		•			•										
22	Curtain Davis Extended				•				•			•		•	•		•			•										
23	Crown Curtain Davis				•			•	•			•									•									
24	S. W. Curtain Davis		•	•	•			•	•			•		•			•			•	•	•								
25	South Curtain Davis		•		•			•	•		•?	•		•	•		•													
26	No.1 Curtain Davis		•		•			•	•		•	•		•	•		•	•		•										
	Pb-Zn DEPOSITS																													
27	Success Extended		•		•			•				•		•	•	•	•						•							
28	Bon Accord														•		•													
29	Owen Meridith														•		•													
30	Success														•		•													
31	Poseiden											•			•		•													
32	Argent Tunnel		•												•									•	•					
33	Lead Blocks		•											•	•		•													
34	McKinnie		•												•		•													
35	Melba				•						•			•	•								•			•				
36	Kapi		•	•	•									•	•		•													
37	Evendon		•		•							•		•	•		•													
38	Carbine		•		•				•		•	•		•	•		•													
39	Curtain Davis Consol		•		•			•			•?	•		•	•															
40	Scout Hut (Higgins)		•		•			•			•	•		•	•															
41	Wallace		•		•			•			•	•		•	•															
42	Moores Pimple				•							•		•	•															
43	Unnamed Prospect													•	•		•													
44	North Comet		•		•																									
45	West Comet														•		•							•						
46	Adelaide				•						•			•	•		•							•			•			
47	Red Lead				•						•			•	•		•							•			•			
48	Comet				•			•						•	•		•										•			
49	Maestries											•		•	•		•										•			
50	Platt										•			•	•									•	•					
51	Banner Cross		•		•						•			•	•		•													
52	Ainslie		•		•									•	•		•													
53	Kominski		•		•							•		•	•		•													
54	South Comet				•						•	•		•	•		•													
55	Mt. Misery				•									•	•															
	Cu-Ni DEPOSITS																													
56	Genets			•								•																		•
57	North Cuni			•	•							•																		•
58	Vaudeau			•	•							•																		•
59	Nickel Reward				•							•																		
60	South Cuni			•	•							•																		•
		TOURMALINE	QUARTZ	PYRRHOTITE	PYRITE	CASSITERITE	WOLFRAMITE	ARSENOPYRITE	TETRAHEDRITE	TENNANTITE	JAMESONITE	CHALCOPYRITE	STANNITE	SPHALERITE	GALENA	SILVER (native)	SIDERITE	MARCASITE	TALC	BISMUTHINITE	CHLORITE	MAGNETITE	STIBNITE	CROCOITE	PYROMORPHITE	EPIDOTE	CERRUSITE	AXINITE	ACTINOLITE	PENTLANDITE

Styles *of Mineralisation in the Renison–Dundas District*

Mineralisation in the Renison–Dundas district consist of the following overlapping types of deposits (Tables 1, 2):

(i) tin-rich deposits,
(ii) copper–antimony–silver deposits,
(iii) lead–zinc–silver deposits,
(iv) copper–nickel deposits.

The most important commodity mined is tin. Tin was mined from a range of deposit styles but the largest ore bodies are represented by the Renison style of stratabound carbonate replacement and related fault and fracture styles of mineralisation. At the turn of the century, however, argentiferous antimonial–copper–lead lodes called 'fahl-ore' and argentiferous lead–zinc ores were also mined successfully in the district from a number of NNW/NNE trending fissure lodes. The copper–nickel deposits at Cuni (Nos 56–60, Fig. 5, Tables 1, 2) were the products of Cambrian mineralisation due to magmatic segregation within mafic dykes. All other styles of mineralisation are associated with the Devonian Pine Hill intrusion which overprints the earlier copper–nickel deposits in the Cuni area. The Cambrian copper–nickel styles of mineralisation will not be discussed further.

Mineralisation in the Renison–Dundas district exhibits a broad telescoped zonation pattern centred upon the Pine Hill Granite (Fig. 6). Leaman and Richardson (1989) consider the Pine Hill Granite to be:

> *"...probably the most important granite in western Tasmania. This granite has introduced an array of mineralisation styles, as well as remobilisation of older volcanic material. Its transverse relationship to the Dundas Trough is probably the critical element. It is almost fully roofed. The roof is irregular and ... mineralisation can be directly correlated to roof form and body distribution.*
> *... zonation studies are likely to be fruitful, as the crest of the intrusion is irregular with key focal points. Renison is presumably one of these."*

The central **tin zone** closest to Pine Hill, with a diameter of approximately 6 km, extends northward and includes the Renison and Exe River deposits together with the Olympic and Athena deposits to the east. The southern extension of this tin zone occurs south of Pine Hill at the Frazer Mine and Green's Prospect. A further separate tin zone approximately 2.5 km in diameter is recognised around both the Razorback and Grand Prize Mines in the southeastern region of the mineral district. A comparison of the tin zones with the granite contours clearly demonstrates an association between proximity to the Pine Hill Granite and apophyses within the roof of the intrusion. Two cross-sections through the Renison–Dundas district (Fig. 7) illustrate the telescoped nature of mineralisation, defined by the mines and prospects in the district, and the close association between mineralisation and distance from the intrusion. Figure 7 (a) is a NNW–SSE cross-section of the Renison–Dundas district through the Renison–Pine Hill–Curtain Davis areas and clearly shows the steep sided nature of the Pine Hill body and the undulating top to the granite–sediment contact. Associated with the intrusion is a telescoped metal zonation that passes from a tin-rich centre, into a copper zone of mineralisation, and out distally into a lead–zinc halo. Figure 7 (b) is a N–S cross-section through both the Pine Hill and Razorback regions, at 370 000 E, and illustrates the close association between tin mineralisation and apophyses in the granite surface in both regions.

In general, it can be inferred from the regional cross-sections of Figure 7 that tin mineralisation in the Renison–Dundas district only occurs within a 1.5 km radius from the Pine Hill Granite–sediment interface. Because uneconomic skarn styles of tin mineralisation occur within the first 500 m of the Pine Hill Granite, initial exploration for economically important 'Renison styles' of tin mineralisation should be undertaken within a 500–1500 m radial distance of the granite contact.

The mineralogy of the deposits within the tin zones have been presented in Tables 1 and 2 and consist of an oxide–silicate stage of mineralisation. This stage of mineralisation consists of tourmalinised sediments around fissure infills containing quartz + arsenopyrite ± pyrrhotite ± pyrite ± cassiterite. Pyrrhotite appears to give way to pyrite outside the thermal metamorphic aureole of the Pine Hill intrusion. Tables 1 and 2 illustrate that the major commodity mined in the tin zone were carbonate replacement styles of mineralisation. Cassiterite deposits with an average grade between 1–2 wt.% were the principal targets, although at the Fraser workings only arsenopyrite was mined.

At the Curtin Davis deposits, which occur on the steep northern face of Godkin Ridge, the oxide–silicate stage has been recognised in the lower most workings, but this has been overprinted by later sulphide and carbonate stages (Herman & White 1989).

A number of the tin deposits (e.g. Razorback, Grand Prize, Karlson-Riley, Greens Prospect) formed as replacement mineralisation along margins of dolomitised Cambrian ultramafic bodies (Table 1). This indicates that the ultramafic bodies and related Cambrian thrusts acted as zones of structural

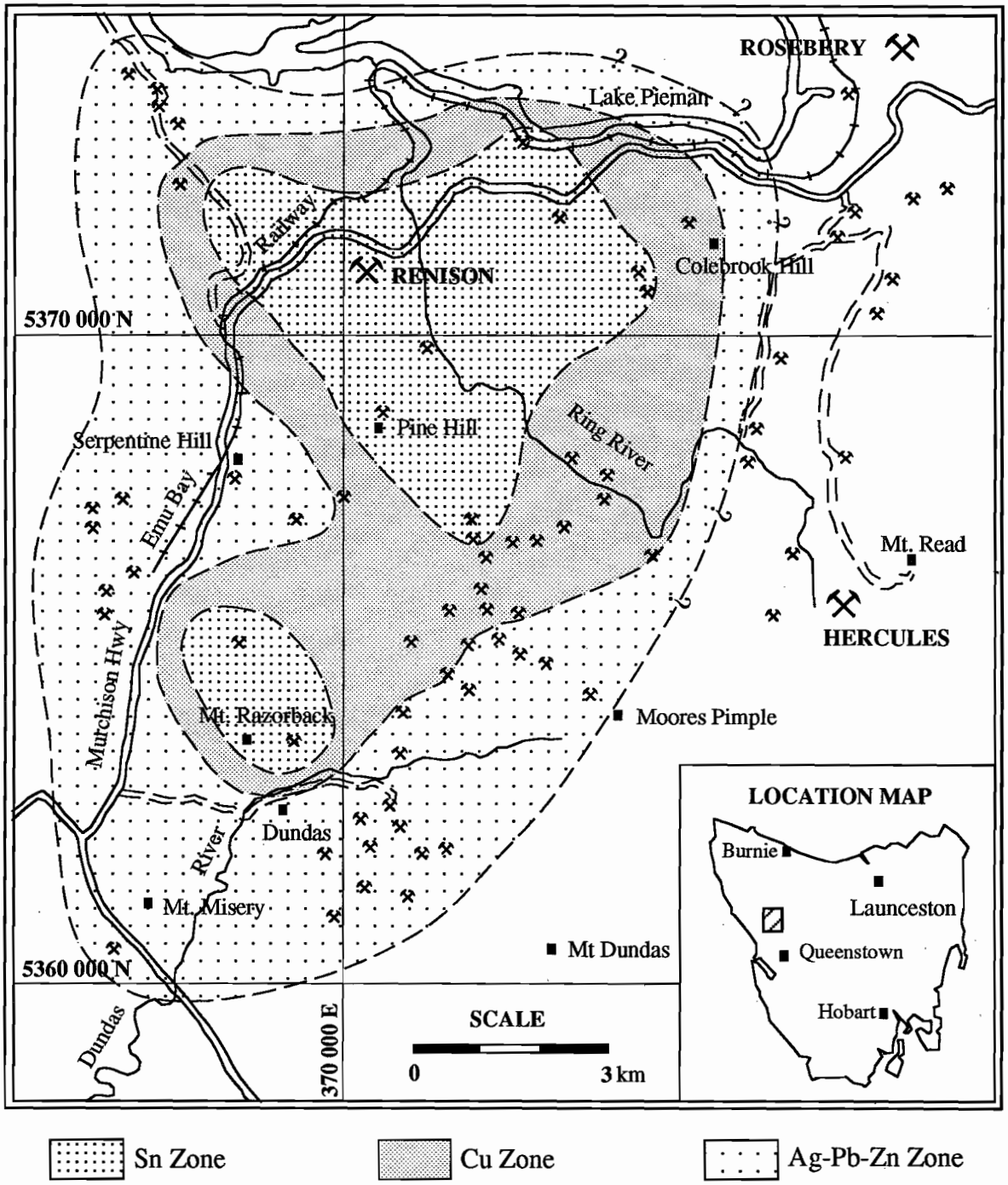

FIG. 6 — Metal zonation in the Renison–Dundas mineral field.

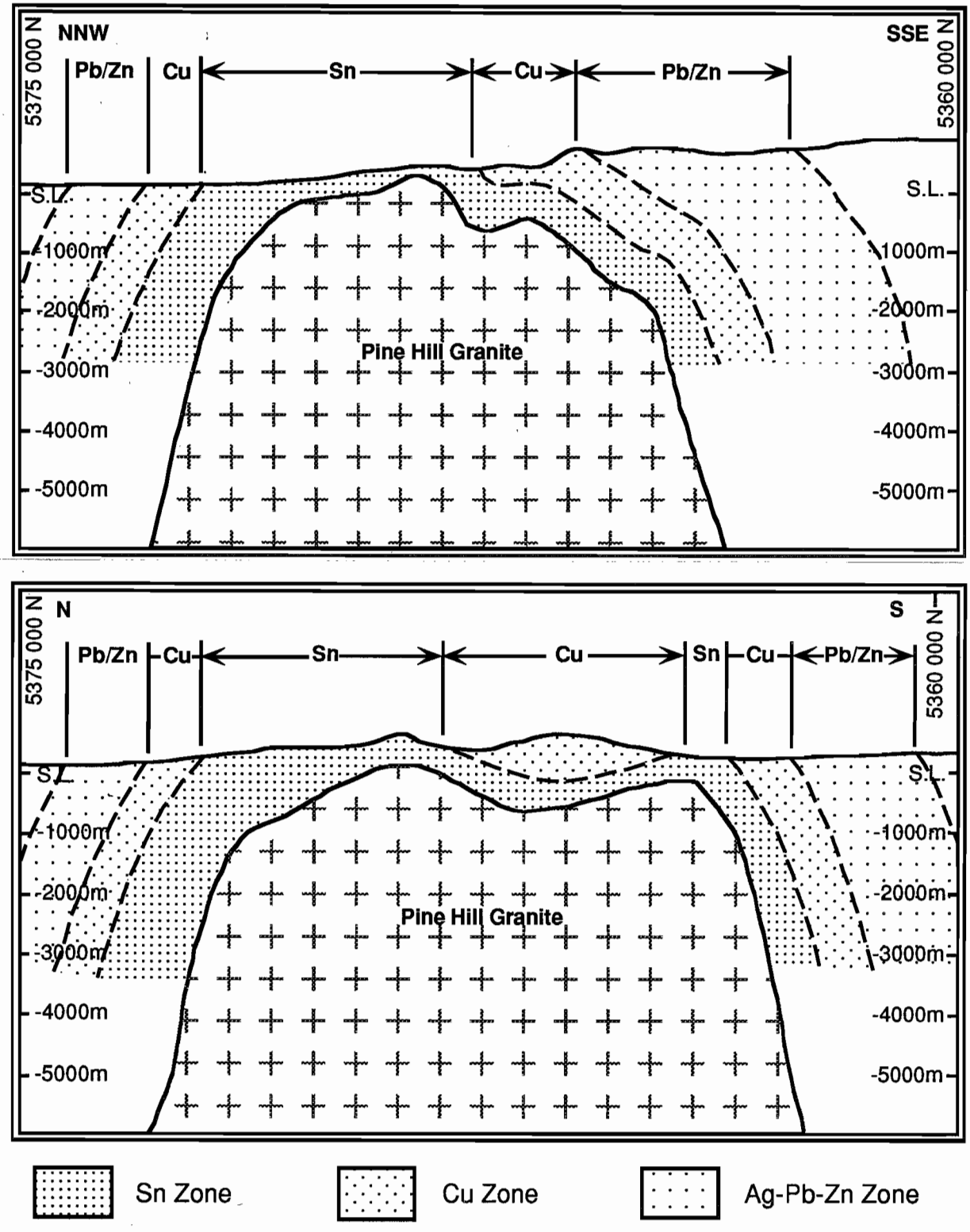

FIG. 7 — Geological cross-sections through the Renison–Dundas mineral field.

weakness and provided a focus for Devonian hydrothermal fluids (Crossing 1991). All of the ultramafic replacement deposits in the district are small scale and presently uneconomic.

Overlapping the central tin zone in the Renison–Dundas district are a number of **copper-rich** deposits that define a 2 km wide annulus of copper mineralisation around the central tin zone (Fig. 6). These deposits include the Curtain Davis workings as well as the Bonnie Dundee, Fahl, Rich P. A., Svengali and Colebrook Hill deposits (Tables 1, 2). The majority of the copper-rich deposits occur along the southeastern margin of the Pine Hill Granite adjacent to the two tin rich areas. The exact significance of this fact is uncertain except to say that it forms an intermediate zone of mineralisation between the central tin zones and the peripheral lead–zinc styles of mineralisation around the Pine Hill Granite. The telescoped nature of the copper mineralisation is shown in Figures 7 (a) and (b) and highlights the fact that copper-rich mineralisation occurs within a zone between 0.5–2 km directly away from the Pine Hill Granite–sediment interface.

The overlapping telescopic nature of mineralisation at the Curtain Davis mines has been briefly described by Herman and White (1989). They recognised that the earliest stage of quartz–arsenopyrite ± pyrite ± pyrrhotite ± cassiterite (equivalent to the oxide–silicate stage of mineralisation) in the lowest levels of the mine workings vary vertically upward into a siderite dominated assemblage containing quartz–pyrite–chalcopyrite–tetrahedrite ± arsenopyrite ± pyrrhotite ± galena ± sphalerite. The sulphides exhibit a variable mode of occurrence from coeval, fine to coarse disseminated inclusions and intergranular fillings in a sideritic gangue, to later cross-cutting veins and stringer styles of mineralisation. Herman & White (1989) interpreted the field associations as representing the vertical upward migration and evolution of a granite derived hydrothermal fluid along dilational open spaced fissures.

Tables 1 and 2 shows that the major commodity in the copper zone is a 'fahl-ore' consisting of tetrahedrite and chalcopyrite. The ore was worked primarily for the silver content of the tetrahedrite which averaged approximately 600 g/t silver (Blissett 1962). The final mineralising event recognised in the copper zone are a series of late stage stringer veins of jamesonite which overprint all previous sulphide stages.

Peripheral to, but overlapping the copper-rich zone is a 3 km wide outer halo of **argentiferous lead zinc deposits** (Fig. 6). The majority of the lead–zinc deposits, like the copper deposits discussed previously, are concentrated along the southeastern margin of the Pine Hill Granite. A number of deposits, however, occur along the western margin of the granite and also overprint the Cuni deposits, and still others occur in the northwestern region of the mineral field. To the east of the Renison–Dundas mineral field Devonian mineralisation overlaps and overprints Cambrian volcanogenic hosted massive sulphide deposits at Rosebery and Hercules. This Devonian overprint is associated with the Heemskirk–Pine Hill–Granite Tor ridge which shallowly underlies the Rosebery district and is expressed by quartz-tourmaline veins along the Rosebery Fault Zone and by a pyrrhotite overprint on portions of the Rosebery and Hercules orebodies (Fig. 5). The complex nature of this relationship has been discussed by Khin Zaw (1991).

The telescoped nature of the lead–zinc mineralisation in the Renison–Dundas mineral field can be seen more clearly in Figures 7 (a) & (b). In these district scale cross-sections it can be inferred that this style of mineralisation occurs within a zone 2–4 km radially outward from the Pine Hill Granite–sediment interface. Within this zone the major producers of silver, and more recently lead and zinc, occur in the southeastern region of the mineral field. The South Comet Mine, for example, started operations in 1911 mining argentiferous galena but was reopened in early 1990 to extract sphalerite left by the earlier operators, and has operated on a small scale employing eight men up until recently. Secondary minerals such as crocoite and cerussite are also mined from this area for sale to local and overseas collectors.

Tables 1 and 2 indicate that the majority of the argentiferous lead–zinc deposits occur as fissure infill or as partial replacements of altered ultramafics bodies. Mineralisation consists of a siderite gangue overprinted by lead–zinc mineralisation. The typical vein assemblage consists of siderite–pyrite–galena–sphalerite ± chalcopyrite ± quartz. Jamesonite overprints all previous stages of mineralisation as either fine stringers and occasionally as coarse veins or large shoots.

$\delta^{18}O_{qtz}$ and Metal Zonation

In the Renison–Dundas district, the morphology of the partially exposed Devonian Pine Hill Granite, responsible for structural deformation and preparation of the overlying sediments, has been determined by geophysical methods (Leaman & Richardson 1989, Leaman 1990, Fig. 2). This has had allowed a far greater understanding of the structural controls on mineralisation at Renison. Research at the Renison Tin Mine has shown that a cooling magmatic hydrothermal fluid ascended the Federal–Bassett Fault prior to reacting with the host dolostone. $\delta^{18}O_{qtz}$

values and fluid inclusion results define two major dilational zones associated with fluid focussing, economic tin mineralisation and metal zonation.

The usefulness of $\delta^{18}O_{qtz}$ values was tested in this project by moving from a mine scale to a district scale of mineralisation. It has been demonstrated that the fracture controlled and telescoped nature of metal zonation in the Renison–Dundas district is associated spatially and temporally with the Pine Hill intrusion. Oxygen isotope analyses of quartz collected from several deposits in the district have been plotted upon a metal zonation diagram in Figure 8. Within the tin zone at Renison and Pine Hill that $\delta^{18}O_{qtz}$ values range from approximately 13.0–15.0‰, and in the Razorback area the range is close to 15.5‰. In the annular copper zone the data is scarce but indications are that the $\delta^{18}O_{qtz}$ values ranges from 15.5–18.0‰. Further out into the silver–lead–zinc zone the $\delta^{18}O_{qtz}$ values are between 18.0‰ and 20.0‰.

I conclude that:

- $\delta^{18}O_{qtz}$ values from fracture controlled mineralisation around mesothermal granitic intrusions, such as exist between the Heemskirk Granite and Granite Tor (i.e. the buried Devonian granite ridge that underlies the study area), mimic the telescoped mineral zonation pattern established on a district scale.
- The application of this method without well defined gravity data of the underlying granite obviously limits the applicability of the method.
- Any effect upon the variability of the $\delta^{18}O_{qtz}$ values due to the composition of the overlying host sequence into which the quartz mineralisation must intrude is yet to be established.
- Estimates of the temperature of mineralisation from fluid inclusion studies are required to determine the isotopic signature of the fluid responsible for mineralisation. The determination of $\delta^{18}O_{fl}$ values for the precipitated quartz would also assist in constraining the nature of the mineralising fluid and may help differentiate fault histories, i.e. Cambrian from Devonian structures.

$\delta^{18}O_{qz}$ in the Pieman River–Mackintosh Dam Area

A preliminary investigation of $\delta^{18}O_{qtz}$ values from vein material in the Pieman River – Mackintosh Dam study area (Figs 1, 2) was undertaken to establish the usefulness of $\delta^{18}O_{qtz}$ values in defining metal zonation patterns across the buried Devonian granite ridge and to possibly differentiate Cambrian fault structures from Devonian fault structures. A number of syn- to post-tectonic quartz veins of varying mineralogies were sampled across the traverse from various host sequences. The location, a geological description, and the $\delta^{18}O_{qtz}$ value of each sample is given in Appendix 1.

Figure 9 (a–d) summarises the data. Figure 9 (a) is a plot of all the data from the host sequences (Murchison Granite, Cambrian volcanics, Farrell Slates, and Owen Conglomerate) from which the samples were collected. The results show a spread of data across the four type categories from 9.6‰ to 18.4‰, with the majority of the data falling in the range 11.0‰ to 16.8‰. These results suggest that the host rocks to quartz veins have very little buffering effect upon the $\delta^{18}O_{qtz}$ values, without considering the nature of each of the quartz veins.

Figure 9 (b) separates the quartz veins in the Cambrian volcanic successions into their vein mineralogy's. The range of $\delta^{18}O_{qtz}$ values varies from 11–16‰. All groups have a similar distribution except perhaps for the Devonian Qz–Tourmaline veins from around Rosebery which vary between 13.9 – 15.3‰.

For the Farrell Slates, Devonian base metal veins have the lowest $\delta^{18}O_{qtz}$ values which range from 9.6‰ to 13.3‰ (Fig. 9c). The lowest value of 9.6‰ comes from a Qz–Flu–Py vein. The two syn-tectonic, flat lying extensional Qz–Carb veins at Tullarbadine also form a tight group that range from 13.6‰ to 14.9‰ but the low number of samples could not justify any certainty in their grouping. This latter group probably reflect rock buffering by the host succession. Carbonate isotope values will assist in evaluating the extent of rock buffering.

The final figure, 9 (d), shows a tight cluster for the $\delta^{18}O_{qtz}$ values in Devonian base metal veins once again that range from 11.3‰ to 13.3‰. The remaining quartz veins of variable mineralogies illustrate a range in $\delta^{18}O_{qtz}$ values which corresponds to syn-tectonic rock buffered values for $\delta^{18}O_{qtz}$.

In brief, the results of the preliminary investigation of oxygen isotope values from quartz in a variety of quartz veins across the transect from the Pieman River to the Mackintosh Dam show that::

- Devonian base metal veins from a range of host sequences are tightly constrained and have $\delta^{18}O_{qtz}$ values less than 14.0‰.
- Detailed gravity interpretations of the Devonian granite morphology will be required to better interpret the nature of metal zonation associated with this granite.
- The syn- to post-tectonic veins not associated with Devonian mineralisation have a quite varied distribution and probably reflect the influence of rock buffering. This will only be established by assessing the isotopic composition of mineral separates from whole-rock samples in which the various styles of quartz veins occur.

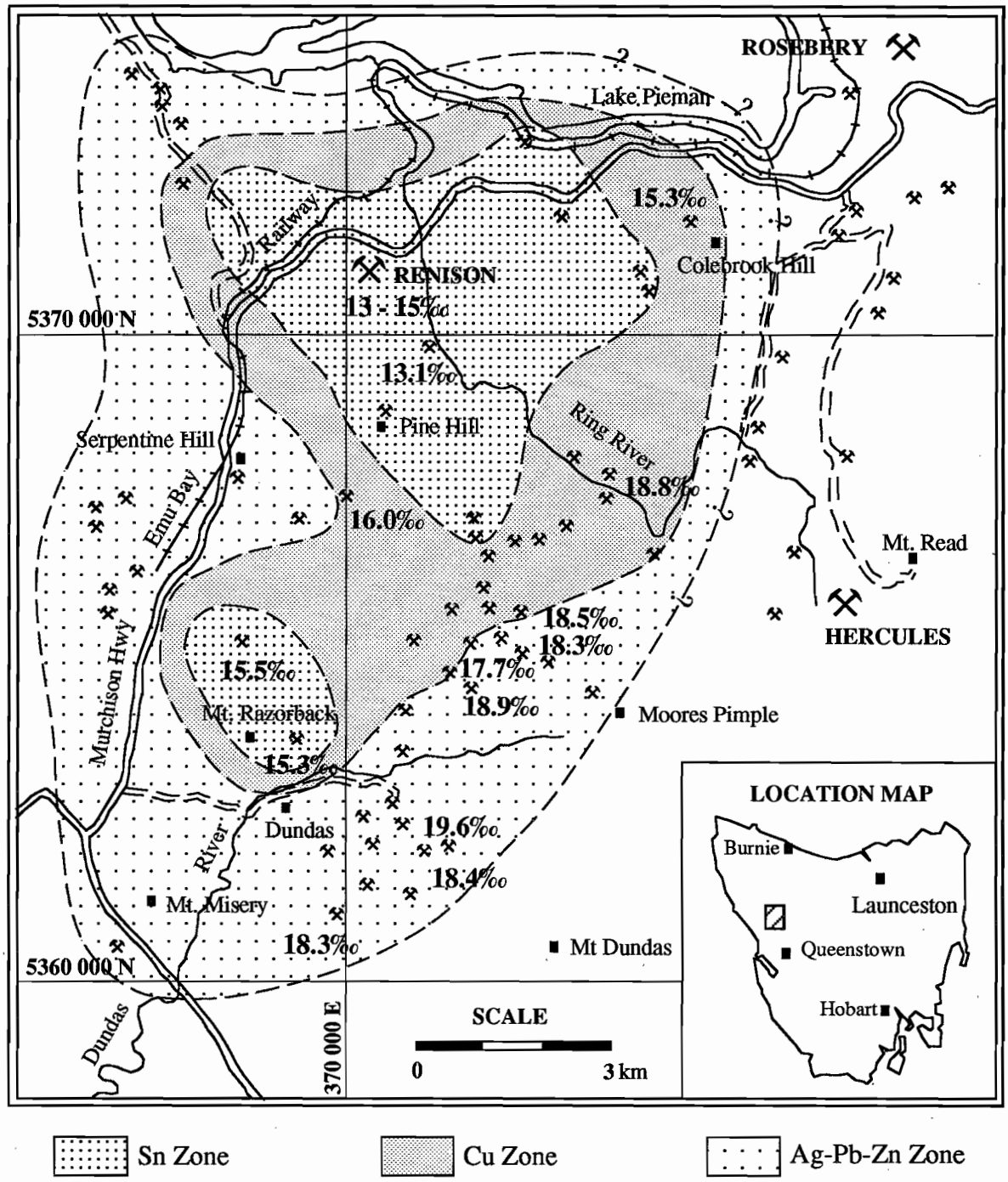

FIG. 8 — Oxygen isotope values for vein quartz mineralisation and metal zonation in the Renison–Dundas mineral field.

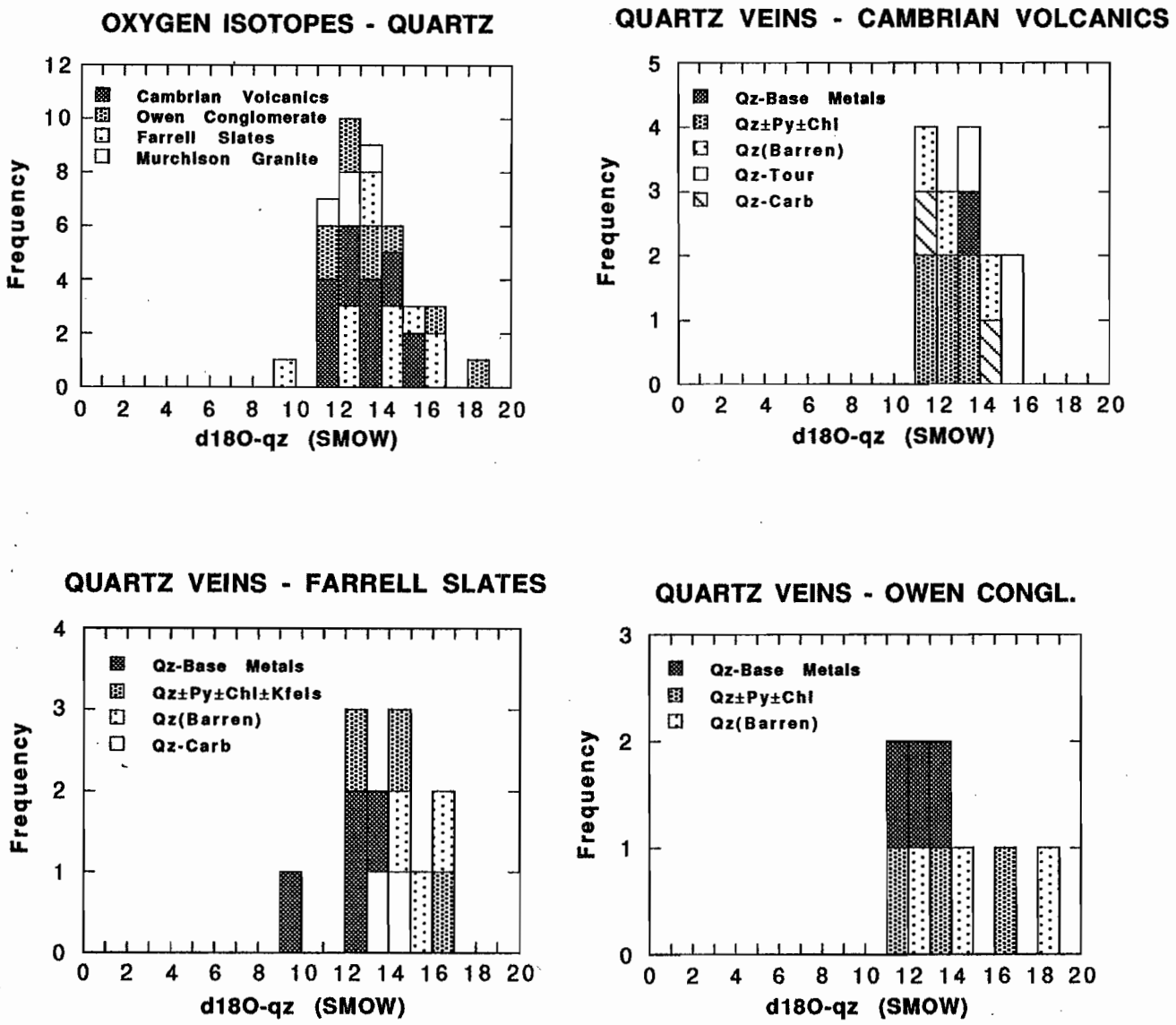

FIG. 9 — Histograms of the oxygen isotope values for vein quartz from the Pieman River – Makintosh Dam traverse. (a) Histogram of $\delta^{18}O_{qtz}$ values for the host sequences. (b) Histogram of $\delta^{18}O_{qtz}$ values for various vein mineralogies in the Cambrian volcanics. (c) Histogram of $\delta^{18}O_{qtz}$ values for various vein mineralogies in the Farrell Slates. (d) Histogram of $\delta^{18}O_{qtz}$ values for various vein mineralogies in the Owen Conglomerate.

- Fluid inclusion studies will be required to determine the oxygen isotope composition of the coexisting mineralising fluid. This aspect of the project has already commenced and will assist in characterising the nature of the mineralising fluid and help to differentiate Cambrian from Devonian fault structures.

Comparative Study of the Lakeside Prospect and the Transect

A detailed investigation of the Lakeside Prospect within the study area by Taheri and Green (1990) provides a useful comparison of the preliminary results. Their investigation into the origin of gold–tin–copper mineralisation looked at $\delta^{18}O_{qtz}$ values for mineralised Devonian quartz veins (Table 3.) along the Henty Fault which separates the Mount Black Volcanics to the west from the Farrell Slates and Murchison Volcanics to the east.

The purpose of their study was to investigate the possible origin(s) of the fluids for these veins by the use of fluid inclusion data to calculate temperatures of formation. Their $\delta^{18}O_{qtz}$ values ranged from 11.3‰ to 14.9‰ and therefore overlapped the isotopic field for our mineralised Devonian veins. Determination of $\delta^{18}O_{fl}$ values for the precipitated quartz–sulphide range from +7.2‰ to +9.1‰ (Table 3) using estimated formation temperatures of 350°C. These fluid values are similar to those calculated for the oxide–silicate stage of mineralisation on the Federal–Bassett Fault at Renison and indicate that the mineralising fluid was derived from a dominantly magmatic aqueous phase.

The $\delta^{18}O_{fl}$ values for water in equilibrium with the late stage barren quartz–carbonate veins are near zero and suggest the dominance of externally derived meteoric fluids during their precipitation.

The Sterling Valley Sn–As mineralisation in the Mount Black Volcanics is considered a deeper analogue of the mineralisation from the Lakeside Prospect having homogenisation temperatures up to 390°C (Green & Taheri 1992). Both the Lakeside and Sterling Valley Prospects are considered by Green & Taheri (1992) to have been adjacent to one another on the Henty fault prior to syn-mineralisation reverse faulting and later sinistral strike slip movement that separated the deposits by 1100 m.

The following conclusions can now be made about the oxygen isotope study of quartz from faults in the study region used to characterise both Cambrian and Devonian structures:

- The mineralised quartz veins within the study area are partly derived from with Devonian magmatic fluids and can be characterised from their mineralogy and oxygen isotope compositions of both the quartz and the mineralising fluid (obtained from fluid inclusion studies).
- The quartz–carbonate veins may be associated with Devonian mineralisation but rock buffering of Cambrian fluids must also be considered. Fluid inclusion studies should resolve any ambiguity in this matter where workable fluid inclusion material is available.
- Until the project has progressed further the characterisation of the remaining quartz vein-sets is uncertain. Future investigations involving fluid inclusion studies should prove beneficial.

TABLE 3 — Oxygen isotopes from quartz at the Lakeside Prospect (Taheri & Green 1990).

Sample No.	Mineralogy	Temp. °C	Oxygen–Qz	Oxygen–H_2O
102843	Qz–Py vein	350.00	13.00	7.20
102844	Qz–Py–Sph vein	350.00	13.50	7.70
102845	Qz–Py	350.00	14.90	9.10
102896	Qz–Sph–Asp	350.00	13.20	7.40
102895	Qz–vein	300.00	14.80	7.40
102894	Qz–Carb vein	200.00	12.10	–0.10
102893	Qz–Carb	200.00	11.80	–0.40
102892	Qz–Carb vein	200.00	11.30	–0.90
102891	Qz in vug	180.00	12.20	–1.40

PART 2

ISOTOPIC COMPOSITION OF HYDROTHERMAL CARBONATES FROM FAULT STRUCTURES

INTRODUCTION

An isotopic study of fault controlled carbonate mineralisation from the Pieman River–Mackintosh Dam region was undertaken to compliment the oxygen isotope investigation of quartz veins used to characterise and differentiate the various histories of both Cambrian and Devonian fault generations and reactivations. It was previously noted that carbonate veins usually post-date the main stages of mineralisation but their isotopic signatures still reflect unique $\delta^{18}O_{carb}$ and $\delta^{13}C_{carb}$ values that may characterise fault generations and reactivations.

Ore deposit research has already noted that Cambrian ore fluids are substantially different to Devonian ore fluids. The isotopic composition of hydrothermal carbonates therefore should provide another possible tool to assist in testing the proposed tectonic model for western Tasmania. The oxygen and carbon isotope values of the carbonates were determined using a VG Micromass 602D mass spectrometer in the Central Science Laboratory, University of Tasmania, using the method of McCrea (1950). The reaction time for the carbonate isotope procedures varied from 24 to 72 hours at 25°C for the various carbonates sampled except for siderites which were reacted at 50°C.

Devonian Carbonates and Fluid – Rock Interaction at Renison

Cassiterite-rich, pyrrhotite replacement of sedimentary Proterozoic dolomites at Renison by Devonian granitic hydrothermal fluids resulted in a world-class primary tin deposit (Patterson et al. 1981, Kitto 1992). The hydrothermal fluids responsible for mineralisation were enriched in CO_2 during the replacement of dolomite by acidic mineralising fluids (Davies 1985, Holyland 1987).

Figure 10 is a plot of isotopic analyses for various carbonates at the Renison Tin Mine. The shape of the mixing curves reflect the isotopic compositions of the hydrothermal fluid and the wallrocks; the extent of mixing in a closed versus open system; the temperature of isotopic exchange; and finally the CO_2 concentration of the mineralising fluid. The data includes both mineral separates and whole rock data which has been compiled from Patterson (1979), Jones & Evans (1985), Holyland (1987), and Rao & Adabi (in prep). In Figure 10 the data represented by solid circles corresponds to mineralogically unaltered dolomites, although some recrystallisation of the dolomites has been recognised in those dolomites with lowest $\delta^{18}O$ and $\delta^{13}C$ values. The cross symbols represent isotope values for the hydrothermal siderites that occurs at the reaction front between the massive pyrrhotite orebodies and the unreplaced sedimentary dolomite horizons. The majority of the siderite $\delta^{18}O$ and $\delta^{13}C$ values are the lightest of all the samples analysed. The square symbols represent minor late stage vein calcite $\delta^{18}O$ and $\delta^{13}C$ values.

The rectangular area labelled "Unaltered Proterozoic Dolomite" has been chosen to represent the host dolomite horizons with an averaged $\delta^{18}O$ value of +28 ‰ (SMOW) and a $\delta^{13}C$ value of +4.5 ‰ (PDB). The point labelled "Magmatic Fluid" is the inferred isotopic composition of a hydrothermal magmatic fluid in equilibrium with the Pine Hill Granite and responsible for carbonate replacement mineralisation at Renison (Kitto 1993). The $\delta^{18}O$ value of +7 ‰ (SMOW) for this fluid was calculated from $\delta^{18}O$ analyses from quartz, together with temperature estimates from coexisting fluid inclusions from the early oxide–silicate stage of mineralisation on the Federal–Bassett Fault and using the fractionation factors from Matsuhisa et al. 1979. The $\delta^{13}C$ value of –6 ‰ (PDB) for the magmatic fluid was chosen as an approximated average igneous carbon value based on discussions in Faure (1977), Hoefs (1980), Ohmoto (1986), and Taylor (1987). The line labelled "Magmatic Carbonate" is the theoretical dolomite-fluid $\delta d^{18}O$–$\delta^{13}C$ fractionation curve for dolomites formed from, or in equilibrium with, the hydrothermal magmatic fluid, of constant composition, and at a range of temperatures from 450°C to 100°C (after Rye & Williams 1981). The $\delta^{18}O$ values for this line were calculated from the fractionation factors of Land (1983), after Sheppard & Schwarcz (1970), and the $\delta^{13}C$ values were calculated using the fractionation factors of Ohmoto & Rye 1979. Hydrothermal carbonates that might fall on this line would represent those carbonates that precipitate within the Federal–Bassett Fault without wallrock interaction.

Rye & Williams (1981) used this approach for fluids in which carbon is almost totally oxidised, and noted that caution would be require if CH_4 was present. Fluid inclusion decrepitation studies by Patterson & Ohmoto (1976) report the presence of CO_2/CH_4 ratios that vary between 1.0 and 0.5 in late stage fluids associated with vein calcites at 200°C. Variations in $\delta^{13}C$ values of carbonates at Renison from all the data available show a maximum range from +5‰ to –8‰ and not from +5‰ to –14‰ as reported in Patterson & Ohmoto (1976) and used by Ohmoto & Rye (1979) as the best example of

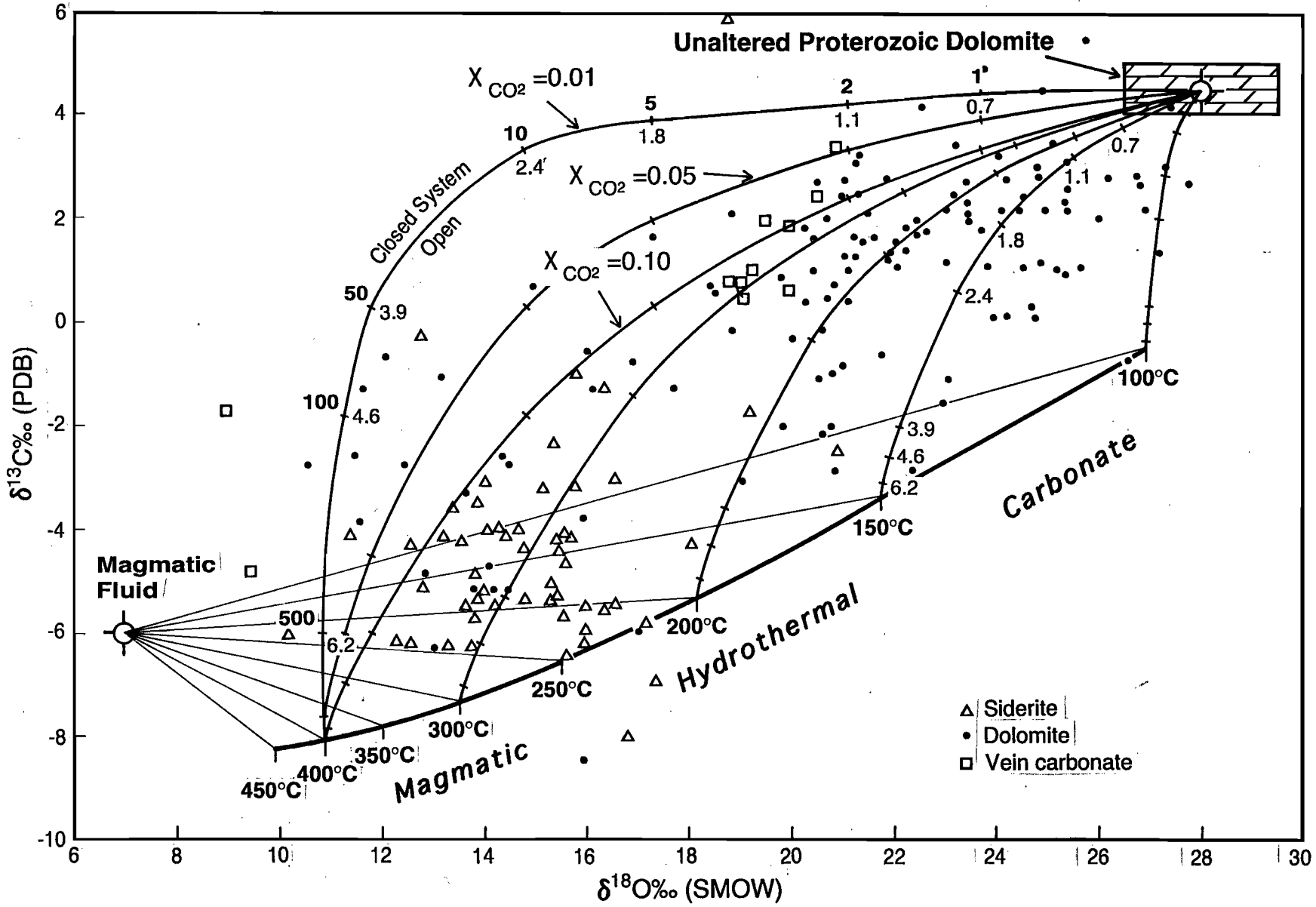

FIG. 10 — Fluid–Rock interaction associated with hydrothermal carbonates at the Renison MIne.

variations in $\delta^{13}C$ values due to the CO_2/CH_4 ratio of fluids near the CO_2/CH_4 boundary. The presence of CH_4 in the *late stage* hydrothermal fluid at Renison has been noted but is not considered the major cause of variations in the $\delta^{13}C$ values of the carbonates associated with the *main stage* of cassiterite mineralisation at the Renison Tin Mine.

Figure 10 suggests that the data can best be interpreted as the progressive interaction of a C and O reservoir typical of Proterozoic dolomites with a reservoir more typical of a felsic Devonian granitic rock. The hydrothermal fluids responsible for carbonate replacement mineralisation at Renison were in equilibrium with an igneous rock prior to injection into the Federal–Bassett Fault and reacting with Proterozoic dolomites. *Decarbonation* is not an important process in this distal skarn environment as the development of silicate mineral assemblages, consisting of talc and tremolite, is restricted to a small zone at the interface between massive pyrrhotite and the siderite reaction front in the host dolomite horizons. Decarbonation cannot explain the substantial isotopic depletions in both $\delta^{18}O$ and $\delta^{13}C$ values of the carbonate in this deposit (Brown et al. 1985, Bowman et al. 1985, Taylor & Bucher-Nurminen 1986).

The many curved lines in Figure 10 connecting the unaltered Proterozoic dolomite with the magmatic hydrothermal carbonates, in equilibrium with a "magmatic fluid" at various temperatures, represent isotopic alteration paths for carbonate host-rocks as a function of water to rock ratios due to *infiltration*. Sverjensky (1981) first calculated theoretical isotopic compositions of host-rock calcites during hydrothermal isotopic alteration as a function of a progressively increasing water to rock ratio at a constant temperature, and applied this technique to the Upper Mississippi Valley-type Pb–Zn district. The same technique was applied by Shelton (1983) to the Mines Gaspe porphyry copper and skarn deposit to explain the isotopic alteration observed in calcites as a function of the water to rock ratio. These equations were applied to the Renison data to calculate the changing isotopic composition of the host-rock dolomites with increasing water to rock ratio. The fractionation factors of Land (1983), after Sheppard & Schwarcz (1970), were used to calculate the $\delta^{18}O$ values, and the fractionation factors of Ohmoto & Rye (1979) were used to calculate $\delta^{13}C$ values. Fractionation factors for $\delta^{18}O$ values in siderite are almost identical to those used for dolomite but only apply to the temperature range 33°C to 197°C (Carothers et al. 1988). As a consequence all fluid–rock calculations have been made for dolomite and applied to the siderite data from Renison.

The three isothermal fluid–rock lines for 400°C, in Figure 10, connecting the Proterozoic dolomite and magmatic hydrothermal dolomite have been calculated for various concentrations of $H_2CO_{3(apparent)}$. The curvature of the mixing curves primarily depends on the concentration of CO_2 in the hydrothermal fluid. Values of 0.01, 0.05 and 0.10 molal were chosen for the major carbon-bearing species and represent possible successive increases or gradients in the concentration of CO_2 in the hydrothermal fluid during the main stage carbonate replacement process, as dissolution of the dolomite takes place resulting in massive cassiterite-rich pyrrhotite orebodies (Patterson 1979, Davies 1985, Holyland 1987). Similar sets of isothermal fluid–rock curves could also have been applied for the remaining temperatures, but for clarity only X_{H2CO3} = 0.10 molal are shown.

The calculated curves for the fluid–rock interaction encompass the entire field of the isotopic data for the Renison carbonates and explain the trends to lighter isotopic values. The mixing curves suggest that a water-to-rock ratio near 6, for an open system. Decreasing temperatures are required to explain the extent of the isotopic exchange of the carbonate-bearing host rocks at the Renison Mine. Fluid inclusion data from the Federal–Bassett Fault and the Transverse Faults support this interpretation as homogenisation temperatures decline along such structures and outward into the wallrocks away from the major pyrrhotite orebodies (Patterson,1979, Davies 1985, Holyland 1987, Kitto 1994).

In conclusionthis simple model of fluid–rock interaction is consistent with the geological situation and explains the chemical and isotopic systematics associated with the carbonate replacement orebodies at the Renison Tin Mine. The fluid modelling carried out so far is simplistic but support the following conclusions:

- A Devonian granitic derived magmatic hydrothermal fluid having a $\delta^{18}O$ value of +7‰ (SMOW) and a $\delta^{13}C$ value of –6.0 ‰ (PDB) ascended the Federal–Bassett Fault at or near 400°C before reacting with sedimentary Proterozoic dolomites with an averaged isotopic composition of $\delta^{18}O$ = +28 ‰ (SMOW) and a $\delta^{13}C$ = +4.5 ‰ (PDB).
- Infiltration was the dominant mechanism responsible the fluid–rock interaction.
- A water to rock ratio near 6 in an open system with declining temperatures from 400°C to less than 150°C accounts for the observed pattern in the $\delta^{18}O$ and $\delta^{13}C$ values.
- The X_{H2CO3} in the hydrothermal fluid most probably increased from 0.01 molal to 0.10 molal as CO_2 was released by dolomite dissolution

during the main stage cassiterite-rich pyrrhotite mineralisation.

- NOTE: Caution needs to be applied when interpreting C/O isotopic data if methane is present inthe hydrothermal fluids because reduced conditions significantly shift $\delta^{13}C$ values.

Isotopic Composition of Cambrian Hydrothermal Carbonates

A plot of carbon and oxygen isotope data for Cambrian hydrothermal carbonates is presented in Figure 11 (a). This data has been compiled from a number of sources which have included Dixon (1980), Yeats (1990), Khin Zaw (1990 & 1992), and Warmeant (1990). This data is tabulated in Appendix 2.

The oxygen and carbon isotope values for Cambrian hydrothermal carbonates generally have a very tightly constrained composition. The majority of the hydrothermal carbonates have a $\delta^{13}C_{carb}$ (PDB) values that range between 0.0‰ and –5.0‰ and $\delta^{18}O_{carb}$ (SMOW) values that range from 8.5‰ to 14.0‰. The couple of rouge $\delta^{13}C_{carb}$ (PDB) values for North and South-end Rosebery undoubtedly represent late stage Devonian quartz–carbonate veins and are not Cambrian in age. Their oxygen and carbon isotope values overlap the Devonian hydrothermal carbonate field from Renison which has been represented on the plastic overlay (Fig. 11a) by the dolomite fractionation curve for Devonian magmatic fluids. The spread in the South Hercules data which show positive increases in $\delta^{13}C_{carb}$ (PDB) and $\delta^{18}O_{carb}$ (SMOW) values has previously been described by Khin Zaw (1992) as representing precipitation of carbonates over a temperature range from 150°C to 250°C and was verified by fluid inclusion studies. This allowed Khin Zaw to calculate a theoretical isotopic composition for the coeval hydrothermal fluid from which the carbonates precipitated (see Figure 11a). This hydrothermal fluid has a $\delta^{13}C_{fl}$ (PDB) value of between –1.0‰ and –2.0‰ and a $\delta^{18}O_{fl}$ (SMOW) value of 2.0‰ to 4.0‰ and is consistent with an evolved Cambrian seawater (Khin Zaw 1992).

The spread in $\delta^{13}C_{carb}$ (PDB) values for all Cambrian hydrothermal carbonates is interpreted to be the result of fluid rock interaction. Like the data presented in Figure 10, progressive fluid-rock interaction will change the isotopic composition of the hydrothermal carbonates to isotopic values nearer to the host sequence. As carbon and oxygen isotopic data for the host successions is currently unavailable fluid–rock calculations explaining the isotopic shifts can not been presented.

Hydrothermal Carbonate Isotopes in the Study Area

A limited number of carbonate samples from the Pieman River–Mackintosh Dam traverse were submitted for carbon and oxygen isotope analysis. The results have been plotted in Figure 11(b) and the results tabulated with sample descriptions in Appendix 1. In addition to this data is a set of analyses, collected by Josie Raftery, from the Murchison Lodes and the New North Farrell deposits. The isotopic analyses from these deposits are included in Table 4.

Figure 11(b) presents the available data from the traversed area, and the results clearly fall into two

Table 4 — Carbon and oxygen isotope analyses from the Farrell Lodes (Raftery, unpubl. data).

Sample no..	Location	Mineralogy	C_{PDB}	O_{SMOW}
JR-86	New North Farrell Mine	Qz-Carb vein breccia with Farrell Slate clasts	-7.496	16.417
JR-87A	New North Farrell Mine	Carb-Sph±Py vein breccia with Farrell Slate clasts	-8.903	17.345
JR-87B	New North Farrell Mine	Carb-Sph-Qz±Py vein	-8.4	17.079
JR-87D	New North Farrell Mine	Carb-Sph-Gal vein	-8.616	16.739
JR-87F(iii)	New North Farrell Mine	Carb-Sph±Qz vein	-8.64	16.602
JR-MP28	Murchison Lodes	Carb-Gal-Sph-Py vein	-7.707	14.907
JR-MP29	Murchison Lodes	Carb-Qz vein in Farrell Slate	-7.676	15.407
JR-MP30	Murchison Lodes	Carb-Qz-Py-Chl±Asp vein	-8.232	13.456
JR-MP71	Murchison Lodes	Carb-Qz vein breccia in Farrell Slate	-6.261	15.411
JR-MP86	Murchison Lodes	Qz-Asp-Carb-Py vein	-8.74	16.038
JR-MP87	Murchison Lodes	Carb-Qz vein in Qz phyric volcanoclastic schist	-5.714	17.254
JR-MP88	Murchison Lodes	Carb-Qz-Py vein in graphitic schists of Farrell Slates	-7.694	16.784

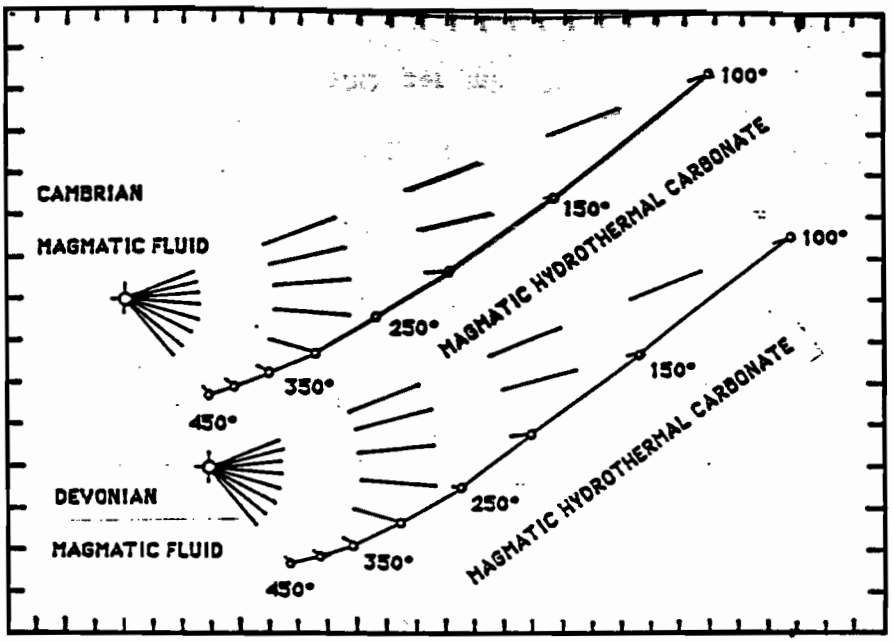
CAMBRIAN
MAGMATIC FLUID
100°
150°
250°
350°
450°
MAGMATIC HYDROTHERMAL CARBONATE
DEVONIAN
MAGMATIC FLUID
100°
150°
250°
350°
450°
MAGMATIC HYDROTHERMAL CARBONATE

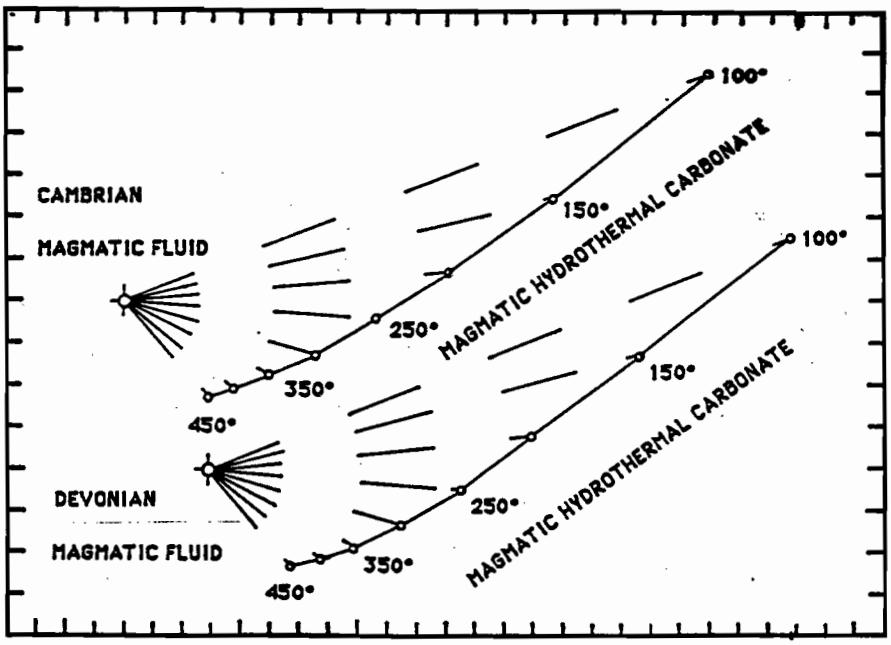
CAMBRIAN
MAGMATIC FLUID
100°
150°
250°
350°
450°
MAGMATIC HYDROTHERMAL CARBONATE
DEVONIAN
MAGMATIC FLUID
100°
150°
250°
350°
450°
MAGMATIC HYDROTHERMAL CARBONATE

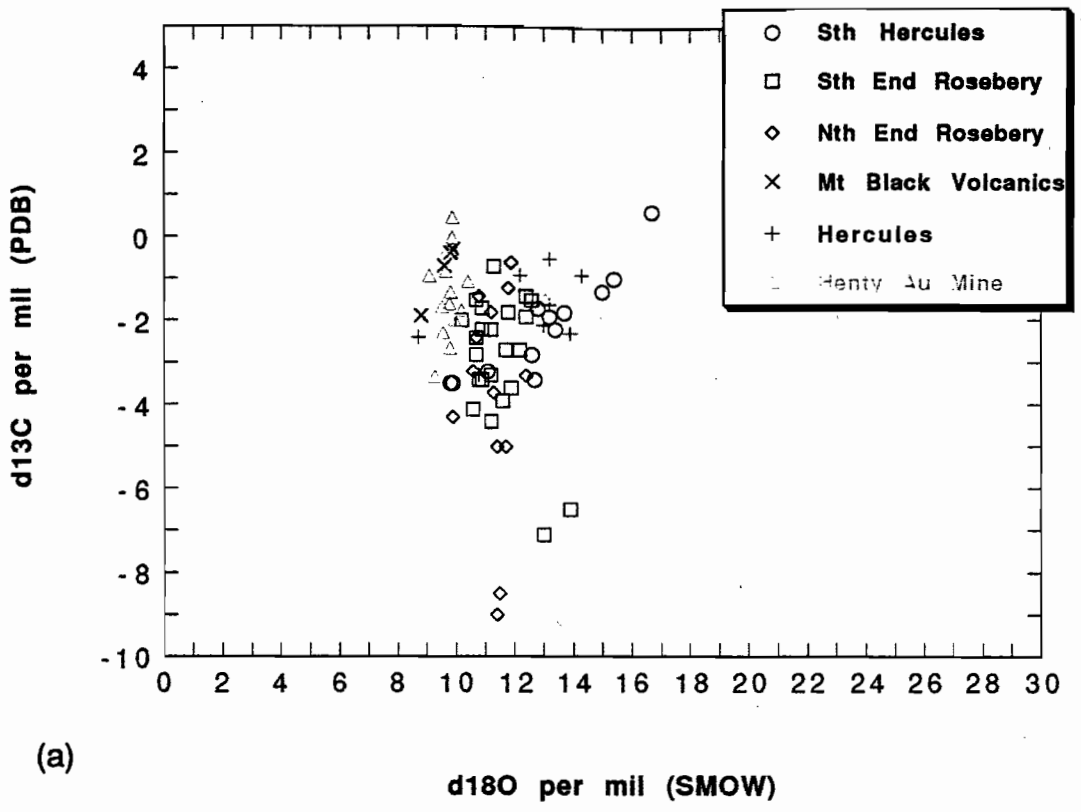

FIG. 11 — (a) Carbon and oxygen isotopic fields for Cambrian hydrothermal carbonates. (b) Carbon and oxygen isotopic fields for carbonate analyses from the Pieman River–Makintosh Dam traverse.

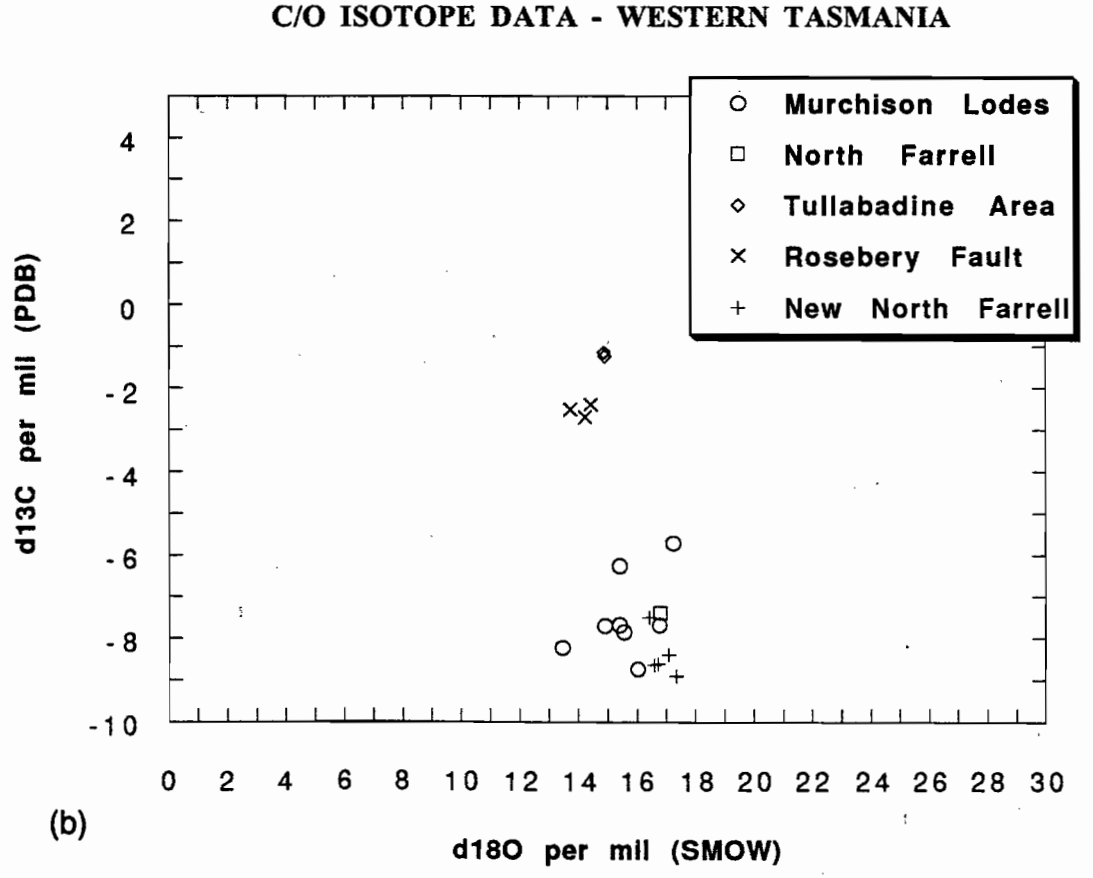

well defined groups. The majority of the data has low $\delta^{13}C_{carb}$ (PDB) values that range from –5.7‰ to –8.9‰ and $\delta^{18}O_{carb}$ (SMOW) values that range from 12.5‰ to 16.3‰. This set of data overlaps the Renison hydrothermal siderite field but has a slightly lower $\delta^{13}C_{carb}$ (PDB) value that may reflect differing CO_2/CH_4 levels in the magmatic fluid compared to those at Renison. Fluid inclusion studies may be able to answer this question.

The second clearly defined field for carbon and oxygen isotopes from the study area, shown in Figure 11 (b), have much higher $\delta^{13}C_{carb}$ (PDB) values that overlaps the lower portion of the Cambrian hydrothermal carbonate field established in Figure 11 (a). Our results represent samples from the Rosebery Fault (at Bastyan Dam) and from the Farrell Slates at Tullabardine. The analyses from the Rosebery Fault are, at this stage, considered to represent remobilised Cambrian sedimentary carbonates but fluid inclusion studies are needed to confirm this interpretation. In handspecimen the carbonates from the Tullabardine area appear to represent syn-post Devonian deformation qz–carb veins but their isotopic signatures fall within the Cambrian field of analyses. Future fluid inclusion research will be required to assist in their interpretation as rock-buffering may also be a consideration.

Recent investigations of latest Proterozoic marine carbonates by Kaufman et al. (1993) have suggested that strong isotopic variations in Sr and C isotope data can be used to detect significant environmental and tectonic changes. A preliminary investigation of Sr and C isotopic variations in fault controlled carbonates may therefore assist in differentiating Cambrian and Devonian structural histories and further test the tectonic model proposed for western Tasmania.

Based on the preliminary research into carbon and oxygen isotopes of hydrothermal carbonates within the traversed area the following conclusions can be reached:

- Cambrian hydrothermal carbonates in western Tasmania associated with VHMS styles of mineralisation have a well constrained field of $\delta^{13}C_{carb}$ (PDB) and $\delta^{18}O_{carb}$ (SMOW) values that characterise fluid circulation along Cambrian structures.
- Devonian hydrothermal carbonates associated with magmatic fluids derived from the buried Heemskirk–Pine Hill–Granite Tor ridge have a unique isotopic signature that assists in the recognition of Devonian fluid circulation along faults; be these faults Cambrian or Devonian structures.
- Fluid inclusion studies are necessary to assist the interpretation of ambiguous carbonate results to enable further constrains on the source of the mineralising fluids.
- Carbon and oxygen isotope values for the rocks hosting vein carbonates are required to undertake fluid–rock calculations in the study area. This will allow fluid circulation models to be developed that can then test the proposed tectonic model for western Tasmania.
- New research into Sr and C isotopes (Kaufman et al. 1993) in carbonates has shown that their isotopic variations can record significant environmental and tectonic changes. This area of research should be considered.

REFERENCES

Allman-Ward, P., C. Halls, A. Rankin and C.M. Bristow. 1982. "An intrusive hydrothermal breccia body at Wheal Remfrey in the western part of the St. Austell granite pluton, Cornwall, England." *In* A. M. Evans (Ed.): *METALLISATION ASSOCIATED WITH ACID MAGMATISM.* John Wiley and Sons Ltd: 1–28.

Bartlett, J. 1993. "Geology of the South Comet Mine Area." Unpubl. B. Sc. (Hons.) thesis, University of Tasmania.

Blissett, A.H., 1962. *Zeehan.* Tas. Dept. Mines. Geol. Surv. Explan. Rept., One mile series K155-5-50.

Both, R.A., T.A. Rafter, M. Solomon and M. L. Jensen, 1969. Sulphur isotopes and zoning of the Zeehan mineral field, Tasmania. *Econ. Geol.* 64: 618–628.

Both, R.A. and K.L. Williams, 1968a. Mineralogical zoning in the lead–zinc ores of the Zeehan field, Part I: Introduction and review. *J. Geol. Soc. Aust.* 15: 121–137.

Both, R.A. and K.L. Williams, 1968b Mineralogical zoning in the lead–zinc ores of the Zeehan field, Part II: Paragenetic and zonal relationships. *J. Geol. Soc. Aust.* 15: 217–243.

Bowman, J.R., J.J. Covert, A.H. Clark and G.A. Mathieson, 1985 The CanTung E Zone scheelite skarn orebody, Tungsten, Northwest Territories: oxygen, hydrogen, and carbon isotope studies. *Econ. Geol.* 80: 1872–1895.

Brooks, C.C. 1962. Geology of the Tullah area. Unpubl. B.Sc. (Hons.) thesis, University of Tasmania: 339 pp.

Brown, P.E., J.R. Bowman, and W.C. Kelly, 1985. Petrologic and stable isotope constraints on the source and evolution of skarn-forming fluids at Pine Creek, California. *Econ. Geol.* 80: 72–95.

Burnham, C.W., 1967. Hydrothermal fluids at the magmatic stage. *In* H.L. Barnes (ed.): *GEOCHEMISTRY OF HYDROTHERMAL ORE DEPOSITS.* Wiley-Intersci., New York: 34–76.

Burnham, C.W., 1979. Hydrothermal fluids at the magmatic stage. *In* H.L. Barnes (ed.): *GEOCHEMISTRY OF HYDROTHERMAL ORE DEPOSITS. Second edition.* Wiley-Intersci., New York: 71–136.

Carothers, W.W., L.H. Adami, and R.J. Rosenbauer, 1988. Experimental oxygen isotope fractionation between siderite-water and phosphoric acid libeated CO_2-siderite. *Geochim. et Cosmochim. Acta* 52: 2445–2450.

Clayton, R.N. and T.K. Mayeda, 1963. The use of pentafluoride in the extraction of oxygen from oxides and silicates for isotopic analysis. *Geochem. et Cosmochim. Acta* 27: 43–52.

Collins, P.L. F., S.G. Brown, E.V. Dronseika and R. Morland, 1989. Mid-Palaeozoic ore deposits. *In* Burrett C. F. and Martin E. L. (eds): *GEOLOGY AND MINERAL RESOURCES OF TASMANIA.* Geol. Soc. of Aust. Spec. Pub. 15.: 270–292.

Collins, P.L.F. and E. Williams, 1986. Metallogeny and tectonic development of the Tasman Fold Belt System in Tasmania." *Ore Geol. Rev.* 1: 153–201.

Crossing, D.J.F., 1991. EL101/87 Dundas and EL13/88 Moores Pimple annual report 1990/91. RGC Exploration Pty Limited (unpubl.).

Davies, B.M., 1985. The nature and mechanism of stratabound mineralisation in the Renison Tin Mine. Unpubl. Ph.D, James Cook University.

Dixon, G.H., 1980. The carbonates at Rosebery: geology, geochemistry, stable isotopes. Unpubl. B.Sc. Hons thesis, University of Tasmania.

Elliston, J., 1950. Dundas mineral field. Unpubl. B.Sc. (Hons.) thesis, University of Tasmania.

Forsythe, D.L., 1969. Progress report on the North Dundas Project, Tasmania. Unpubl. report New Consolidated Gold Fields (A'sia) Pty Limited.

Gilbert, J.M. and C.F. Park, 1986. *THE GEOLOGY OF ORE DEPOSITS.* 4th Edn. Freeman and Co..

Green, G.R., 1990. Palaeozoic Geology and Mineral Deposits of Tasmania. *In* F. E. Hughes (ed.): *GEOLOGY OF THE MINERAL DEPOSITS OF AUSTRALIA AND PAPUA NEW GUINEA.* The Australian Institute of Mining and Metallurgy, Melbourne: 1207–1223.

Green, G.R., H. Ohmoto, J. Date, and T. Takahashi, 1983. Whole-rock oxygen isotope distribution in the Fukazaw-Kosaka area, Hokuroku district, Japan, and its potential application to mineral exploration. *Econ. Geol. Monogr.* 5: 395–411.

Groves, D.I., 1968. The cassiterite-sulphide deposits of western Tasmania. Unpubl. PhD. thesis, University of Tasmania.

Gulson, B.L. and P.H. Porritt, 1987. Base metal exploration of the Mount Read Volcanics, western Tasmania: lead isotope signatures and genetic implications. *Econ. Geol.* 82: 291–307.

Heinrich, C.A., 1990. The chemistry of hydrothermal tin (–tungsten) ore deposits. *Econ. Geol.* 85: 457–481.

Heinrich, C.A. and P.J. Eadington, 1986. Thermodynamic predictions of the hydrothermal chemistry of arsenic, and their significance for the paragenetic sequence of some cassiterite-arsenopyrite-base metal sulfide deposits. *Econ. Geol.* 81: 511–529.

Heinrich, C.A., R.W. Henley, and T.M. Seward, 1989. *HYDROTHERMAL SYSTEMS.* Adelaide: Australian Mineral Foundation.

Henley, R.W. and A. McNabb, 1978. Magmatic vapor plumes and ground-water interaction in porphyry copper emplacement. *Econ. Geol.* 73: 1–20.

Herman, W. and M. White, 1989. *A reconnaissance of old workings in the Central and North Dundas mineral fields, Tasmania.* Unpub. report RGC Exploration Pty. Ltd.

Hoefs, J., 1980. *STABLE ISOTOPE GEOCHEMISTRY. 2nd Edition* Springer-Verlag: New York, Heidelberg, Berlin.

Holyland, P., 1987. Structure and hydrodynamics of the Renison Tin Mine. Unpubl. Ph.D thesis, University of Queensland.

Jackson, N.J., A.N. Halliday, S.M.F. Sheppard and J.G. Mitchell, 1982. Hydrothermal activity in the St. Just mining district, Cornwall, England. *In* A. M. Evans (ed.): *Mineralisation Associated with Acid Magamatism.* Wiley, Chinchester: 137–179.

Jones, M. and D. Evans, 1985. Trace element and stable isotope variations in rocks of the Renison Mine Sequence. Tenison mine, unpubl. report.

Kaufman, A.J., S.B. Jacobsen, and A.H. Knoll, 1993. The Vendian record of Sr and C isotopic variations in seawater: Implications for tectonic and paleoclimate. *Earth & Planet. Sci. Lett.* 120: 409–430.

Kelly, W.C. and R.O. Rye, 1979. Geologic, fluid inclusion, and stable isotope studies of the tin-tungsten deposits of Panasqueira, Portugal. *Econ. Geol.* 74: 1721–1822.

Kelly, W.C. and F.S. Turneaure, 1970. Mineralogy, paragenesis and geothermometry of tin and tungsten deposits of the Eastern Andes, Bolivia. *Econ. Geol.* 65: 609–680.

Kitto, P.A., 1992b. The geological and structural controls on mineralisation at the Renison Tin Mine. *Bull. Geol. Surv. Tasm.* 70: 97–117.

Kitto, P.A., 1993. Oxygen isotopes as an indicator of large-scale hydrothermal paleoflow and economic Sn mineralisation, Renison Mine, western Tasmania. *In* Second National Meeting SGEG in Armidale: 34–35.

Kitto, P.A., 1993b. Exploration criteria for Renison style deposits and recommendations for the Renison Mine Lease, EL 101/87 and EL 13/88. Unpubl. mine report, Renison Tin Mine.

Kitto, P.A., 1994. Structural controls on hydrothermal paleoflow and metal zonation at the Renison Tin Mine, western Tasmania, Australia. *In* Large, R.R. (ed): In the Footsteps of Solomon in Western Tasmania. Centre for Ore Deposit & Exploration Studies, University of Tasmania: 20–21.

Kitto, P.A. and R.F. Berry, 1992. Structural controls on mineralisation at the Renison Tin Mine, western Tasmania. *In* 11th Aust. Geol. Convention in Ballarat: 70–71.

Kutina, J., 1963. Problems of post-magmatic ore deposition, a symposium. Geol. Surv. Czech.: 588 pp.

Kyser, T.K., ed., 1986. *SHORT COURSE IN STABLE ISOTOPE GEOCHEMISTRY OF LOW TEMPERATURE FLUIDS.* Vol. 13. Mineralogical Association of Canada.

Land, L.S., 1983. The application of stable isotopes to studies of the origin of dolomite and to problems of diagenesis of clastic sediments" *In* Stable Isotopes in Sedimentary Geology, 4.1-4.22. Soc. Econ. Paleo. Mineral., Short Course.

Large, R.R. and D.L. Huston. 1986. The zinc number [100/Zn/(zn + Pb)], a new geochemical discrimination for mineral exploration in the Mount Read Volcanics. *In* Large, R.R. (ed.): The Mount Read Volcanics and Associated Ore Deposits. Geol. Soc. Aust. (Tas. Div.): 57–60.

Leaman, D.E., 1980. Applied geophysics in Tasmania – a summary of surveys. Tasmanian Department of Mines unpubl. report 1980/41.

Leaman, D.E., 1990. Renison mine lease gravity survey. Renison Mine. Unpubl. report from Leaman Geophysics

Leaman, D.E. and R.G. Richardson, 1989. The granites of west and north-west Tasmania: a geophysical interpretation. *Bull. Geol. Surv. Tas.* 66: 146pp.

Lehmann, B., 1990. *METALLOGENY OF TIN.* Vol. 32. Lecture notes in Earth Sciences. Springer-Verlag, Berlin: 1990.

Lehmann, B. and C. Mahawat, 1989. Metallogeny of tin in central Thailand: a genetic concept. *Geology* 17: 426–429.

Loftus Hills, C., 1921. The progress of geological research in Tasmania since 1902. *Pap. Proc. Roy. Soc. Tas.:* 111–146.

Lutley, W.M., 1975. Cassiterite-sulphide mineralisation at Queen Hill, Zeehan, western Tasmania. Unpubl. MSc thesis, University of Adelaide.

Lynch, J.V.G., F.J. Longstaffe, and B.E. Nesbitt, 1990. Stable isotope and fluid inclusion indications of large scale hydrothermal paleoflow, boiling, and fluid mixing in the Keno Hill Ag–Pb–Zn district, Yukon Territory, Canada. *Geochem. et Cosmochim. Acta* 54: 1045–1059.

Matsuhisha, Y., J.R. Goldsmith, and R.N. Clayton, 1979. Oxygen isotope fractionation in the system quartz-albite-anorhtite-water. *Geochim. et Cosmochim. Acta* 42: 1131–1140.

McCrea, L.M., 1950. The isotope chemistry of of carbonates and a paleotemperature scale. *Jour. Chemistry Physics* 18: 849–857.

Montgomery, A., 1896. Report on the Zeehan–Dundas Mineral Field. Mines Office, Launceston.

Munha, J., F.J.A.S. Barriga and R. Kerrick, 1986. High ^{18}O ore-forming fluids in volcanic hosted base metal massive sulphide deposits: geologic, $^{18}O/^{16}O$, & D/H evidence from the Iberian pyrite belt: Crandon Wisconsin; and Blue Hill, Maine. *Econ. Geol.* 81: 530–552.

Ohmoto, H., 1986. Stable Isotope Geochemistry of Ore Deposits. *In* J. W. Valley, H. P. Taylor, and J. R. O'Neil (eds): *STABLE ISOTOPES IN HIGH TEMPERATURE GEOLOGICAL PROCESSES* 16. Mineralogical Society of America: 491–560.

Ohmoto, H. and R.O. Rye, 1979. Isotopes of sulfur and carbon. *In* H.L. Barnes (ed.): *GEOCHEMISTRY OF HYDROTHERMAL ORE DEPOSITS.* Wiley Intersci., New York: 509–567.

Park, C.F. Jnr., 1955. The zonal theory of ore deposits. *Econ. Geol.* 50th Anniv. Vol.: 226–248.

Patterson, D.J. 1979. The geology and mineralisation at Renison Bell, western Tasmania. Unpubl. Ph.D. thesis, University of Tasmania.

Patterson, D.J., H.H. Ohmoto and M. Solomon, 1981. Geological setting and genesis of cassiterite-sulfide mineralisation at Renison Bell, western Tasmania. *Econ. Geol.* 76: 393–438.

Plimer, I.R., 1987. Fundamental parameters for the formation of granite related tin deposits. *Geol. Rundschau* 76: 23–40.

Pollard, P.J. and R.G. Taylor, 1986. Progressive evolution of alteration and tin mineralisation: controls by interstitial permiability and fracture related trapping of magmatic fluid reservoirs in tin granites. *Econ. Geol.* 81: 1795–1800.

Polya, D.A., M. Solomon, C.J. Eastoe, and J.L. Walshe, 1986. The Murchison Gorge, Tasmania — A possible cross-section through a Cambrian massive sulfide system. *Econ. Geol.* 81: 1341–1355.

Pouba, Z. and M. Stemprok. 1970. Problems of hydrothermal ore deposition. *In* IUGS Ser. A, no.2 in Stuttgart: 393pp.

Reid, A.Mc., 1925. The Dundas mineral field. *Bull. Geol. Surv. Tas.* 31: 102.

Rivers, W.M., 1975. The geology and geochemistry of the Tullah area. Unpubl. B.Sc. (Hons.) thesis, University of Tasmania: 164 pp.

Ruxton, P.A. and G. Plummer. 1984. Economic geology and fluid inclusion history of the Scamander mineral field and Great Pyramid tin deposit, NE Tasmania. *In* Baillie P. W. & Collins P. L. F. (eds): Mineral Exploration and Tectonic Processes in Tasmania. Geol. Soc. Aust. (Tas. Div.): 45–47.

Rye, D.M. and N. Williams, 1981. Studies of the base metal sulfide deposits at McArthur River, Northern Territory, Australia: III. The stable isotope geochemistry of the HYC, Ridge and Cooley deposits. *Econ. Geol.* 76: 1–26.

Shelton, K.L., 1983. Composition and origin of ore-forming fluids in a carbonate-hosted porrphyry copper and skarn deposit: A fluid inclusion and stable isotope study of Mines Gaspe, Quebec. *Econ. Geol.* 78: 387–421.

Sheppard, S.M.F. and H.P. Schwarcz, 1970. Fractionation of carbon and oxygen isotopes and magnesium between coexisting metamorphic calcite and dolomite. *Contrib. Mineral. Petrol.* 26: 161–198.

Shimazaki, H. and M. Kusakabe, 1990. Oxygen isotope syudy of the Kamioka Zn–Pb skarn deposits, central Japan. *Mineral. Deposita* 25: 221–229.

Solomon, M., 1981. An introduction to the geology and metallic ore deposits of Tasmania. *Econ. Geol.* 76: 194–206.

Solomon, M. and D.I. Groves, (in press). *AUSTRALASIAN ORE DEPOSITS.* Oxford University Press.

Stanton, R.L., 1972. *ORE PETROLOGY.* McGraw–Hill.

Sun, S.S. and P.J. Eadington, 1987. Oxygen isotope evidence for the mixing of magmatic and meteoric waters during tin mineralisation in the Mole Granite, New South Wales, Australia. *Econ. Geol.* 82: 43–52.

Sverjensky, D.A., 1981. Isotopic alteration of carbonate hostd rocks as a function of water to rock ratio — an example from the Upper Mississippi Valley zinc-lead district (Scientific Communication). *Econ. Geol.* 76: 154–157.

Taheri, J. and G.R. Green, 1990. The origin of gold-tin-copper mineralisation at the Lakeside Deposit, western Tasmania. Geol. Rep. Mt. Read Volc. Proj. Tasm. 5. Division of Mines and Mineral Resources.

Taylor, B.E., 1987. Stable isotope geochemistry of ore-forming fluids." *In* T. K. Kyser (ed.): *Short Course in Stable Isotope Geochemistry of Low Temperature Fluids*, 13. Mineralogical Association of Canada, Saskatoon.

Taylor, H.P., 1967. Oxygen isotope studies of hydrothermal mineral deposits. *In* H.L. Barnes (ed.): *GEOCHEMISTRY OF HYDROTHERMAL MINERAL DEPOSITS.* Wiley Intersci., New York.

Taylor, H.P., 1974. The application of hydrogen and oxygen isotope studies to problems of hydrothemal alteration and ore deposition. *Econ. Geol.* 69: 843–883.

Taylor, H.P., 1979. Oxygen and hydrogen isotope relationships in hydrothermal mineral deposits. *In* H.L. Barnes (ed.): *GEOCHEMISTRY OF HYDROTHERMAL ORE DEPOSITS. Second edition.* Wiley Intersci., New York: 236–277.

Truesdell, A.H., 1984. Stable isotopes in hydrothermal systems. In R.W. Henley, A.H. Truesdell, and P.B. Barton (eds): *FLUID-MINERAL EQUILIBRIA IN HYDROTHERMAL SYSTEMS. Rev. Econ. Geol.* 1: 129–142.

Twelvetrees, W.H., 1900. Report on the mineral districts of Zeehan and neighbourhood. Tasmanian Government Geologist Office: 105.

Twelvetrees, W.H., 1906. Report on the Renison Bell tin-field. Rep. to secr. of mines, Tasmania.

Waller, G A., 1902. Report on the tin ore deposits of North Dundas. Rep. to secr. mines, Tasmania.

Warmeant, P., 1990. The geology, geochemistry and mineralisation of the Mount Black Volcanics. Unpubl. B.Sc. Hons. thesis, University of Tasmania.

Whitney, J.A., 1975. Vapor generation in a quartz monozite magma: a synthetic model with application to porphyry copper deposits. *Econ. Geol.* 70: 346–358.

Yeats, C., 1989. The geology and mineralisation of the Henty Au Prospect. Unpubl. B.Sc. Hons. thesis, University of Tasmania.

Zaw, Khin, 1991. The effect of Devonian metamorphism and metasomatism on the mineralogy and geochemistry of the Cambrian VMS deposits in the Rosebery–Hercules district, western Tasmania. Unpubl. Ph.D. thesis, University of Tasmania: 302 pp.

Zaw, Khin and R.R. Large, 1992. The precious metal-rich South Hercules mineralisation, western Tasmania: a possible sub-seafloor replacement volcanic-hosted massive sulfide deposit. *Econ. Geol.* 87: 931–952.

APPENDIX 1 — Field descriptions and isotopic analyses of geological samples discussed in the accompanying report.

FIELD NO.	LOCATION	MINERALOGY	SAMPLE DESCRIPTION	DIP/DIP DIRN.	SLIDE	Oxygen-qz	C13-(PDB)	O18-(SMOW)
PK-1A	388640E/5374560N Lake Makintosh-Sofia Tunnel	Py-Qz-Sph-Chl vein in Murchison volcanics	Vein in Murchison Volc. on contact b/w Owen cong. and chloritised Murchison Volc. with the Cambrian Murchison Granite immediately beneath. The shear zone is syn/post min's with sinistral shear sense or west side up.	Vein 71° to 060°	Fl-Sph	13.30		
PK-1B	388640E/5374560N Lake Makintosh-Sofia Tunnel	Qz-Chl-Py alteration in Owen conglomerate	Alteration in Owen congl. on contact b/w Owen cong. and chloritised Murchison Volc. with the Cambrian Murchison Granite immediately beneath. The shear zone is syn/post min's with sinistral shear sense or west side up.	Vein 71° to 060°				
PK-1C	388640E/5374560N Lake Makintosh-Sofia Tunnel	Qz-Sph-Py alteration in Owen conglomerate	Vein in Owen congl. on contact b/w Owen cong. and chloritised Murchison Volc. with the Cambrian Murchison Granite immediately beneath. The shear zone is syn/post min's with sinistral shear sense or west side up.	Vein 71° to 060°	Fl-Sph	13.30		
PK-1D	388640E/5374560N Lake Makintosh-Sofia Tunnel	Py-Sph-Chl alteration in graded Owen conglomerate?	Alteration in graded Owen congl? on contact b/w Owen cong. and chloritised Murchison Volc. with the Cambrian Murchison Granite immediately beneath. The shear zone is syn/post min's with sinistral shear sense or west side up.	Shear 71° to 060°	Fl-Sph			
PK-2A	388640E/5374560N Lake Makintosh-Sofia Tunnel	Qz crystals in vug for F.I.'s in Owen Conglomerate	Qz crystals in a hydraulic breccia, hosted by qz-arenaceous unit in Owen congl. Breccia fragments have variably oriented cleavage fragments. Kinematic indicators show 2 fault movt's (i) reverse, (ii) wrench. (10m from PK-1)		Fl-Qz	12.00		
PK-3A	388640E/5374560N Lake Makintosh-Sofia Tunnel	Qz vein (buck qz) in Owen congl.	Syn-tectonic milky qz vein with extensional crack-seal textures cross cutting the cleavage. Kinematic striations indicate 2 fault reactivations (i) sinistral-reverse pitching 41°E, (ii) dirn? pitching 77° E. Vein in Owen congl.	Vein 77° to 206°		18.40		
PK-3B	388640E/5374560N Lake Makintosh-Sofia Tunnel	Owen congl.-arenite unit	Arenite unit in Owen congl. sampled next to PK-3A for Oxygen isotopes.			14.00		
PK-4A	388600E/5374530N Lake Makintosh car park	Qz-Py-(Sph) dissem in Owen conglomerate	Disseminated sulphide on the sheared contact b/w Cambrian Murchison Granite and the Owen Congl. Sulphide is hosted in the brecciated Owen. (Photo-Ron)	Contact-Shear 89° to 073°		11.30		
PK-4B	388600E/5374530N Lake Makintosh car park	Py-Qz veinlet in Owen congl. 35cm from cont.	Owen conglomeratic quartzite with a minor veinlet 35cm from the contact.			11.80		
PK-4C	388600E/5374530N Lake Makintosh car park	Qz-Sph-Py vein in Murchison granite	1.5cm sulphide vein 8m into the Murchison granite, and west of PK-4B	Vein 70° to 285°	Fl-Sph	11.70		
PK-5A	388600E/5374560N Lake Makintosh next to shed	Qz-Py-Sph-Chl vein in Murchison granite	Qz-chl-sulph vein in Murchison granite with a K-fels depletion zone of a few cm Late/syn jointing assoc with vein have chl. selvages dev. around them instead o musc. (Photo-Ron)	Vein 81° to 285°	(i)Fl-Sph (ii)Fl-Qz	13.40		
PK-5B	388600E/5374560N Lake Makintosh next to shed	Alteration Murchison granite at edge Qz-Py vein	Alteration front in the Murchison granite out from a Qz-Py vein. Alteration is evident by K-fels being replaced by musc. Late/syn jointing assoc with vein have chl.selvages dev. around them instead of musc.	Vein 64° to 308°	PTS			
PK-6A	388300E/5374170N Tunnel Road Saddle	Qz-Py-Gal vein at contact b/w Owen congl. & Murch. gr.	Shear zone b/w Owen congl. and the Murchison granite with qz-sulphide vein. Chlorite sits on striated joint surfaces and is equivalent to the cleavage develop. Chl. is stretched out along the cleavage in the Devonian shear zone and cut K-fels veins in the Murchison granite.		Fl-Qz	12.10		
PK-6B	388300E/5374170N Tunnel Road Saddle	K-fels rich Murchison gran.	In the Murchison gran. 9m from the sheared contact with the Owen congl. the granite is K-fels rich. This sample has K-fels kinematic fibres on its surface.		PTS			
PK-6C	388300E/5374170N Tunnel Road Saddle	Kfels-Chl alteration in the Murchison granite	In the Murchison granite 7m from the sheared contact with the Owen congl. the granite has Kfels-Chl alteration features.		PTS			
PK-6D	388300E/5374170N Tunnel Road Saddle	Chl±Kfels alteration in the Murchison Granite	In the Murchison granite 1.5m from the sheared contact with the Owen congl. the granite has Chl±Kfels alteration features.		PTS			
PK-7A	387220E/5375390N Murchison Gorge Rd.	Qz-Py vein in Murchison volc. with dissem. Chl-Py	Murchison Volcanics with disseminated Chl-Py alteration and cut by Qz-Chl-Py vein with extension crack-seal fibres. The surface of the outcrop has a lineation parallel to the fibre veins and offset of the vein on this surface is 2m	Vein 38° to 059° Fault 61° to 211° Lineation 42° to 257°	(i)PTS (ii)PTS	11.00		
PK-7B	387220E/5375390N Murchison Gorge Rd.	Qz-Chl vug in Murchison volc. with dissem. Chl-Py	Qz(crystals)-Chl in a vuggy vein in the Murchison Volcanics		Fl-Qz			
PK-7C	387220E/5375390N Murchison Gorge Rd.	Qz-Chl-Kfels vein in Murchison Volcanics	Qz-Chl-Kfels mineralisation from the edge of the PK-7B vein		PTS			
PK-7D	387220E/5375390N Murchison Gorge Rd.	Py-Qz-Chl vein in the Murchison Volcanics	Sinuous crack-seal Qz-Py-Chl veins upto 1m long representing low strain zone - extensional flat veins similar to the Henty Fault. Py & Chl possibly represent remobilised Cambrian mineralisation. It is not assoc. with Devonian Pb-Zn mineralisation which is not seen here. The crack-seal natue of these veins is					

FIELD NO.	LOCATION	MINERALOGY	SAMPLE DESCRIPTION	DIP/DIP DIRN.	SLIDE	Oxygen-qz	C13-(PDB)	O18-(SMOW)
			limited to the margin and Qz-Chl infills the central part of the vein.					
PK-8A	386250E/5376110N Murchison Gorge Rd.	Qz-Hem-Py vein on contact Owen & Eastern Qz-Phyric S.	Contact b/w Owen congl. and the Eastern Qz-Phyric Sequence . A vocanoclastic unit with interbedded conglomeratic material. The eastern qz-phyric sequ. is sericitised & not chloritised as previous locations. Sericitic alteration sits in the cleavage which is oriented N-S (same as Henty Zone) compared to 340° as at earlier locations.		PTS	13.80		
PK-9A	385940E/5376220N Murchison Gorge Rd.	Qz-Kfels-Chl vein in Farrell Slates	Qz-Kfels-Chl crackseal vein and Qz vein in equilibrium with Seric-Kfels alteration of Farrell Slates 50m from the eastern zone of the Henty Fault Zone. Also present are a number of horizontal sigmoidal crack-seal veins suggesting horizontal compression. These veins are upto 0.5m		PTS	12.60		
PK-10A	385870E/5376280N Murchison Gorge Rd.	Chlorite spotted volcanocl. in Farrell Slates	Chlorite spotted volcanoclastic in the Farrell Slates representing ex-pumice fragments flattened during diagenesis and stretched parallel to cleavage.		PTS			
PK-11A	385690E/5376530N Murchison Opencut	Qz(buck) vein in Farrell Slates at Murchison Opencut	Barren buck quartz vein from the hangingwall of the Murchison Opencut on the Murchison Line of Lodes (eastern side).			16.60		
PK-11B	385690E/5376530N Murchison Opencut	(i) Sph-Py-Qz-Carb (ii) Gal-Sph-Py-Qz-Carb (iii) Asp-Sph-Py-Qz-Carb (iv) Qz-Carb-Sph-Gal-Py (v) Py(amorp)-Sph-Gal-Car	Ore samples from the Murchison Opencut. Sample (i) contains Qz material in carbonate that may be O.K. for F.I.'s	Trend of lode 030°	Fl-Sph	13.30	-7.85	15.57
PK-12A	385820E/5379090N New North Farrell Mine	Gal-Carb-Qz dissem in Farrell Slates	Gal-Carb-Qz disseminated mineralisation in Farrel Slates (See last AMIRA Rpt. for info on New North Farrell Mine)	Trend of lode 010°	PTS-large			
PK-12B	385820E/5379090N New North Farrell Mine	Carb-Gal veinlets in Farrell Slates (ore dump)	Carb-Gal veinlets in the Farrel Slates from the New North Farrell Mine dumps		PTS			
PK-12C	385820E/5379090N New North Farrell Mine	Qz vein with Gal veinlets in Farrell Slates	Qz vein with late Gal veinlets cross-cutting and hosted in the Farrell Slates					
PK-12D	385820E/5379090N New North Farrell Mine	Qz-Carb-Gal-Sph vein in Farrell Slates (ore dumps)	Qz vein with Carb-Gal-Sph veinets cross-cutting and hosted in the Farrell Slates. Take from the New North Farrell Mine dumps.		PTS	15.50	-7.39	16.79
PK-12E	385820E/5379090N New North Farrell Mine	Kinked Carbonate vein in Farrell Slates (ore dumps)	Kinked Carbonate vein in Farrell Slates from the New North Farrell ore dumps.		PTS-large			
PK-13A	387570E/5382400N Makintosh Dam	Qz-Chl vein on Henty Fault	Qz-Chl vein in Henty Fault zone on eastern side Makintosh Dam Spillway. Henty Fault benn reactivated 4x (i) Cambrian thrusting assoc. with ultramafics (ii) Normal faulting (iii) Folding due E-W compression (iv) ?		PTS	16.00		
PK-13B	387570E/5382400N Makintosh Dam	Silicified Owen conglomerate on contact Henty Fault	Silicification of the Owen Conglomerate on the contact of the Henty Fault.					
PK14-A	379950E/5380160N Pieman Rd (field test loc.#2)	Qz-Chl crack-seal vein on fault in Central Volcanic Com.	Central Volcanic Complex consisting of massive coarse volcanoclastics with reaction rims on the flow banded rhyolites. The fault contains 1cm wide veins that are brecciated impling that they pedate the last reactivation on the fault. The veins consist of Qz-chl crack-seal textures. Deformation suggests that an earlier ductile phase of deformation predated later brittle deformation. (i) dextral movement on the fault is indicated by the cleavage rotation into the ft. (ii) sinistral movement indicated by the en-echelon veins	Fault 89° to 282° Wrench striations 3°S	PTS-large	11.90		
PK-15A	379780E/5380570N Pieman Rd-Boco Creek	Qz vein with crack-seal text in Central Volcanic Complex	A 10cm qz vein with crack-seal texture weakly developed. An Fe2O3 in fill of some vugs may be ex-carbonate. (Boco Creek Siding at LPD 50 km sign)		Fl-Qz			
PK-15B	379780E/5380570N Pieman Rd-Boco Creek	Qz vein in Central Volcanics Complex (F.I.'s)	Qz vein with clear euhedral crystals in a pumaceous volcanoclastic of the Centra Volcanic Complex.	Vein 30° at 032°	Fl-Qz	12.10		
PK-16A/B	377420E/5378500N Rosebery Fault-Bastyan Dam	Carb-Qz-Py vein in Dundas correlates next Rosebery Ft.	Carb-Qz-Py vein in the Dundas correlates at the edge of the cataclasite zone on Rosebery Fault. The carbonate dominates the mineral assemblage and pyrite is disseminated throughout the sediments with minor amounts in the carbonate. The Dundas correlates resembles a black slate.	Rosebery Fault 45° to 090°	PTS	16.80	-2.40	14.41
PK-17A	377480E/5378470N Rosebery Fault-Bastyan Dam	Silicified Carb vein in hang-ingwall volcanoclastics	A silicified Qz vein in the hangingwall volcanoclastics to the Rosebery Group in the Central Volcanoclastic. 100m above the Rosebery Fault and 30m from the gate to the Bastyan Dam off the Lower Pieman Dam road.		PTS		-2.70	14.22
PK-17B	377480E/5378470N Rosebery Fault-Bastyan Dam	Sph-Carb associated with chlorite veinlets	Chloritised feldspathic volcanoclastics with Sph-Carb associated with veinlets		PTS			
PK-17C	377480E/5378470N Rosebery Fault-Bastyan Dam	Carb vein & Qz vein in HW volcanoclastics	Carbonate and Qz veins in volcanoclastic unit in hangingwall of the Rosebery Ft. Vein formation related to the Rosebery Ft. but is post-cleavage. Sph assoc with		PTS	11.20	-2.51	13.72

FIELD NO.	LOCATION	MINERALOGY	SAMPLE DESCRIPTION	DIP/DIP DIRN.	SLIDE	Oxygen-qz	C13-(PDB)	O18-(SMOW)
			late carbonate. Chlorite is pre-to syn-cleavage and accentuates the cleavage.					
PK-18A	385420E/5380040N Lake Rosebery-Makintosh Bdg	Kfels-Alb-Chl overprinted by Epid-Qz-(Kfels) in CVC.	Central Volcanics Complex consisting of Kfels-Alb-Chl overprinted by Epid-Qz-Kfels at ~400°C. Qz occurrence some what controlled by brittle fractures in Epid Alteration not really different to alteration in the Murchison Volcanics. Alteration probably controlled by porosity differences, ie., alteration of early carbonate produced by volume controlled mineral replacement.		PTS-large	13.00		
PK-18B	385420E/5380040N Lake Rosebery-Makintosh Bdg	Late Qz vein in CVC	Barren Qz vein cross-cutting the CVC		PTS	14.00		
PK-19A	388060E/5384040N Near Tullabadine boat ramp	Qz veins with crack-seal text in Farrell Slates	Crack-seal quartz veins in Farrell Slates shows fibres developed normal to the vein edge. Suggests that the Devonian east-west compression seen in the striat are similar to the Henty Fault.	Vein 15° to 068°	Fl-Qz	14.90		
PK-19B	388060E/5384040N Near Tullabadine boat ramp	Carbonate vein in the Farrell Slates	Siderite(?) vein in the Farrell Slates probably rock buffered.	Vein 40° to 122°	PTS	13.60	-1.23	14.90
PK-20A	387590E/5383270N Quarry Tullabadine Rd	Qz-Carb-(Py) en-echelon veins in Farrell Slates	Qz-Carb-(Py) extensional, flat lying en-echelon veins developed off more vertical fibre veins. Two sets of flat lying extensional veins occur. (i)Early set show en-echelon development off the main vertical fibre vein (ii) Late set show flat flat horizontal vein development.	Fibre Veins 49° to 298° Fibres Pitch 60°S Extensional Veins (i) 21° to 025 (ii) 50° to 105°			-1.15	14.89
PK-20B	387590E/5383270N Quarry Tullabadine Rd	Qz-Carb-Chl fibre vein in Farrell Slates	Qz-Carb-Chl fibre vein in Farrell Slates against which the extensional fibre veins develop as flat lying en-echelon veins containing Qz-Carb.		PTS	14.90		
PK-21A	385340E/5375090N Murchison Hwy-Sth Tullah	Qz-Py-Gal-(Bte)? vein in Farrell Slates	Qz-Py-Gal-(Bte)? vein sets on the Murchison Hwy south of Tullah but before the Anthony Rd turn off. A number of generations of mineralisation can be seen of which Gal-Py-Qz was the last. 10-20cm wide.	Vein 61° to 246°	Fl-Qz			
PK-21B	385340E/5375090N Murchison Hwy-Sth Tullah	Gal-Sph-Py-Qz vein in Farrell Slates	Qz-Sph-Py-Qz-vein in the Farrell Slates on the Murchison Hwy south of Tullah but before the Anthony Rd turn off. 10-20cm wide.	Vein 77° to 236°	Fl-Sph	12.60		
PK-21C	385340E/5375090N Murchison Hwy-Sth Tullah	Qz-Flu-Py vein in the Farrell Slates	Qz-Flu-Py vein 2cm wide and occurring 10cm north of 21B.		Fl-Qz	9.60		
PK-21D	385340E/5375090N Murchison Hwy-Sth Tullah	Gal-Py vein in Farrell Slates volcanoclastic unit	Gal-Py vein 1-5cm wide overprinting an earlier Qz-Kfels? vein in a volcanoclastic unit in the Farrell Slates	Vein 82° to 252°	Fl-Qz/Sph	12.40		
PK-21E	385340E/5375090N Murchison Hwy-Sth Tullah	Qz-Kfels-Carb en-echelon veins in Farrell Slates	Flat extensional Qz-Kfels-Carb en-echelon veins (?? with crack-seal texture ??) occurring on the margins of sub-vertical veins (faults?) with base metal mineralisation. Source of the Kfels: (i) Kfels in the volcanoclastics been remobilised around the en-echelon veins. (ii) Sourced from the granites -Cambrian/Devonian?- but the distribution of Kfels doesn't support this interpretation as it occurs on the margins of these veins. (iii) Textural variation of the host rocks approaching the veins changes and the cleavage is stronger away from the vein - implying the development of syn-cleavage veins with associated extensional en-echelon veins developed normal to the main vein which also has late sulphides associated with brittle reactivations	Extensional Veins (i) 62° to 092° (ii) 38° to 090°	PTS	14.70		
PK-22A	385620E/5374340N Anthony Rd 2km Tullah T-off	Qz-Py-Chl vein in Quartz Phyric Sequence	Silicified fault in the quartz Phyric Sequence. The fault contains Py-Chl veins and in the handspecimen can see an alteration zonation	Fault 63° to 260°	PTS	12.60		
PK-22B	385620E/5374340N Anthony Rd 2km Tullah T-off	Qz-Chl-Kfels en-echelon veins in Qz-Phyric Sequence	10m east of 22A massive quartz phyric volcanics sequence has 30-50cm high near verticle en-echelon Qz-Chl-Kfels veins. These steep en-echelon veins represent overturning of a syncline as approach the Henty Fault. Further along the road the en-echelon veins represent the same generation of veins but are much flatter.		PTS	12.50		
PK-22C	385620E/5374340N Anthony Rd 2km Tullah T-off	Py-Qz-(Gal-Sph) alteration zone in Qz-Phyric Sequence	An alteration zone of Py-Qz with minor Gal-Sph but Kfels depleted in quartz Phyric Sequence.		Fl-Qz/Sph			
PK-22D	385620E/5374340N Anthony Rd 2km Tullah T-off	Kfels-Qz alteration in Qz-Phyric Sequence	A zone of Kfels-Qz alteration in the quartz Phyric Sequence		Fl-Qz			
PK-22E	385620E/5374340N Anthony Rd 2km Tullah T-off	Chloritic alteration in Qz-Phyric Sequence	A zone of chloritic alteration in the Quartz Phyric Sequence.		PTS			
PK-23A	386660E/5369690N	Epidote alteration in the	Murchison Granite with epidote alteration developed on Devonian? fault(thrust)		PTS	12.40		

FIELD NO.	LOCATION	MINERALOGY	SAMPLE DESCRIPTION	DIP/DIP DIRN.	SLIDE	Oxygen-qz	C13-(PDB)	O18-(SMOW)
	Anthony Dam Rd-150m down	Murchison Granite	surface. Good Qz-Epid fibres developed on the surface					
PK-23B	386660E/5369690N	Kfels-Epid altered	Sample Kfelpar-epidote altered Murchison granodiorite. Appears to be a		PTS			
	Anthony Dam Rd-150m down	Murchison Granite	concentration of Kfelspar along the Qz-Epid striated veins.					
PK-24A	381940E/5373230N	Qz vein in the Mt Black	Quartz vein in the Mt Black volcanics but without any sign of crack-seal textures	Vein	PTS	11.30		
	Murchison Hwy-Mt Black	Volcanics	developed. The Mt Black Volcanics have quite a chloritic nature to them.	67° to 285°				
PK-24B	381940E/5373230N	Qz-Chl vuggy vein in the	15m north of PK-24A is a Qz-Chl vuggy vein sub parallel to the other vein.		Fl-Qz			
	Murchison Hwy-Mt Black	Mt Black Volcanics						
PK-25A	378410E/5373310N	Tour-Qz vein in Footwall	Tourmaline-Quartz vein at Rosebery below the bottom Pub within the Footwall	Vein	PTS	13.90		
	Rosebery below bottom Pub	Volcanics of Rosebery Mine	Volcanics of the Rosebery Orebody. The vein sits within the cleavage of the	53° to 079°				
			volcanics and has a brecciated texture.					
PK-26A	378240E/5372620N	Tour vein & silicification	Tourmaline vein and silicification in the Footwall Volcanics of the Rosebery host	Vein	PTS			
	Sth Rosebery TownBoundary	in Footwall Volcanic	rocks. The vein is 1cm wide and only 30m away from the Rosebery Ft to the we	63° to 082°				
PK-27A	377780E/5371720N	Tour-Py vein overprinting	Tourmaline with minor pyrite overprinting quartz in the Footwall Volcanics of		PTS	15.30		
	Salisbury Mine	Qz in the Footwall Volcanics	the Rosebery Hostrocks.					
PK-28A	377640E/5371370N	Tour disseminations in the	Tourmaline disseminations in the Footwall Volcanics of the Rosebery Fault	Fault		15.20		
	Chamberlain Mine	Footwall Volcanics	(Very poor sample)	53° to 122°				
PK-29A	378440E/5374000N	Qz-Rhod bouden from J-lens	Quartz -Rhodochrosite bouden from the J-lens of the Rosebery Orebody			14.00	???	
	Rosebery Mine	Rosebery Mine						

APPENDIX 2 — A compilation of carbon and oxygen isotopes from Cambrian hydrothermal carbonates, western Tasmania.

NORTH END - ROSEBERY

SAMPLE NO.	REFERENCE	LOCATION	MINERALOGY/TEXTURE	C-PDB	O-SMOW
60482-950mN	Dixon, 1980	N.end, Rosebery/A&B lens	spherulitic, colloform carbonate	-4.30	9.90
1120mN-1,15L	Khin Zaw, 1990	N.end, Rosebery/A&B lens	massive carbonate	-5.00	11.40
1120mN-3,15L	Khin Zaw, 1990	N.end, Rosebery/A&B lens	spotty carbonate	-1.80	11.20
1120mN-4,15L	Khin Zaw, 1990	N.end, Rosebery/A&B lens	spotty carbonate	-1.20	11.80
1250mN-1,15L	Khin Zaw, 1990	N.end, Rosebery/A&B lens	vein carbonate-chlorite-chalcopy	-2.40	10.70
R3374@114.5m	Khin Zaw, 1990	N.end, Rosebery/A&B lens	massive pink carbonate	-5.00	11.70
R3394@175.3m	Khin Zaw, 1990	N.end, Rosebery/A&B lens	vein carbonate	-9.00	11.40
R3394@175.3m	Khin Zaw, 1990	N.end, Rosebery/A&B lens	vein carbonate	-8.50	11.50
R3421@116.5m	Khin Zaw, 1990	N.end, Rosebery/A&B lens	spotty carbonate	-1.40	10.80
R3456@288.5m	Khin Zaw, 1990	N.end, Rosebery/A&B lens	vein carbonate	-3.70	11.30
R4297B@35.5m	Khin Zaw, 1990	N.end, Rosebery/A&B lens	vein carbonate-chlorite-quartz	-3.30	12.40
R4482@72.5m	Khin Zaw, 1990	N.end, Rosebery/A&B lens	spherulitic carbonate	-0.60	11.90
R4482A@72.8m	Khin Zaw, 1990	N.end, Rosebery/A&B lens	vein carbonate-chlorite-quartz	-3.20	10.60

SOUTH END - ROSEBERY

SAMPLE NO.	REFERENCE	LOCATION	MINERALOGY/TEXTURE	C-PDB	O-SMOW
60372-196mN	Dixon, 1980	S.end, Rosebery/D,E,G,H lens	recrystallised massive carbonate	-3.40	10.80
60390-238mN	Dixon, 1980	S.end, Rosebery/D,E,G,H lens	packed carbonate spherulite	-1.80	11.80
60417-219mN	Dixon, 1980	S.end, Rosebery/D,E,G,H lens	carbonate concretion	-3.90	11.60
60419-227mN	Dixon, 1980	S.end, Rosebery/D,E,G,H lens	recrystallised brecciated carbonate	-3.40	10.90
60469-260mN	Dixon, 1980	S.end, Rosebery/D,E,G,H lens	nodular carbonate pod	-1.50	10.70
60477-255mN	Dixon, 1980	S.end, Rosebery/D,E,G,H lens	zoned dolomite rhomb	-2.70	11.70
60486-455mN	Dixon, 1980	S.end, Rosebery/D,E,G,H lens	colloform, layed carbonate	-2.70	12.20
60488-245mN	Dixon, 1980	S.end, Rosebery/D,E,G,H lens	vein carbonate-quartz	-4.40	11.20
60498-139mN	Dixon, 1980	S.end, Rosebery/D,E,G,H lens	massive carbonate (nodular?)	-0.70	11.30
17L-1	Khin Zaw, 1990	S.end, Rosebery/D,E,G,H lens	spherulitic carbonate	-1.50	12.60
R1477-5@992'	Khin Zaw, 1990	S.end, Rosebery/D,E,G,H lens	spotty carbonate	-1.90	12.40
R1477-9@1047'	Khin Zaw, 1990	S.end, Rosebery/D,E,G,H lens	massive pink carbonate	-2.40	10.70
R1625@1016'	Khin Zaw, 1990	S.end, Rosebery/D,E,G,H lens	bleby pink carbonate	-2.80	10.70
R1770-14@?	Khin Zaw, 1990	S.end, Rosebery/D,E,G,H lens	bleby or patchy carbonate?	-4.10	10.60
R3011-25@182'	Khin Zaw, 1990	S.end, Rosebery/D,E,G,H lens	bleby brown carbonate	-6.50	13.90
R3011-25@182'	Khin Zaw, 1990	S.end, Rosebery/D,E,G,H lens	bleby brown carbonate	-7.10	13.00

R3024-4@142'	Khin Zaw, 1990	S.end, Rosebery/D,E,G,H lens	brecciated, bleby carbonate	-3.60	11.90
R3034-10@112'	Khin Zaw, 1990	S.end, Rosebery/D,E,G,H lens	vein carbonate	-1.70	10.90
R3491-1@17'	Khin Zaw, 1990	S.end, Rosebery/D,E,G,H lens	massive pink carbonate	-2.20	11.20
60351-273mS	Dixon, 1980	S.end, Rosebery/D,E,G,H lens	recryst. mass carb.(relict colloform)	-2.00	10.20
60366-583mS	Dixon, 1980	S.end, Rosebery/D,E,G,H lens	bleby or poddy carbonate	-3.30	11.20
60396-238mS	Dixon, 1980	S.end, Rosebery/D,E,G,H lens	brecciated, blebby carbonate	-2.20	10.90
60397-226mS	Dixon, 1980	S.end, Rosebery/D,E,G,H lens	recrystallised massive carbonate	-1.40	12.40

HERCULES

SAMPLE NO.	REFERENCE	LOCATION	MINERALOGY/TEXTURE	C-PDB	O-SMOW
H802@114'	Khin Zaw, 1990	Hercules	massive pink carbonate	-0.90	14.30
H802@71'	Khin Zaw, 1990	Hercules	vein pink carbonate	-2.30	13.90
H802A@71'	Khin Zaw, 1990	Hercules	massive pink carbonate	-1.60	13.20
H1032-4B@200'	Khin Zaw, 1990	Hercules	bleby or patchy carbonate	-0.50	13.20
H831-4B@80'	Khin Zaw, 1990	Hercules	massive pink carbonate	-3.30	10.80
H1033-2@120'	Khin Zaw, 1990	Hercules	spotty carbonate	-0.90	12.20
H1062-4@199'	Khin Zaw, 1990	Hercules	spotty carbonate	-2.40	8.70
M lens	Khin Zaw, 1990	Hercules	massive carbonate	-2.10	13.00

SOUTH HERCULES

SAMPLE NO.	REFERENCE	LOCATION	MINERALOGY/TEXTURE	C-PDB	O-SMOW
H1108-1@29.5m	Khin Zaw, 1990	South Hercules	massive carbonate	-1.30	15.00
H1108-1@29.5m	Khin Zaw, 1990	South Hercules	vein pink carbonate-quartz	-2.20	13.40
H1132-5@74.0m	Khin Zaw, 1990	South Hercules	pink carbonate	-3.50	9.80
H1132-3@64.0m	Khin Zaw, 1990	South Hercules	massive pink carbonate	-3.20	11.10
H1142-5@45.7m	Khin Zaw, 1990	South Hercules	vein pink carbonate	-1.90	13.20
H1117-B@21.0m	Khin Zaw, 1990	South Hercules	bleby pink carbonate	-1.00	15.40
H1108-4@36.2m	Khin Zaw, 1990	South Hercules	coalesced spherulitic carbonate	-1.80	13.70
H1108-3A@34.5m	Khin Zaw, 1990	South Hercules	vein pink carbonate	-2.80	12.60
H1108-3A@34.5m	Khin Zaw, 1990	South Hercules	massive pink carbonate	0.60	16.70
H1108-10A@50.2m	Khin Zaw, 1990	South Hercules	spherulitic carbonate	-3.50	9.90
H1108-10A@50.2m	Khin Zaw, 1990	South Hercules	vein pink carbonate	-3.40	12.70
H1108-3B@35.2m	Khin Zaw, 1990	South Hercules	massive pink carbonate	-1.70	12.80

MOUNT BLACK VOLCANICS

SAMPLE NO.	REFERENCE	LOCATION	MINERALOGY/TEXTURE	C-PDB	O-SMOW
74R 7	Warmeant, 1990	Mount Black Volcanics	massive carbonate	-0.70	9.60
74R 7	Warmeant, 1990	Mount Black Volcanics	massive carbonate	-0.30	9.90
60 R	Warmeant, 1990	Mount Black Volcanics	massive carbonate	-0.40	9.80
MBD 2 G	Warmeant, 1990	Mount Black Volcanics	vein carbonate	-1.90	8.80

HENTY GOLD MINE

SAMPLE NO.	REFERENCE	LOCATION	MINERALOGY/TEXTURE	C-PDB	O-SMOW
HP013-588.8m	Yeats, 1989	Henty Gold Mine	Fe-calcite with silica-hem-py	-1.07	10.42
HP013-589.8m	Yeats, 1989	Henty Gold Mine	Calcite with minor silica-ser	0.45	9.88
HP013-590.1m	Yeats, 1989	Henty Gold Mine	Fe-calcite with silica-ser-py alt.	-1.49	13.07
HP013A-587.3m	Yeats, 1989	Henty Gold Mine	Calcite with coarse pyrite bands	-0.83	9.66
HP013A-587.3m	Yeats, 1989	Henty Gold Mine	Fe-calcite with coarse pyrite bands	-0.95	9.09
HP047-446.3m	Yeats, 1989	Henty Gold Mine	Calcite with silica-ser alteration	-1.76	10.20
HP047-446.3m	Yeats, 1989	Henty Gold Mine	Fe-calcite with silica-ser alt.	-2.30	9.57
HP047-447.3m	Yeats, 1989	Henty Gold Mine	Calcite with minor ser alt.	-1.60	9.78
HP047A-447.35m	Yeats, 1989	Henty Gold Mine	Calcite with sericite alteration	-1.99	9.96
HP047A-447.35m	Yeats, 1989	Henty Gold Mine	Fe-calcite with sericite alteration	-1.69	9.52
HP047A-449.3m	Yeats, 1989	Henty Gold Mine	Fe-calcite with silica-hem-py	-1.33	9.82
HP049A-933.5m	Yeats, 1989	Henty Gold Mine	Pure white calcite	-0.31	9.89
HP049A-933.5m	Yeats, 1989	Henty Gold Mine	Pure white calcite	-0.02	9.87
HP049A-933.5m	Yeats, 1989	Henty Gold Mine	Pure white Fe-calcite	-0.36	9.67
HP071-266.3m	Yeats, 1989	Henty Gold Mine	Hanging wall calcite-hematite vein	-2.66	9.81
HP077-258.1m	Yeats, 1989	Henty Gold Mine	Hanging wall calcite-hematite vein	-3.34	9.29

Rosebery Fault — cleavage domains

Ron F. Berry
CODES Key Centre

ABSTRACT

A study of the cleavage relationships along the Rosebery Fault demonstrated a close spatial relationship between the fault and a late N-striking cleavage (S_2). This cleavage occurs in the hanging wall at Rosebery but in the footwall in the Pieman River. The form of the cleavage reflects the thermal conditions during Devonian granitoid emplacement. An earlier cleavage was recognised at all localities. In general, this cleavage was not visible in the most intense zones of S_2 cleavage development but a zone of overprinting was found on the edge of the zone of S_2 development. The earlier cleavage has a composite origin including both a NNW-striking Devonian cleavage and a N-striking cleavage of Devonian or Cambrian age.

INTRODUCTION

Section 8 of the project, is a detailed study of the spatial and temporal relationships of the cleavage formation, folding and faulting along the Rosebery Fault from Rosebery Lodes to the Pieman River. The aim was to look for evidence that the Rosebery Fault had a Cambrian history. The previous work along this section of the Rosebery Fault had failed to detect any evidence for such and early history but had not concentrated on the cleavage relationships near the fault.

The original interpretation from this section was that a NNW-striking regional cleavage is overprinted by a local N-striking cleavage. The NNW cleavage is considered a Devonian structure based on the fact that this is the orientation of cleavage in Silurian and Devonian rocks in the Huskisson syncline and that the cleavage in the younger rocks is similar in intensity and style to that in the Cambrian stratigraphy. The N-striking cleavage is a local effect developed within 500 m of the Rosebery Fault and was interpreted to have no separate regional significance. Aerden (1991) had reported similar local overprinting of a regional cleavage.

The work concentrated at accessible locations with good outcrop. These can be roughly grouped in three locations.

PIEMAN RIVER

The Pieman River provides excellent near continuous outcrop across the Rosebery Fault. At this point the hanging wall is rigid Central Volcanic Complex (CVC) and shows a modest cleavage development in quartz feldspar-rich volcaniclastic rocks. For example at location 2 (Fig. 1, 37756E 537844N), 60 m east of the fault, only one cleavage is visible in hand specimen and this strikes 330°–350°. In thin section there is a very weak preferred orientation of white mica in this rock.

Fifty centimetres west of the Rosebery Fault the CVC is strongly altered. In hand specimen there is little evidence of the fault structure. In thin section the texture has been strongly modified with extensive alteration but there is no strong foliation.

At the Rosebery Fault there is a distinct 5 m cataclastic zone. The hanging wall side of this zone is a 5 cm zone of white pug largely produced from the hanging wall block. The remainder of the cataclasite zone is composed of cataclastic rock derived from the footwall quartz dominated metasediments. Within this zone only the cataclastic cleavage is recognisable.

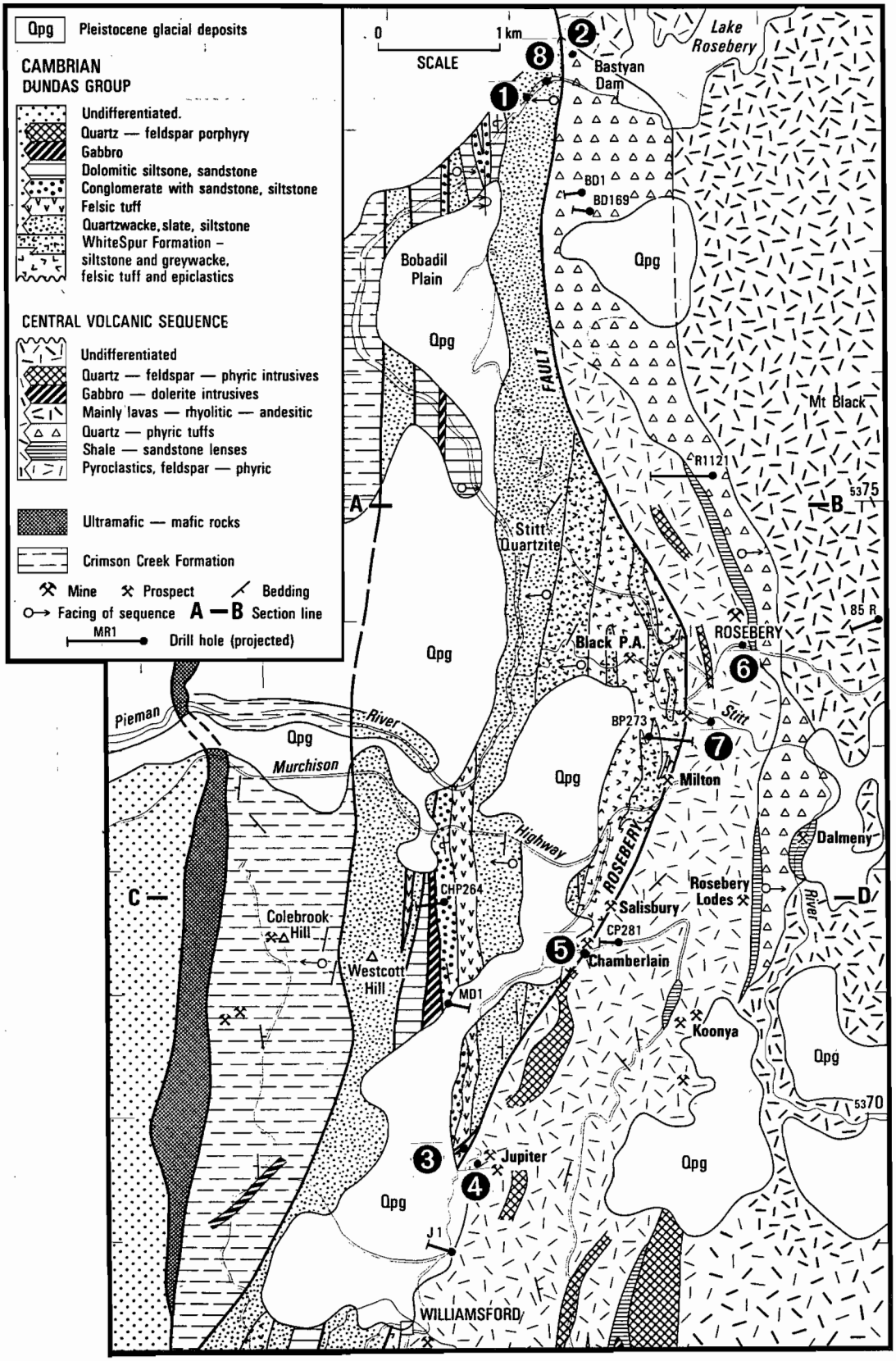

FIG. 1 — Geology of the Rosebery area showing locations mentioned in the text. Geology from Corbett & Lees (1987).

The next 60 m into the footwall is proto-cataclasite. In outcrop this section is dominated by a fault related cleavage. This is also a zone of intense carbonate-quartz veining. The cleavage disrupts all layering and the quartz-ankerite veining. It overprints the regional cleavage. In thin section, the foliation within the fault zone is dominated by pressure solution and while the earlier cleavage is folded and faulted there is no evidence for new white mica. Carbonate is the most mobile phase and is concentrated into veins and strain shadows.

On the edge of this proto-cataclasite zone, the later deformation is less intense and for a few metres the interference between the two deformation events can be recognised as folds (Figs 2, 3a). Both bedding and the regional NNW cleavage are folded and the axial plane cleavage is parallel to the cataclastic cleavage in the adjacent zone (Figs 2, 4). The axial plane cleavage to these folds is exclusively a pressure solution surface. I could find no evidence that white mica was newly crystallised in this orientation. There is some rotation into this direction. Associated with this cleavage are a few fibre veins which are ankerite-dominated with minor quartz.

Further into the footwall of the Rosebery Fault no overprinting cleavage is recognised even though folds of the same geometry are exposed (Fig. 2). The high strain overprint is very restricted in its distribution. At location 1 in Figure 1, far from the Rosebery Fault, there is a single cleavage. The large variation in mica orientation around sand grains makes it difficult to pick up any other orientation. The foliation here apparently includes a component of the original bedding foliation represented by the detrital white mica.

WILLIAMSFORD ROAD

South of Rosebery the Rosebery Fault is exposed at several localities. Near the Jupiter prospect there is an intense cleavage in the fault zone and footwall. The cleavage has a zone of shallow dip at the fault position, about 50°/115°, but otherwise is steep to the east. The zone of a single strong N-striking cleavage is at least 200 m wide in this area. The regional cleavage is very difficult to find within this zone which is roughly symmetrical with respect to the position of the Rosebery Fault as mapped by Lees (1987)

Diamond shaped cleavage patterns were recognised in massive rocks in the footwall (e.g. location 3, 376610E 537010N 150 m west of the fault). Here the two orientations are an early pervasive cleavage dipping 89° to 245° and a late spaced cleavage dipping 84° to 268°. In thin section, white mica occurs in discrete zones against a matrix of very fine grained quartz and feldspar. (?devitrified glass). There are two discrete sets of mica surfaces. An early closer spaced set which is crenulated and a late wider space and discontinuous cleavage (Fig. 3b). Both surfaces are very weak.

At location 4 (37663E 536955N),in the hanging wall of the Rosebery Fault near Jupiter, a diamond shape pattern was recognised with a weaker cleavage striking 330° in a zone dominated by a cleavage striking 010° (78°/088°,74°/095° nearby).

Sample 93/2 comes from 50 m from the major fault position. At this locality only one cleavage is visible in hand specimen. In thin section, the dominant cleavage show evidence of an extensional crenulation cleavage and the interpretation is more

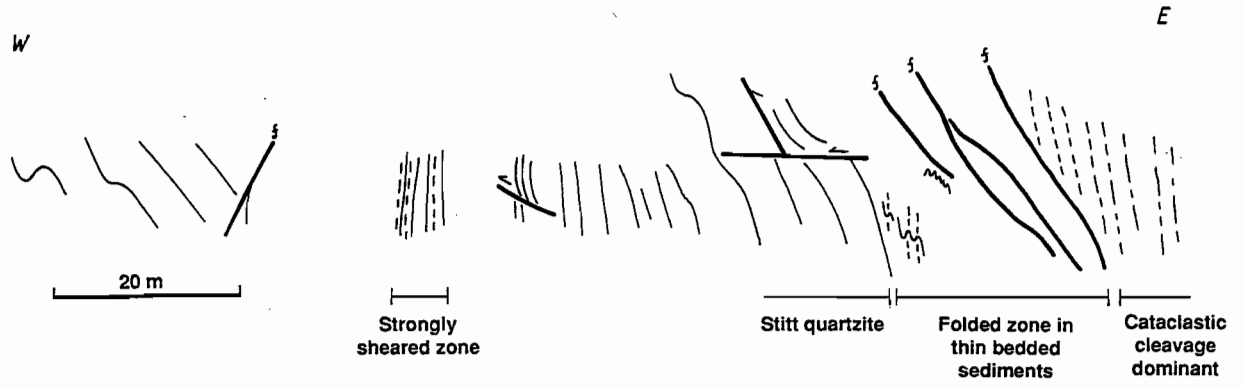

FIG. 2 — Sketch of structure west of the Rosebery Fault in the Pieman River.

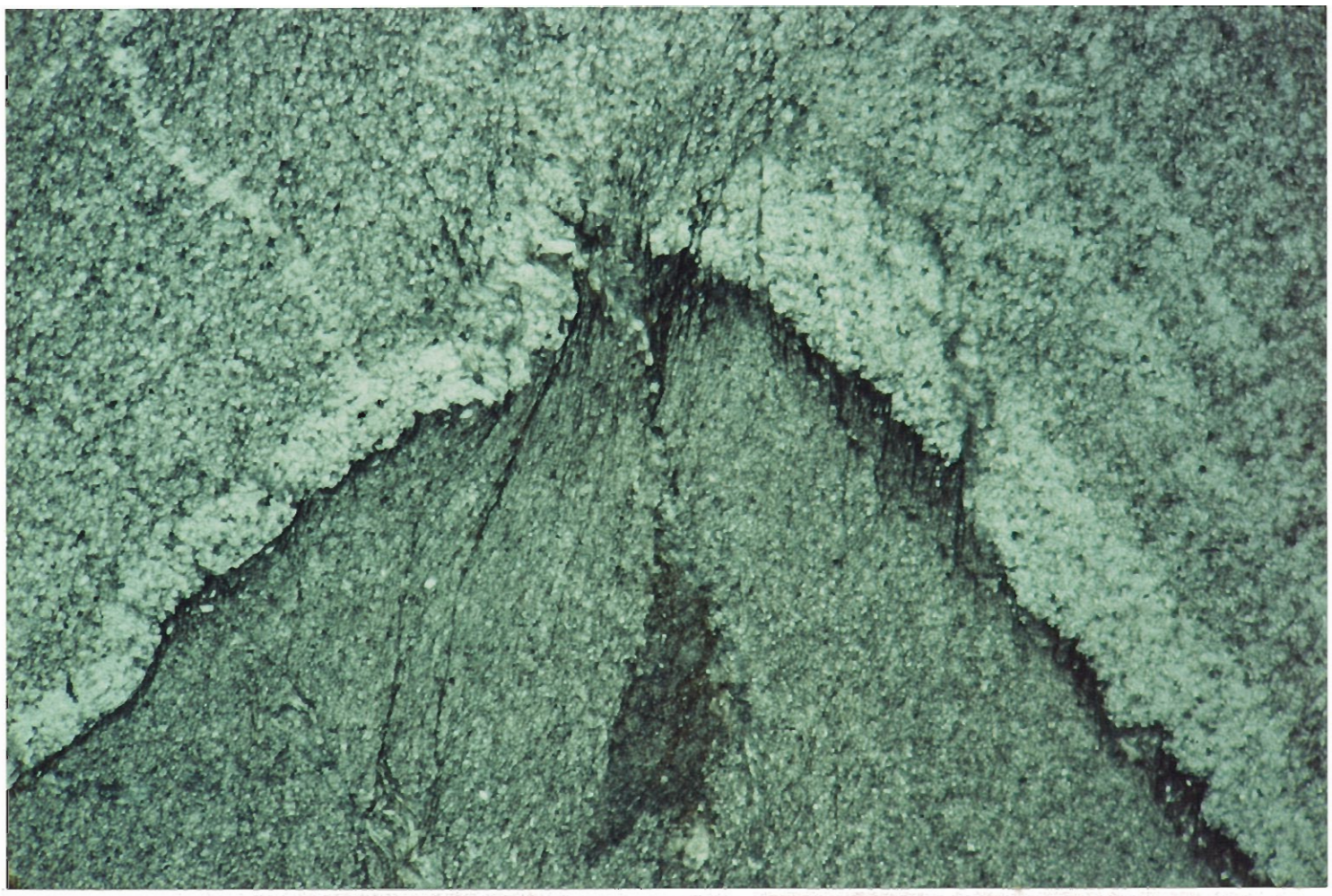

FIG. 3 — (a) Photographs of F_2 folds on the margin of the cataclasite zone in the Pieman River. Note the axial plane structure which is a pressure solution surface. The field of view is 10 × 15 mm.

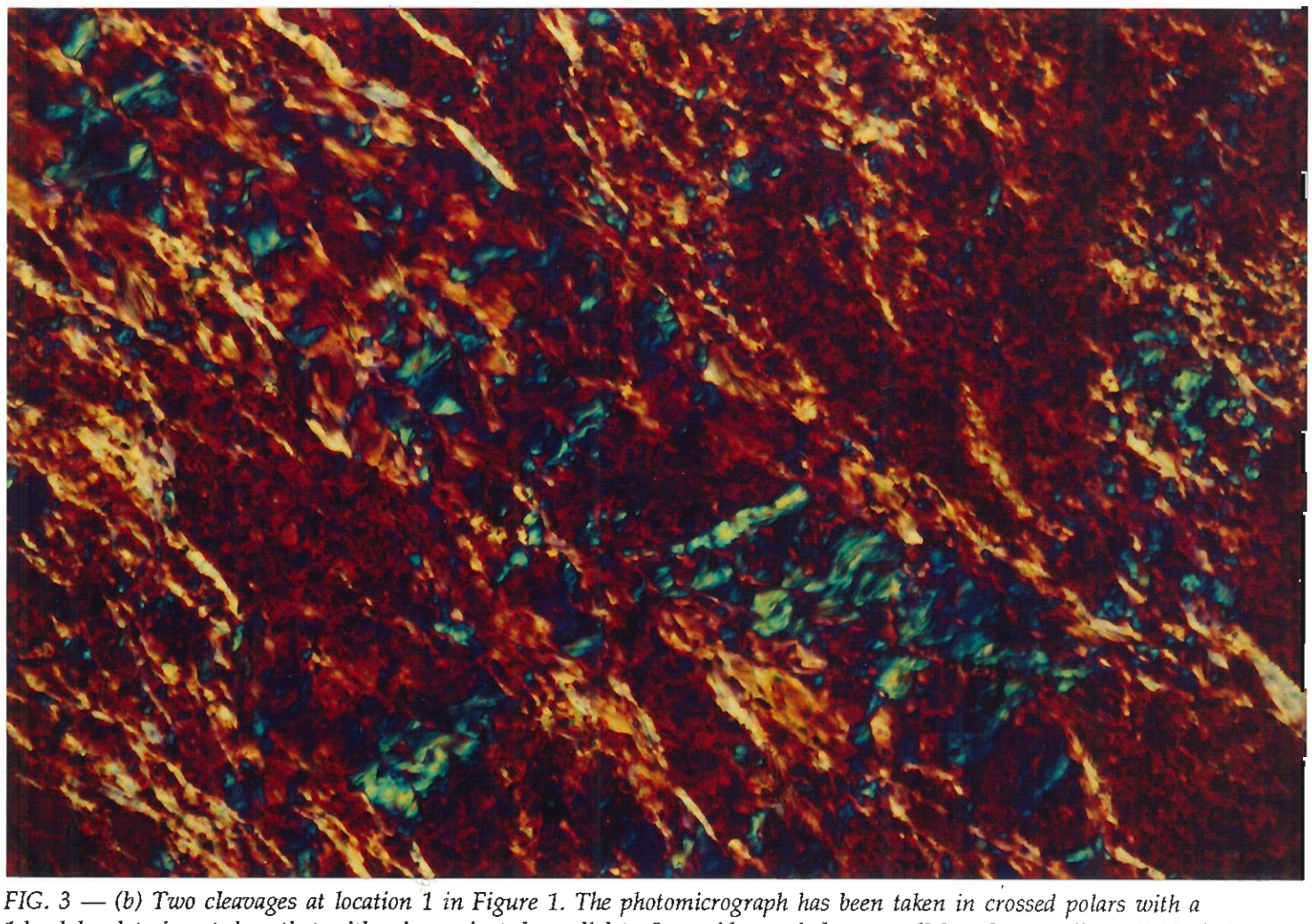

FIG. 3 — (b) Two cleavages at location 1 in Figure 1. The photomicrograph has been taken in crossed polars with a 1 lambda plate inserted so that with micas oriented parallel to S_1 are blue and those parallel to S_2 are yellow. Field of view is 0.3 × 0.5 mm.

blank

difficult. I interpret this structure as a composite fabric resulting from rotation of a pre-existing fabric into the new orientation. An alternative is to assume this is a strongly rotational fabric in which the texture is mylonitic. The argument against the latter interpretation is the complete lack of evidence for strong rotation in the larger crystals and the general lack of highly rotational textures. The recognition of composite fabrics where early cleavages are close in orientation to later cleavages has been documented in a number of areas. The main feature to be recognised here is that the initial separation of 30° means the two cleavages can only be discerned when the strain is low so that the initial fabric is not strongly rotated or the deformation mechanism does not involve any homogeneous flattening. A discussion of the latter effect is given below..

In some locations, such as in the footwall to Rosebery Lodes, extensional crenulation cleavages have been interpreted as sense of shear indicators. Without any prior consideration of whether the crenulations are synchronous with the coexisting cleavage or any other evidence for a strongly rotational cleavage and extensive recrystallisation this style of interpretation is invalid. Shear bands can only be used after a mylonitic origin is demonstrated.

At Chamberlain, on the Mt Read Road, the Rosebery Fault occupies a zone of intense cleavage development with a steep cleavage striking 010°–020°. Here the zone of fault cleavage is about 100 m wide. At the extreme western end of outcrop (location 5 in Fig. 1) in the roadside the fault cleavage is weaker and it is possible to recognise another cleavage direction. At this locality the two space cleavages have strikes of 350° and 010°.

In thin section this rock has two cleavage orientations. The white mica is concentrate in patches and seams within a fine grained quartz ?feldspar matrix. The mica has two distinct extinction directions 30° to 50° apart. The earlier cleavage is weaker and has an irregular shape associated with the extensional crenulations which also define areas of strong concentration of S_2 parallel white mica. Again, the form has some similarities with mylonite texture but these rocks are not strongly deformed. The quartz phenocrysts are essentially undeformed. There are no rotational fabrics associated with these phenocrysts. Even area of recrystallised quartz are not strongly stretched. There are no rotated pressure shadows. In fact pressure shadows are very weakly developed. As all these indicate a very low strain for this rock a progressive rotational strain is not an acceptable interpretation for the composite cleavage development.

At this locality, the hanging wall to the Rosebery Fault is composed of rocks that are very massive and have a weak cleavage striking 350°. In conclusion in the near vicinity of the Rosebery Fault there is a strong cleavage striking 000°–010° but on the edge of a zone of strain about 100 m wide a 330°–345° striking cleavage is also visible.

ROSEBERY MINE LEASE

At Rosebery, the geometry of the Rosebery Fault is slightly different. Firstly the major footwall alteration to the Rosebery deposit has substantially modified the mineralogical composition of the area east of the Rosebery Fault, that is the hanging wall is much softer because of the alteration. The immediate effect is that the local additional cleavage associated with the Rosebery Fault is widespread in the hanging wall to the fault. For example, at location 6 (Fig. 1) in the immediate footwall to the Rosebery deposit, two cleavages are readily recognised in thin section. S_2 dominates the fabric but an apparently earlier weak cleavage is visible. The general appearance again is of an extensional crenulation cleavage.

The rocks west of the fault are not substantial altered and a similar distribution of footwall strain to that in the Pieman River might have been expected. Despite excellent exposures along the Flume Road no equivalent of the footwall cataclasites at the Pieman River were found. My rationalisation of this difference is that the sericite-altered zone east of the Rosebery Fault is softer than the Rosebery Group and therefore the ductile strain associated with the Rosebery Fault is partitioned into the sericite alteration. Further north where the CVC is not strongly altered the ductile strain is partitioned into the Rosebery Group. To the south there is less contrast between the walls and both sides have a zone of ductile strain.

The Rosebery Group west of the Mine lease has an additional complicating feature. In this zone the dominant cleavage strikes 350°–015° rather than expected 340°–355°. This cleavage has the same appearance as the regional NNW cleavage elsewhere. This could be interpreted as:

1. A complete overprint by the S_2 cleavage.

   This seems very unlikely since this cleavage orientation is maintained up to 1 km from the fault.

2. An anomalous original orientation for the Devonian S_1.

   The assumption here is that the Devonian NNW cleavage has a modified orientation because of

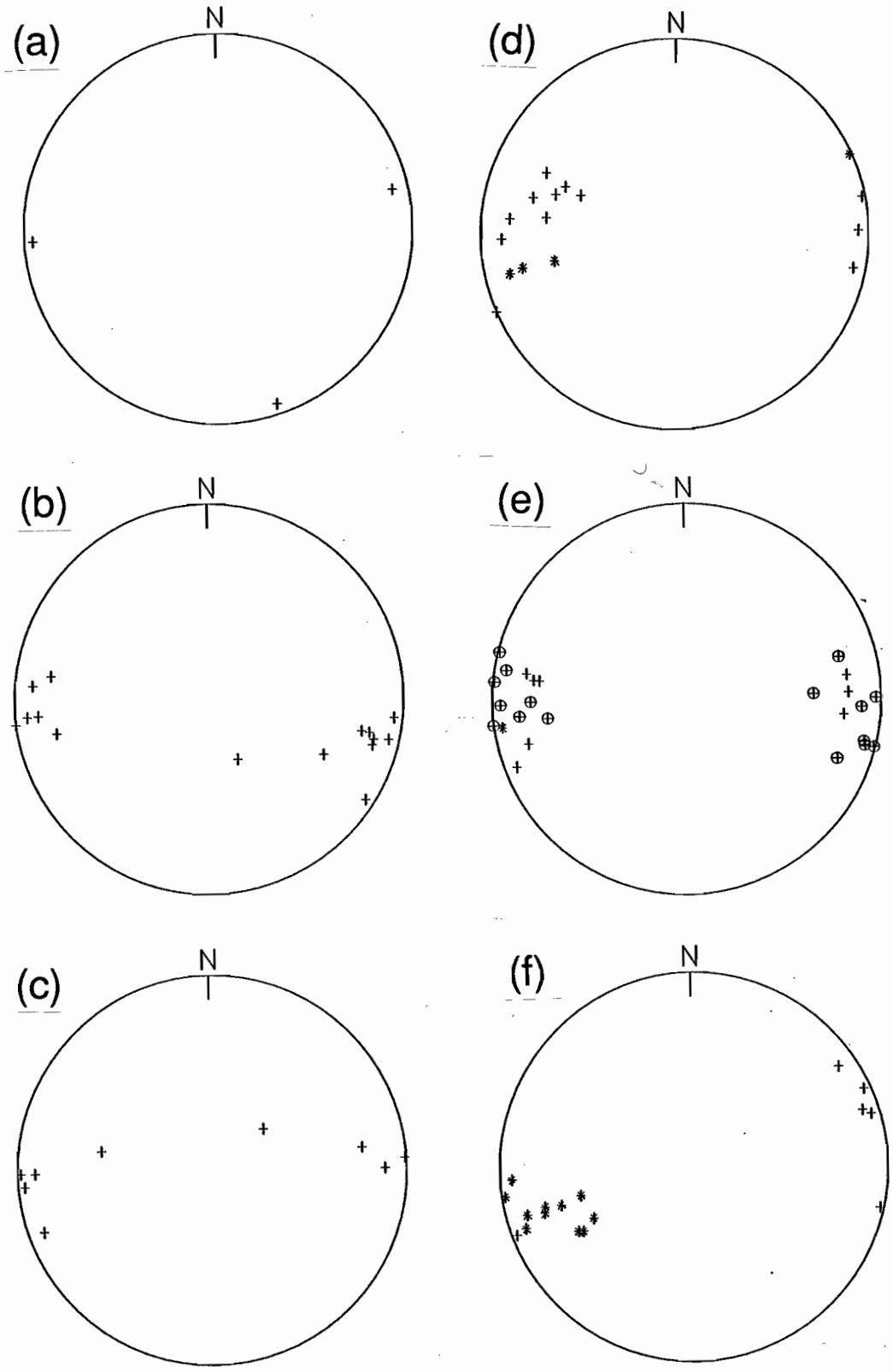

FIG. 4 — Equal area stereographic projections of structural data. (a) southern region poles to bedding, (b) Rosebery area poles to bedding, (c) Pieman River area poles to bedding, (d) southern region poles to cleavage, (e) Rosebery area poles to cleavage, (f) Pieman River area poles to cleavage.

rheological constraints near the Rosebery Fault. No clear evidence for a different morphology here has been recognised. Further, 5 km north of this section, near Bobadil Dam, a weak NNW-striking cleavage crosscuts bedding and a slaty cleavage giving a possible transected fold geometry. In thin section the major slaty cleavage is sub parallel to the bedding and this cleavage forms very weak crosscutting crenulations with some pressure solution.

3. A composite origin for these slaty cleavage rocks.

We have remarked in previous reports that the Devonian slaty cleavage transects the dominant N trending folds but that the axial plane structures associated with the early fold generation has remained elusive. Most of our evidence suggests the Cambrian folds were gentle to open and thus may no have had a substantial axial plane structure. High angle unconformities (greater than 45°) are relatively rare. Cambrian cleavages were reported from zones outside the locus of Devonian deformation (Berry & Keele 1993). The dominance of a slaty cleavage in this section which predates a NNW trending cleavage and is apparently axial plane to the N-trending Cambrian structures suggests this is a zone in which Cambrian deformation was stronger and created a substantial Cambrian cleavage. Whereas in other areas the evidence for an early cleavage is largely obliterated and the relicts cannot be distinguished from a sedimentary fabric, here the cleavage is strong and clearly tectonic in origin. This does not preclude a Devonian origin since N-trending folds effect Devonian rocks in the King River (Berry 1992) and, at Black Bluff, Seymour (1980, 1989) has recognised N-trending folds overprinted by NNW-trending folds in Ordovician rocks. It does, however, complicate the relatively simple model which can be applied in most of this section of the Rosebery Fault. In both the west coast examples the N-trending fold dominance is in the footwall of major reverse faults.

DIAMOND-SHAPED CLEAVAGE PATTERNS

It is important to realise that, in this area, only massive silica rich rocks in which the cleavage forming process was dominated by pressure solution rather than grain rotation have been found with a clear diamond shaped cleavage pattern. This may reflect the fact that for the close angle between cleavages, the tendency for slaty cleavage is to overprint the existing fabric by partial rotation rather than start a new cleavage. Within the Rosebery Group the N-striking cleavage is strong and the NNW strike is only recognised as crenulation. There is some rotation of the cleavage but not enough to make this the dominant feature except in a few isolated exposures. The strength of this N-striking cleavage at this site is circumstantial evidence that the Rosebery fault was active before the regional NNW cleavage.

MINERAL CHEMISTRY

An initial study was made into the mineral chemistry associated with different cleavages. A sample with two cleavages from the southern outcrops was analysed in detail. The rock contains the assemblage muscovite chlorite albite quartz. In this assemblage the Mg-Si/tschermaks exchange in muscovite is controlled by temperature and chlorite composition. Na exchange with albite may also be a useful indicator of temperature although no calibration exists for this. A detailed analysis of the chemical composition of the muscovite failed to find any substantial difference between S_1 and S_2 muscovite in this rock. The only element which is significantly different is fluorine and there is no mineral buffering this element (Table 1). The conclusion, then is that S_2 muscovite grew only partly as a result of recrystallisation in this rock. The K must have come from albite or relict K -feldspar now completely consumed. Based on existing compositions of chlorite and S_2 muscovite the temperature was about 310°C at the time of this event.

The sample from the immediate footwall to the Rosebery deposit (location 6) is composed of muscovite and quartz. In this rock with no other mineral components to react with it is not surprising that S_1 and S_2 muscovites are identical in composition.

Just south of Rosebery, where the Stitt River crosses the Murchison Highway (location 7), a rock containing the assemblage quartz-muscovite-biotite-K feldspar was analysed (Table 1). The biotite in this rock occurs as decussate aggregates indicating it largely post-dates the ductile deformation. The appearance of biotite in K-feldspar bearing assemblages of appropriate composition is generally considered to occur at 350°C and at about 400°C biotite should be found in a wide range of compositions. The limited appearance of biotite near Rosebery suggests the temperature was in the range 350–400°C. This assemblage has been calibrated as a geobarometer by Massone & Schreyer (1987). Unfortunately the effect of minor components has not yet been adequately dealt with but a simple minded application of the calibration suggests pressures of 5 kb. This is similar to the value reported by Green et al.

TABLE 1

	SiO2	TiO2	Al2O3	FeO	MnO	MgO	CaO	Na2O	K2O	H2O	F	Total
Location 7												
Biotite	35.26	1.96	15.77	23.92	0.30	7.85	0.00	0.03	9.40	3.47	0.62	97.95
Biotite	35.00	2.01	15.69	23.94	0.33	8.17	0.06	0.06	9.01	3.52	0.52	97.77
Biotite	35.48	2.06	15.36	23.56	0.35	8.42	0.00	0.03	9.49	3.46	0.72	98.21
Muscovite	45.73	0.52	28.04	5.50	0.08	2.42	0.03	0.08	10.60	4.21	0.14	97.21
Muscovite	48.73	0.44	30.06	4.54	0.00	2.18	0.08	0.06	9.02	4.41	0.14	99.53
Muscovite	49.29	0.43	29.88	4.98	0.01	2.28	0.00	0.03	9.83	4.40	0.26	101.12
Muscovite	49.22	0.16	32.96	1.86	0.00	1.39	0.01	0.21	9.90	4.51	0.09	100.22
K Feldspar	63.92	0.03	18.03	0.18	0.02	0.01	0.00	0.45	15.72	0.00	0.00	98.32
Location 8												
S1 Muscovite	49.87	0.27	32.56	1.72	0.03	1.71	0.04	0.10	8.61	4.46	0.21	99.38
S1 Muscovite	50.74	0.22	32.39	1.96	0.00	1.73	0.05	0.10	8.09	4.49	0.23	99.76
S2 Muscovite	49.88	0.29	33.79	1.56	0.00	1.28	0.04	0.20	9.59	4.49	0.27	101.11
S2 Muscovite	49.00	0.08	34.82	0.79	0.01	0.64	0.02	0.12	8.92	4.41	0.31	98.80
S2 Muscovite	50.63	0.20	34.23	1.63	0.00	1.17	0.06	0.19	9.00	4.59	0.15	101.70
S2 Muscovite	49.55	0.23	32.65	1.68	0.00	1.67	0.04	0.09	8.87	4.55	0.00	99.33
Location 3												
S1 Muscovite	49.30	0.06	36.38	0.46	0.05	0.92	0.13	0.51	9.04	4.43	0.49	101.27
S1 Muscovite	49.65	0.34	33.30	1.11	0.00	1.78	0.06	0.24	8.61	4.39	0.40	99.46
S1 Muscovite	49.65	0.07	36.75	0.57	0.00	0.75	0.10	0.53	8.46	4.59	0.20	101.47
S1 Muscovite	53.44	0.11	32.41	0.45	0.00	0.65	0.04	0.46	8.12	4.53	0.29	100.21
S1 Muscovite	49.91	0.08	34.78	0.41	0.03	0.77	0.06	0.60	8.56	4.33	0.58	99.53
S1 Muscovite	49.39	0.03	36.12	0.43	0.03	0.82	0.18	0.78	7.95	4.45	0.40	100.18
S1 Muscovite	48.87	0.03	36.61	0.45	0.00	0.67	0.09	0.59	8.68	4.51	0.27	100.50
S2 Muscovite	49.82	0.09	36.06	0.54	0.02	0.81	0.11	0.74	8.74	4.49	0.38	101.41
S2 Muscovite	51.40	0.01	35.36	0.54	0.00	0.98	0.08	0.44	8.04	4.59	0.25	101.44
S2 Muscovite	50.18	0.04	36.36	0.53	0.00	0.85	0.10	0.38	8.18	4.58	0.23	101.20
S2 Muscovite	48.84	1.42	36.18	0.38	0.00	0.64	0.00	0.52	7.32	4.50	0.30	99.79
S2 Muscovite	51.06	0.00	35.81	0.56	0.00	0.85	0.07	0.42	8.45	4.69	0.04	101.91
S2 Muscovite	50.56	0.09	36.81	0.35	0.01	0.75	0.08	0.55	8.67	4.68	0.12	102.52
S2 Muscovite	49.68	0.07	35.90	0.55	0.00	0.96	0.09	0.59	8.88	4.53	0.28	101.24
Chlorite	25.38	0.00	22.75	24.62	0.01	14.32	0.02	0.02	0.13	3.50	0.25	90.76
Chlorite	25.19	0.05	21.86	26.13	0.00	14.03	0.08	0.04	0.01	3.60	0.00	90.97
Chlorite	24.87	0.02	22.45	26.53	0.00	14.04	0.01	0.01	0.04	3.53	0.18	91.49
Location 6												
S1 Muscovite	49.76	0.39	31.56	1.90	0.00	1.93	0.04	0.14	10.48	4.45	0.24	100.63
S1 Muscovite	47.89	0.33	30.72	1.90	0.09	1.90	0.04	0.16	10.88	4.19	0.48	98.10
S1 Muscovite	49.89	0.36	29.30	1.79	0.08	1.64	0.02	0.15	10.59	4.25	0.39	98.07
S1 Muscovite	49.73	0.35	31.63	2.05	0.07	1.91	0.09	0.13	10.31	4.45	0.23	100.73
S2 Muscovite	45.67	0.35	29.10	1.91	0.01	1.84	0.00	0.09	10.68	4.09	0.23	93.74
S2 Muscovite	48.48	0.32	30.99	2.10	0.11	1.98	0.04	0.10	10.88	4.36	0.21	99.36
S2 Muscovite	46.96	0.33	28.56	2.01	0.00	1.80	0.02	0.12	10.42	4.13	0.23	94.33
S2 Muscovite	42.75	0.39	27.59	1.90	0.00	1.72	0.00	0.12	10.15	3.86	0.22	88.48
S2 Muscovite	48.45	0.39	31.44	2.17	0.00	1.91	0.01	0.13	11.14	4.36	0.29	100.00

1981 using sphalerite pyrrhotite assemblages and dismissed by him as unreliable. The cross section of Berry (1993) suggests a thicker overlying sequence but 3 kb seems to be the upper pressure limit expected from any existing structural models during Devonian granite emplacement. At Renison the mineralisation is compatible with pressures around 1 kb.

At the Pieman River, no S_2 muscovite could be recognised. The rock textures are much less recrystallised suggesting metamorphic temperatures are much lower. During S_2 there is no evidence for new grains of muscovite forming and this may reflect the distance to the Devonian Granites at this locality. The lack of S_2 white micas suggests the temperature is already dropping during the cataclastic overprint in contrast to what is happening over the granite ridge where temperatures peaked after the fault cleavage.

In the area around Rosebery many faults contain late quartz tourmaline veins. These are post-kinematic. Where they cross cleavage they are not folded in contrast to early veins which are strongly folded. A brief study of the tourmaline-bearing veins suggest that the movement at the time they were formed was extensional east–west. This is consistent with the structures at Renison.

CONCLUSIONS

The general model of a fault related cleavage along the Rosebery Fault works very well within the section investigated. The variations in morphology of this cleavage reflect the changing circumstances along the fault. At each locality the fault related cleavage occurred in the softer units near the fault but this varied between footwall and hanging wall. The cleavage morphology reflects the strongly varying temperature conditions between those sites which are close to Devonian granitoids and those that are far away.

The NNW cleavage was recognised throughout the area but in the section immediately west of Rosebery the evidence suggests and older cleavage with only a very weak overprint by the NNW direction. The full significance of this are requires further consideration.

REFERENCES

Aerden, D.G.A.M., 1991. Foliation-boudinage control on the formation of the Rosebery Pb-Zn orebody, Tasmania. *J. Struct. Geol.* 13: 759–776.

Berry, R.F., 1992. Victoria Pass to Queenstown regional section. Unpubl. report to AMIRA P291 Report 3: 22–30.

Berry, R.F., 1993. Rosebery section. Unpubl. report to AMIRA P291 Final Report: 1–15.

Berry, R.F. & Keele, R.A., 1993. Cambrian structure in western Tasmania. Unpubl. report to AMIRA P291 Final Report: 55–68.

Corbett, K.D. & Lees, T.C., 1987. Stratigraphic and structural relationships and evidence for the Cambrian deformation at the western margin of the Mt Read Volcanics, Tasmania. *Aust. J. Earth Sci.* 34: 45–68.

Green, G.R., Solomon, M. & Walshe, J.L., 1981. The formation of the volcanic-hosted massive sulfide ore deposit at Rosebery, Tasmania. *Econ. Geol.* 76: 304–338.

Lees, T.C., 1987. Geology and mineralisation of the Rosebery Hercules area, Tasmania. Unpubl. MSc thesis, University of Tasmania.

Massonne, H. & Schreyer, W., 1987. Phengite geobarometry based on the limiting assemblage with K-feldspar, phlogopite, and quartz. *Contrib. Min. Pet.* 96: 212–224.

Seymour, D.B., 1980. The Tabberabberan orogeny in northwest Tasmania. Unpubl. PhD thesis, University of Tasmania.

Seymour, D.B., 1989. Sequential development of the structural trends. *In* Burrett C.F. & Martin E.L. (eds): Geology and mineral resources of Tasmania. *Geol. Soc. Aust. Spec. Pub.* 15: 241.

Sulfur isotopes as a guide to Cambrian structures in the Mount Read Volcanic Belt — first progress report

G. Davidson and P. Kitto
CODES Key Centre

ABSTRACT

Work on the application of laser ablation sulfur isotope methods to the detection/characterisation of Cambrian structures has concentrated on the north end of Rosebery to date, but no isotopic data is yet available. A review of relevant publications on seafloor and ancient settings indicates that this study will be ground-breakng research, in that very few previous studies have examined the background variation of sulfur isotopes in submarine volcanic sequences. The review indicates that areas of shallow seawater convection are likely to be the most isotopically detectable, although there are reasons to believe that the recharge zones of large deep convection cells might also be detectable. Future work will concentrate on areas of probable shallow convection, such as the low-grade alteration north of Rosebery, and transects across known Cambrian structures.

INTRODUCTION

Fine disseminated hydrothermal pyrite is a very common feature in the Cambrian rocks of the Mount Read Volcanic Belt. It is particularly common in the alteration zones of massive sulfide mineralisation. To date, the very fine grain size of this pyrite has prevented its evaluation as a tool for locating fossil Cambrian structures or associated mineralisation. Both the trace element geochemistry (for instance, Co, Ni, Se), and the isotopic composition of such pyrite has potential for characterising paleo-fluid flow in the Mount Read volcanic pile. A technological advance in the form of the laser oblation sulfur isotope facility at the University of Tasmania now permits the isotopic analysis of this fine sulfide, and for the first time this work can proceed.

This report will concentrate on sulfur isotopes in the Mount Read volcanics, outlining a theoretical framework in which to understand sulfur isotopic variation in submarine volcanic packages. To date a very thorough sulfur isotope data base is available for Mount Read Volcanic Belt mineral deposits (e.g. Solomon et al. 1988, Gemmell & Large 1993).

SAMPLING TO DATE

The sampling rationale for this project is to examine sulfur isotope profiles across and within Cambrian structures, to assess whether sulfur isotopes record the circulation of Cambrian fluids.

The north end of the Rosebery ore bodies was selected as the first test of sulfur isotopic variation, because (1) pyrite is definitely present throughout the footwall sequence; (2) the potential overprint of Devonian fluids is minimal (but its effect will be assessed); (3) drill samples are available up to 1.7 km north at and below the same stratigraphic level as the mineralisation, (4) good stratigraphic control is available; and (5) Rosebery likely occurs on a major Cambrian structure or structures. Previous structural work indicates that Cambrian structures in this area dip steeply north in the plane of the steeply east-dipping north-south striking stratigraphic sequence. This area contains enough drillholes along strike from the most northerly "B-lens" mineralisation to potentially construct a sulfur isotope profile which is transverse to known Cambrian structures.

Samples are listed in Appendix 1. Profile locations are shown in Table 1. Sulfur isotopic analysis is underway but values were not available at the time

Hole	collar northing	collar easting	collar RL	Section intersected	Distance from ore (m)
60R	1210N	657E	3651RL	Intersects B-lens ore. Includes H'wall black shale, upper footwall	0
49R	1385N	51E	3548RL	B-lens periphery Includes H'wall black shale, upper footwall	175
57R	1394N	521E	3594RL	B-lens periphery Includes H'wall black shale, upper footwall	184
109R	1782N	350E	3563RL	Deep hole from black shale through the ore position, footwall pumiceous volcanics to the Rosebery Fault.	572
71R	2178N	398E	3530RL	H'wall black shale, transitional host sequence, upper footwall	968
107R	2991N	612E	3399RL	H'wall black shale, transitional host sequence, upper footwall	1781

Table 1 — *Holes sampled at the north end of Rosebery for sulfur isotope variation. Locations are in mine coordinates.*

of writing; the approach used here is to comprehensively analyse only three holes, and if useful variation is observed, analyse the remaining holes to fill in the isotopic picture. Profiles are being analysed from B-lens (60R), 968m from B-lens (71R), and 1781m from B-lens.

REVIEW: SULFUR ISOTOPES IN SUBMARINE VOLCANIC SEQUENCES

The relationship between fluid movement, rifting, and mineralisation — inferences from mid-ocean ridges

It is widely known that seawater is the dominant primary fluid circulating in submarine volcanic sequences. Seawater enters submarine volcanic sequences along faults, fractures, and areas of primary porosity such as hyaloclastite piles, coarse resedimented breccias, drained lava tube zones, etc, and apparently descends through the pile, to be heated across the geothermal gradient. This circulation process is greatly enhanced by convection around sub-surface plutons, where heat-flow is very high. A package of mid-ocean ridge rocks which initially forms at the point of rifting is subjected to high temperature fluid upflow above the pluton soon after formation. Such high temperature upflow may produce seafloor exhalation, and possibly economic VHMS deposits, underlain by pipes or broader zones of alteration. As spreading continues, this package of rocks moves off-axis, through the cooler zone of fluid recharge, with the consequence that low temperature mineral products overprint high temperature assemblages. With further spreading, the rock package is subjected to greater invasion by cool oxidised seawater, and mineral assemblages are affected by seafloor weathering. The movement of altered packages of rock through a stationary hydrothermal convection cell characterises very mature spreading centres such as the mid-ocean ridges; the

extent of mobility in less mature rift settings, such as that represented by the Mount Read Volcanics, is probably much less (% extension is much smaller), and hence the imposition of low temperature alteration assemblages on high temperature alteration assemblages at individual sites through the belt is attributable to in-situ waning of convection.

The causes of sulfur isotope variation in seafloor volcanic piles

The main source of information on the sulfur isotope geochemistry of seafloor volcanic sequences has been modern and ancient seafloor massive sulfide deposits. Sulfur isotope values of these are now very well characterised. However, very few studies of background or recharge zone sulfur variation exist in the literature, either because, as has been the case for the Mount Read Volcanics, regional sulfide grains were too small for analysis, or because researchers have concentrated on deposit variation.

The sources of sulfur for VHMS deposits are regarded as:

1. dominantly "rock" sulfur, mainly consisting of leached host-rock sulfur with lesser amounts of isotopically identical magmatic sulfur; and
2. subordinate volumes of sulfur sourced from inorganic seawater sulfate reduction.

The variation of sulfur isotopes in VHMS deposits through time provides a constraint to the relative importance of these sources. The seawater sulfate component must have been great enough to cause the global Phanerozoic VHMS deposit sulfur curve to follow the seawater sulfate curve through time. This would not occur if rock sulfur was the only sulfur source for this deposit-type.

Sulfur cycling in submarine volcanic packages proceeds as follows. Seawater is drawn down from the seafloor within the recharge zones of convection cells. During the heating that accompanies fluid descent, most sulfate is deposited as anhydrite or magnesium-hydroxysulfate, because of the reverse solubility of these phases (i.e. the phases become less soluble as the fluid heats) (Shanks et al. 1981). Estimates of the amount of sulfate removed by this process vary, from approximately one third (Alt & Chaussidon 1989), based on the molar concentration of Ca in seawater, to almost all the sulfate, based on the concept that excess Ca is available to the hydrothermal fluid liberated by wallrock alteration (Shanks et al. 1981). Certainly recent drilling on the seafloor has identified regions of anhydrite-filled veins and disseminations which are consistent with the concept of large-scale removal of sulfate in the recharge zones of seafloor convection systems (Alt 1985). However, one of the great puzzles of seafloor hydrothermal systems is the lack of evidence of such sulfate concentrations in ancient volcanic stratigraphy. This lack of evidence suggests that the anhydrite concentration is removed during the post-hydrothermal convection history, probably by seawater leaching at temperatures below 150°C.

The remaining seawater sulfate is rapidly reduced to dissolved sulfide, by reaction with Fe-bearing phases in hostrocks, when the modified seawater is heated above 200°C in a deep fluid reservoir. This is now thought to be a "batch" process, meaning that the entire sulfate concentration is reduced, rather than some part of it, producing a volume of dissolved sulfur which has the average concentration of the original sulfate, although individual molecules of sulfur in the fluid will vary widely in their isotopic composition. Modern seawater sulfate has a value of 20.3‰, whereas most modern VHMS deposits have sulfur between 0 and 10‰, indicating that reduced seawater sulfate must contribute to the sulfur value, but that it is not a dominant component.

The dominant component is thought to be rock sulfur. Heated seawater in volcanic sequences becomes acid, and is generally not in equilibrium with volcanic sulfide. Volcanic sulfide is therefore dissolved by the fluid. Volcanic sulfide is normally present as either pyrrhotite or pyrite, with minor base-metal sulfides. Basaltic rocks on average have much higher concentrations of sulfur (averaging 300 ppm) than acid volcanics (approximately 20× less; Solomon et al. 1988), and hence are likely to be more efficient sulfur sources for hydrothermal fluids. Strongly pyrrhotitic footwall rocks may form a special case, because initially sulfate will react with pyrrhotite to form pyrite, a reaction occurs which consumes sulfate sulfur rather than releasing it to the hydrothermal fluid. The hydrothermal fluid will be buffered by the pyrrhotite, and become strongly reduced, although it will not remain so once the pyrrhotite is largely reacted.

Igneous rock sulfur generally has a $\delta^{34}S$ value 0 ± 2‰, and this value is widely applied in isotopic studies. However, in settings comparable to the Mount Read Volcanic Belt, it appears higher values are the norm, which is attributed to heavy sulfur enrichment in the mantle overlying subduction zones, caused by reaction with fluids evolving from the down-going slab. For instance, Ueda & Sakai (1984) report an average value for Japanese arc Quaternary volcanic rocks — regardless of silica content — of $\delta^{34}S = +4.7 \pm 2.0$‰. Moreover, these authors cite reconnaissance values from the Hellenic, New Zealand and Marianas arcs suggesting that heavy igneous sulfur is a widespread feature of island arc volcanics. Again, the value of igneous sulfur has not

been globally well characterised because of its very fine grain size. No reliable, background, pristine igneous sulfide values have as yet been obtained from the Mount Read Volcanic Belt, but it is possible, given the arguments of Ueda & Sakai (1984), that it is heavier than mid-ocean ridge or continental igneous province sulfur (also ~0‰). Magmas degassing directly into the hydrothermal fluid would also contribute heavy sulfur. Quantifying these values for the Mount Read Volcanics is important because they control estimates of host-rock versus seawater-sulfate contributions. For instance, given that arc felsic igneous rocks contain significantly less total sulfur than basic rocks, greater contributions from seawater sulfate might be expected in these settings.

Several lines of evidence suggest that the isotopic value of sulfide in VHMS deposits is transferred directly from the deep hydrothermal reservoir. For instance, Gemmell & Large (1993) demonstrate that VHMS ore at the Hellyer deposit, Tasmania, has the same $\delta^{34}S$ value as ore-stage veins in the alteration pipe at least 700 m below the paleo-sea-bottom. Modern measurements of exhaling fluids indicate that no sulfate is present, indicating complete subsurface reduction prior to exhalation. These measurements strongly suggest that sulfate in barite lenses at the top of hydrothermal mounds is derived directly from seawater, rather than from sulfate in the exhaling fluid. Where the constituent sulfate in the barite is heavier than that of surrounding seawater, it must be surmised that incomplete sulfate reduction occurred at the interface between the exhaling fluid and cold seawater, and that some of the residual heavy sulfate was incorporated into barite.

There is also evidence that seawater sulfate reduction occurs in shallow subsurface convection cells adjacent to exhaling vent zones, as the first phase in the formation of a hydrothermal system, and then throughout its life. Alt & Chaussidon (1989) document a modern seafloor example of this phenomenon, but the best characterised ancient example comes from Hellyer (Gemmell & Large 1993). At the initiation of the hydrothermal cell, Gemmell & Large (1993) hypothesise that connate seawater, trapped in vesicles and interpillow zones of footwall sequences, are heated by a growing geothermal gradient around an intruding pluton. Water to rock ratios are either not high enough in this zone, or temperatures are too low, to leach much rock sulfur, but temperatures are high enough to cause complete reduction of trapped seawater sulfate, which is deposited in veins and as disseminations adjacent to the main evolving alteration pipe. As a consequence, a zone of heavy disseminated sulfide is deposited in the footwall adjacent to the main ore zone. The size of this zone is uncertain, but at Hellyer it extends at least 200 m from ore. There is no evidence that this sulfur makes a volumetrically significant contribution to the sulfur in the ore mound. Heavy sulfur continues to be deposited through the life of the system in the shallow convection cell, possibly because of incomplete reduction in the cell. Gemmell & Large (1993) attribute this incomplete reduction to near-exhaustion of the mineral reductants in this area, but a second option is that the temperature of circulation is such that the reduction is sluggish; for instance, Sakai & Dickson (1978) measured the half-time of exchange between sulfate and sulfide as a few minutes at 350°C, whereas at 200°C it is a few years. Thus lower temperatures would ensure only partial reduction for shallowly convecting cells.

Applications of sulfur isotopes to locating Cambrian structures

1. *Can sulfur isotopes detect the down-going limb of large convection cells, located on fossil Cambrian structures?*

Very little is known about this; the following is a summary of ideas on the subject.

Some evidence indicates that once convection ceases, mineral sulfate is dissolved and removed from the system, and hence would not be now identifiable. A second possiblity is that mineral precipitation helps seal the system, preserving mineral sulfate up until metamorphism. During metamorphism it is possible that in the presence of ferrous iron-bearing phases, and unconnected evolving metamorphic fluid generated by dehydration, the sulfate minerals would be reduced in-situ to dissolved sulfide, and precipitated as pyrite with $d^{34}S$ close to the original sulfate value. In the Cambrian rocks of the Mount Read Volcanics, this would be close to 30‰. Thus areas of fossil recharge may contain very heavy sulfide values, perhaps surrounded by rocks with igneous sulfide values of ~4‰. This would be a recognisable feature.

2. *Can sulfur isotope studies detect Cambrian structures associated with shallow convection, either along strike from major fluid movement sites, or as part of low temperature fluid movement events?*

The evidence from Hellyer regarding shallow convection cells suggests that shallow convection would also be recognisable as a concentration of heavy sulfur sulfides which would grade towards the rock sulfur value where fluids from the deep hydrothermal reservoir had penetrated into the particular structure of interest. The scale of these systems is not known.

3. *Can the peripheries of large VHMS systems be recognised with sulfur isotopes?*

The work of Gemmell & Large (1993) strongly suggests that sulfur isotopes in the footwall should grade inward towards VHMS ore from the background value of Cambrian arc igneous sulfur (~4‰), through a zone of heavy sulfur representing the shallow convection zone (10–30‰), to the lighter values of the main alteration pipe (mostly 4–15‰; Solomon et al. 1988, Gemmell & Large 1993). However, the extent of the shallow convection zone is unknown, and needs further study.

4. *Can low temperature deep Cambrian systems be recognised from their sulfur isotopes?*

Green & Taheri (1992) document pyritic zones in Cambrian volcanics at Boco (13 km N of Rosebery) with $\delta^{34}S$= –1.2 to 4.7‰. These are similar to values at other barren pyrite alteration zones, such as Chester, Basin Lake, and Cattley Range. Green & Taheri (1992) suggest that such areas experienced sufficient alteration to leach igneous sulfur and redeposit it as pyrite with an igneous signature, but that this occurred at too low a temperature or W/R ratio for seawater sulfate reduction. This interpretation will be assessed in this study using fine-grained sulfide data.

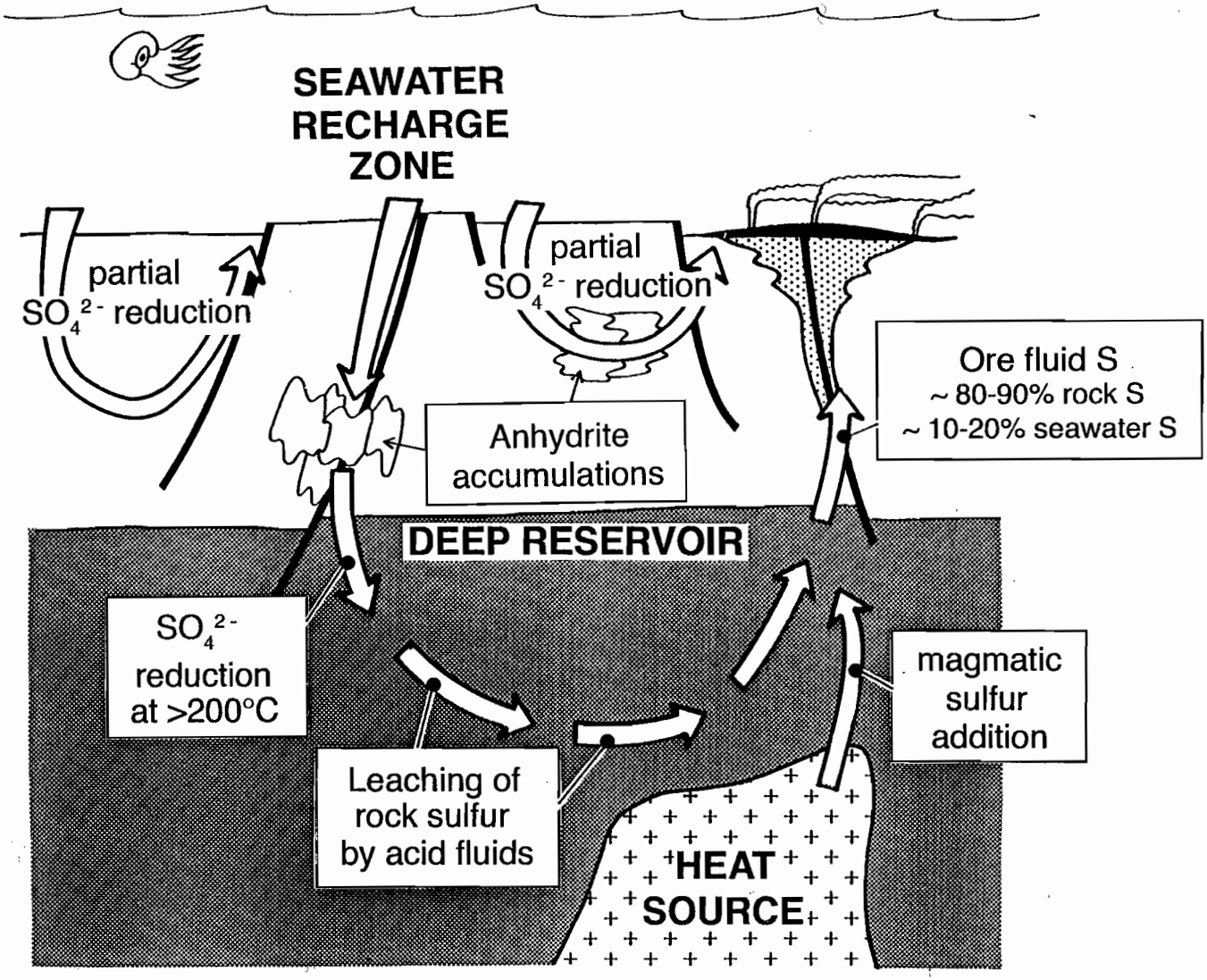

FIG. 1 — *Conceptual diagram of disseminated sulfur isotope variation in the Mount Read Volcanic Belt.*

INCORPORATION OF THIS REVIEW INTO A RESEARCH PLAN

The main aims of this sub-project, which are influenced by this review, are to:

1. Obtain corroboration of the increase of sulfur values in shallow convection zones by studying the Rosebery north end footwall sulfur isotope variation. This work is in progress. Clearly the approach will be justified if a second example of heavy sulfur in a shallow convection system can be found.

2. Extend the work to traverses across other Cambrian structures identified from other criteria.

3. Determine the primary igneous sulfide background in the Mount Read Volcanics.

REFERENCES

Alt, J.C. & Chaussidon, M., 1989. Ion microprobe analyses of the sulfur isotopic composition of sulfides in hydrothermally altered rocks, DSDP/ODP hole 504B. *Proc. of the Ocean Drilling Program., scientific results* 111: 41–45.

Alt, J.C., Saltzman, E.S. & Price, D., 1985. Anhydrite in hydrothermally altered basalts: DSDP Hole 504B. *In* Anderson, R.N, Honnoroez J., Becker K. et al. (eds): *Initial Reports DSDP 83*. US Govt Printing Office, Washington: 283–288.

Gemmell, J.B. & Large, R.R., 1993. Evolution of a VHMS hydrothermal system, Hellyer deposit, Tasmania, Australia: sulphur isotope evidence. *Resource Geology Special Issue* 17: 108–119.

Green, G.R. & Taheri, J., 1992. Stable isotopes and geochemistry as exploration indicators. *Bull. Geol. Surv. Tasmania* 70: 84–91.

Sakai, H. & Dickson, F.W. , 1978. Experimental determination of the rate and equilibrium fractionation factors of sulfur isotope exchange between sulfate and sulfide in slightly acid solutions at 300°C and 1000 bars. Earth Plan. Sci. Letts. 39: 151–161.

Shanks, W.C., Bischoff, J.L. & Rosenbauer, R.J., 1981. Seawater sulfate reduction and sulfur isotope fractionation in basaltic systems: interaction of seawater with fayalite and magnetite at 200–350°C. *Geochimica et Cosmochim.* 45: 1977–1995.

Solomon, M., Eastoe, C.J., Walshe, J.L. & Green, G.R., 1988. Mineral deposits and sulfur isotope abundances in the Mount Read Volcanics between Que River and Mount Darwin, Tasmania. *Econ. Geol.* 83: 1307–1328.

Ueda, A. & Sakai, H., 1984. Sulfur isoope study of Quaternary volcanic rocks from the Japanese Islands arc. *Geochimica et Cosmochim.* 48: 1837–1848.

APPENDIX 1

DDH/m	Mine sequence	Sample description
DDH 107R		
107R-546.6m	Black Shale	Py in 2mm veinlet
107R-558.5m	Black Shale	Disseminated Py in epiclastic sandstone
107R-601.1m	HW epiclastics	Disseminated Py in Qz-Fels phyric volcaniclastics
107R-621.0m	HW epiclastics	Disseminated Py in Qz-phyric volcaniclastics
107R-639.7m	HW epiclastics	Disseminated Py in Qz-Fels phyric volcaniclastics
107R-651.4m	Host rock	Laminated Fels-phyric shales
107R-652.5m	Host rock	Disseminated Py in Qz-Fels phyric volcaniclastics
107R-661.1m	FW volcanics (pumiceous breccia)	Disseminated Py in semi-massive Fels-phyric sandstone
107R-669.9m	FW volcanics (pumiceous breccia)	Disseminated Py in siliceous Fels-phyric volcaniclastic/epiclastic
107R-677.3m	FW volcanics	Disseminated Py veined by late carbonate
107R-688.3m	FW volcanics (pumiceous breccia)	Disseminated Py in massive pumiceous breccia
107R-711.1m	FW volcanics (pumiceous breccia)	Disseminated Py in massive pumiceous breccia
107R-722.3m	FW volcanics (pumiceous breccia)	Disseminated Py in massive pumiceous breccia & 5cm siderite alteration zones
107R-728.0m	FW volcanics (pumiceous breccia)	Disseminated Py in massive pumiceous breccia with silicified Fels phyric texture
DDH 49R		
49R-984.0'	FW volcanics (pumiceous breccia)	Disseminated Py in pumiceous volcaniclastic
49R-954.0'	FW volcanics (pumiceous breccia)	Disseminated Py in pumiceous breccia
49R-956.0'	FW volcanics (pumiceous breccia)	Disseminated Py in pumiceous breccia
49R-998.0'	FW volcanics (pumiceous breccia)	Disseminated Py-Po in pumiceous breccia
49R-935.0'	Host rock (split)	Thin epiclastic layers interbedded with Py-black shales
49R-925.0'	Black Shale	Py-black shales
49R-898.0'	Black Shale	Black shales with abundant Carb-Py veining
49R-840.0'	Black Shale	Black shales with abundant Carb-Py veining
49R-815.0'	Black Shale	Black shales with Py-nodules
49R-800.0'	HW epiclastics	Disseminated Py in turbiditic mass flows?
DDH 57R		
57R-2250.0'	Black Shale	Black shales with thin laminated turbidite layers containing disseminated Py & minor carbonate veins
57R-2273.0'	Black Shale	Black shales with disseminated Py cubes
57R-2290.0'	Black Shale	Disseminated Py in laminated epiclastics
57R-2301.0'	Mineralised Black Shales	Graphitic?-Py cut by 15cm wide Qz-Rhod vein
57R-2325.0'	Host Rock	Disseminated Py±Sph±Qz in fine grained epiclastic
57R-2362.0'	FW Volcanics?	Siliceous epiclastic with Py-Sph-Chl veinlets
57R-2437.0'	FW Epiclastics	Disseminated Py in Qz-Fels phyric sequence
57R-2437.0'	FW Epiclastics	Disseminated Py in Qz-Fels phyric sequence
N.B. THE EARLY SAMPLES FROM THIS HOLE MAY BE FROM A DEFLECTION		
57R-2391.0'	Ore Zone	Disseminated Py-Sph-Gal in chloritised host
57R-2424.0'	FW Volcanics	Disseminated Py in fels-phyric chloritised volcanics
57R-2460.0'	FW Volcanics	Disseminated Py in epiclastics
57R-2495.0'	FW Volcanics	Disseminated Py(±Po) in volcaniclastics
57R-2535.0'	FW Volcanics	Disseminated Py-Sph in volcaniclastics
57R-2546.0'	FW Volcanics	Disseminated Py-Sph in volcaniclastics
DDH 71R		
71R-1648.0'	Black Shale	Disseminated Py in carbonate veinlets
71R-1707.0'	Black Shale	Laminated Black shale with Py veinlets. Po disseminated throughout core but not in this piece
71R-2096.5'	HW epiclastics	Disseminated Py in Qz-Fels phyric pumiceous breccia

APPENDIX 1 cont.

DDH/m	Mine sequence	Sample description
71R-2107.0'	HW epiclastics	Disseminated Py in Qz-phyric pumiceous breccia
71R-2133.0'	Host Rock	Disseminated Py in cherty siltstone
71R-2174.0'	Host Sequence	Disseminated Py in Fels-phyric pumiceous breccia
71R-2210.0'	FW Volcanics	Disseminated Py in chloritic Fels-phyric pumiceous breccia
71R-2245.0'	FW Volcanics	Disseminated Py nodules in chloritic Fels-phyric pseudo pumiceous breccia
71R-2286.0'	FW Volcanics	Disseminated Py in pumiceous breccia
71R-2325.0'	FW Volcanics	Disseminated Py nodules in chloritic Fels-phyric pseudo pumiceous breccia with Qz-Chl crack-seal veins in core of zone
71R-2351.0'	FW Volcanics	Disseminated Py in Kfels-Chl altered fels-phyric pseudo pumiceous breccia
DDH 109R		
109R-510.0m	Black Shale	Disseminated Py in turbiditic-conglomeric mass flow with black shale clasts
109R-530.0m	Black Shale	Disseminated Py in calcite veined black shale
109R-550.0m	Black Shale	Disseminated Py in laminated Black shale with minor calcite veinlets
109R-559.5m	Host Rock	Disseminated Py in a pumiceous Fels-phyric epiclastic with chloritic-calcite veins
109R-569.6m	Transition Zone	Disseminatd Py in pumiceous mass flow-
109R-580.0m	Transition Zone	Disseminatd Py in pumiceous mass flow with chloritic veinlets
109R-591.2m	FW Volcanics	Disseminatd Py in pumiceous mass flow with prolific Qz-Chl crack-seal veins
109R-599.2m	FW Volcanics	Disseminatd Py in pumiceous mass flow with both chloritic veinlets and Qz-Carb veins
109R-611.3m	FW Volcanics	Fels-phyric mass flow with minor Py in a chloritic interval
109R-620.5m	FW Volcanics	Fels-phyric mass flow with Py disseminated along fractures
109R-629.4m	FW Volcanics	Fels-phyric mass flow with minor disseminated Py
109R-642.0m	FW Volcanics	Fels-phyric mass flow with Py disseminated along fractures
109R-649.6m	FW Volcanics	Disseminated Py in Fels-phyric mass flow with Chl-Qz veining
109R-671.5m	FW Volcanics	Disseminated Py in Fels-phyric mass flow with chloritic alteration
109R-738.7m	FW Volcanics	Chloritic-Kfels alteration of Qz-Kfels phyric mass flow similar to Anthony Rd.
109R-790.1m	FW Volcanics	Disseminated Py in siliceous Fels-phyric mass flow
109R-839.5m	FW Volcanics	Disseminated Py in Fels-phyric mass flow
109R-841.4m	FW Volcanics	Tour-Qz veining and brecciation together with Py veinlets (Dev.)
109R-871.5m	FW Volcanics	Fels-phyric mass flow with disseminated Py
109R-892.0m	FW Volcanics-5m from Rosebery	Pumiceous Fels-phyric mass flow with carbonate overprint Fault
109R-895.0m	Rosebery Fault	Siliceous brecciation zone with Carb(±Tour) overprint
DDH 60R		
60R-2827.0'	Black Shale	Disseminated Py in laminated black shale with carbonmate veinlets parallel to schistosity
60R-2850.0'	Black Shale	Disseminated Py in laminated black shale with carbonmate veinlets parallel to schistosity

APPENDIX 1 cont.

DDH/m	Mine sequence	Sample description
60R-2890.0'	Black Shale	Disseminated Py at the contact between black shales and minor mass flow unit
60R-3001.0'	Porphyry????	Disseminated Py in Fels-phyric (Porphyry?) unit with Qz-Carb veins
60R-3095.0'	Ore Zone	Massive Py-Sph Gal
60R-3106.0'	Ore Zone	Py-Sph vein
60R-3154.5'	FW Volcanics	Disseminated sulphides and stringer veins
60R-3197.0'	FW Volcanics	Disseminated Py and Qz-Carb veining
60R-3213.0'	FW Volcanics	Disseminated Py in chloritic volcaniclastic
60R-3253.0'	FW Volcanics	Disseminated Py in chloritic volcaniclastic
60R-3290.0'	FW Volcanics	Disseminated Py in chloritic volcaniclastic
60R-3325.0'	FW Volcanics	Disseminated Py in sericitised Qz matrix
60R-3346.0'	FW Volcanics	Disseminated Py in siliceous volcaniclastic
60R-3368.0'	FW Volcanics	Disseminated Py in siliceous volcaniclastic
60R-3385.0'	FW Volcanics	Disseminated Py in volcaniclastic

Lithostratigraphic correlation in the Dundas and Central Volcanic Complex: a progress report

Ron F. Berry
CODES Key Centre

ABSTRACT

The Mt Read Volcanics have been subdivided into three depositional cycles each with a distinct basin geometry and history. Samples of sandstones have been collect from each of these cycles, Detailed petrography on these rocks has been started with a view to finding distinguishing characteristics for each cycle and variations within the belt for individual facies. Initially this characterisation will be aimed at the heavy mineral suites in these sandstones.

INTRODUCTION

A major aim of the combined ARC-AMIRA project is to find new methods to enhance lithostratigraphic correlation within the Dundas Group and between the sections of the Mount Read Volcanics generally. This includes attempting to check existing lithostratigraphic sections. The major rationale of this work is to tighten up the structural interpretations in the existing regional sections and to provide a framework for basin analysis.

Several lines of evidence have already been put forward for correlation. Biostratigraphy has been used as a basis for correlation (e.g. Jago 1979, Pemberton & Corbett 1992). Major advances in lithostratigraphic correlation have been made in the northern section of the Mount Read Belt (Pemberton & Corbett 1992, McKibben 1993). McPhie & Allen (1992) suggested alternative correlations based on volcanic facies analysis in the Hellyer to Hercules section. Southeast of the Henty Fault the stratigraphic correlation remains very difficult despite a large amount of work.

The main aim of this section is to provide alternative tests of existing correlation and to look for new correlations. For example, the McPhie & Allen (1992) correlations depend on the existence of a unique pair of facies. The intention in this project is to look at the compositions of these facies to see if they have the same mineralogical and chemical composition or at least these vary smoothly from outcrop to outcrop.

STRATIGRAPHIC CORRELATION

As part of this project, a literature review has been attempted to define the options available in lithostratigraphic correlation. I have set up a classification based on three cycles of deposition. A provisional interpretation is made below.

Cycle 1 **Denison Group biostratigraphic correlates**
All the units which are Idamean or younger.

- Higgins Creek succession on the Boco Road and possible correlates, e.g. Westcott Argillite/ Salisbury Conglomerate
- Upper Dundas Group–Fernfields Conglomerate, Comet Slate, Fernflow Conglomerate, Climie Formation, Misery Conglomerate.
- Northern section of the Strahan Sheet in the Queensberry Mine area and west of The Sisters
- Newton Creek Sandstone, Owen Conglomerate
- Mt Zeehan Conglomerate

Comments
(a) the basin geometry is well established with both east and western marginal facies recognisable. Deeper water facies recognised in the western zone from Queensberry Mine to Higgins Creek.
(b) very active uplift of Tyennan block dominates the sedimentary record.

Cycle 2 **Tyndall cycle of deposition**
upper Boomerangian/Mindallyian
(in the north the base of this unit is approximately the facies marker unit of McPhie & Allen (1992))

- Tyndall Group–Comstock Tuff, Dora Conglomerate and volcaniclastic conglomerates in the south
- Southwell Subgroup/ Mt Cripps Subgroup in the north
- Razorback Conglomerate/Farrell Rivulet Quartzwacke–Brewery Junction Formation
- White Spur Formation–Stitt Quartzite–?parts of Westcott Argillite
- At Pinnacles quartz-feldspar porphyry sandstones - mafic magnetite bearing sandstones
- Radfords Creek group in Dial Range Basal chert beds similar to Razorback Conglomerate
- Trial Ridge beds in the Adamsfield trough

Comments
(a) this cycle is missing to very thin in the Murchison Gorge to Lake Selina area.
(b) the base of the cycle shows a shallow water facies in the south (basal unconformity south of Queenstown, limestone unit in Comstock valley) shallow water facies in the west (Razorback Conglomerate) but is below wavebase in the centre and north.
(c) very active explosive volcanism and rejuvenation active deposition are a feature.

Cycle 3 **Yolande Cycle of deposition**
Undillian/lower Boomerangian (predate granite intrusions)

- Miners Ridge Sandstone–Yolande River Group–Central Volcanic Complex
  In the far south the Miners Ridge Sandstone is thin but the mapping in the north of the Lyell sheet suggests the metasedimentary dominated stratigraphy is thicker east of The Sisters and south of the Henty Fault.
- Sticht Range Formation–Eastern Quartz phyric sequence
- Sticht Range Formation — Back Peak beds
- Redlead Conglomerate–Hodge Slate
- Black Harry Beds–Animal Creek Greywacke–Que Hellyer Volcanics–Que River Shale
- Central Volcanic Complex–Animal Creek Greywacke–Que Hellyer Volcanics–Que River Shale
- Lower sandstone- mudstone-conglomerate package of Huskisson Syncline
- Cateena Group in the Dial Range

Comments
(a) the top of the cycle is marked by mudstones in the north and by an unconformity in the south
(b) the base of the cycle is exposed along the eastern margin, in the Dundas area, and in the Miners Ridge.
(c) the Central Volcanic Complex is towards the top of this cycle in the south and west but apparently in the middle to lower part in the north. Is volcanism migrating to the south with time?

CONTENTIOUS CORRELATIONS

The Cambrian stratigraphy along the lower King River has no biostratigraphic control. The Strahan sheet mapping suggested a volcanic stratigraphy overlain by micaceous sandstone suggesting correlation with the White Spur Formation-Stitt Quartzite cycle of deposition but the structure reported by (Keele 1992) indicates a fault contact between the units and leaves open the possibility this is Yolande River Group/Miners Ridge Sandstone.

Poltock (1992) reported in detail on lithologies within the Henty Fault Wedge. He recognised a Henty Valley sequence which he correlated with Miners Ridge and the Yolande River (cycle 3 above), or the Crimson Creek Formation, and a Halls Rivulet and Ewart Creek sequences which he correlated with Tyndall Group (cycle 2).

In the Fossey Mountain trough the Gog Greywacke has unreliable late Cambrian fossils suggesting correlation with the Radfords Group and Stitt Quartzite. The St Valentines sequences also contain fossils suggesting a Tyndall cycle of sedimentation.

McKibben (1993) identified the phases associated with the magnetic sandstone package near Silver Falls as titano-magnetite, ilmenite and clinopyroxene. He suggested correlation of this unit with a magnetic unit in the Mt Cripps Subgroup and with magnetic clinopyroxene-bearing units in the Tyndall Group south of Queenstown. However the Westcott Argillite and upper Dundas Group (cycle 1) have magnetic units but the compositions of the associated mineralogy has not been defined. The mineralogy of these magnetic units needs to be checked to confirm the existing correlation. Some aspects of this problem are being carried out by graduate students at CODES outside the AMIRA project.

WORK IN PROGRESS

The main field activity in this section at present is a reconnaissance study of the distribution of heavy minerals in sandstones along the belt. Sandstones along the belt can be roughly divided into basement dominated and volcanic dominated types. Both occur in cycles 2 and 3 above. Cycle 1 is largely sedimentary and metamorphic in provenance. Samples from all cycles and scattered across the belt have been included in the initial study.

Heavy minerals are a good test of the provenance of sandstones. They potentially survive minor alteration and deformation. The phases are characteristic of their source. The distribution should say something about the basin architecture.

In addition if certain sources only become available during the history of the belt a separation of the stratigraphy should be possible. For example the existing problem with the definition of the Tyndall Group. At present some granitic clasts are required to recognise this group. It is likely that the unroofing of the Cambrian granitoids will add new compositions of heavy minerals to the sequence and that these will be distributed more widely than the visible granitic clasts.

Forty samples have been collected and crushed gently as recommended by Henningsen (1967). The fine sand fraction from these rocks will be extracted by sieving, washed and then separated by heavy liquids. The resulting heavy fraction will be mounted and polished. For some minerals a microprobe analysis will obtained. For example, tourmaline compositions are characteristic of different sources (Henry & Dutrow 1992). The separations are in process.

REFERENCES

Brown, A.V., 1986. Geology of the Dundas-Mt Lindsay-Mt Youngbuck region. *Bull. Geol. Surv. Tasm.* 62: 221pp.

Henningsen, D., 1967. Crushing of sedimentary rock samples and its effect on shape and number of heavy minerals. *Sedimentology* 8: 253–255.

Henry, D. J. & Dutrow, B.L., 1992. Tourmaline in a low grade clastic metasedimentary rock: an example of the petrogenetic potential of tourmaline. *Contrib. Min. Pet.* 112: 203–218.

Jago, J.B., 1979. Tasmanian Cambrian biostratigraphy - a preliminary report. *J Geol. Soc. Aust.* 26: 223–230.

Keele, R.A., 1992. The King River regional cross-section: a transect through the Dundas Trough. AMIRA project P291 Report 4: 11–30 (unpubl.)

McKibben, J.A.J., 1993. The geology and geochemistry of the North Pinnacles Ridge, western Tasmania. Unpubl. BSc Hons. thesis, University of Tasmania.

McPhie, J. & Allen, R.L., 1992. Facies architecture of mineralised submarine volcanic sequences: Cambrian Mount Read volcanics, western Tasmania. *Econ. Geol.* 87: 587–596.

Pemberton, J. & Corbett, K.D., 1992. Stratigraphic-facies associations and their relationship to mineralisation in the Mt Read Volcanics. *Bull. Geol Surv. Tasm.* 70: 167–176.

Poltock, R.A., 1992. Henty Fault wedge. Unpubl. M. Econ. Geol. thesis, University of Tasmania.